2-1-2012

Strength and ductility of bulk nanostructured aluminum processed by mechanical milling

Nesma Tarik Mohamed Aboulkhair

The American University in Cairo

School of Sciences and Engineering

Strength and Ductility of Bulk Nanostructured Aluminum Processed by Mechanical Milling

By

Nesma Tarik Mohamed Aboulkhair

A thesis submitted in partial fulfillment of the requirements for the degree

Of

Master of Science in Mechanical Engineering

Under the supervision of

Dr. Amal M. K. Esawi

Professor, Department of Mechanical Engineering

The American University in Cairo

Fall 2011

The American University in Cairo

Strength and Ductility of Bulk Nanostructured Aluminum Processed by Mechanical Milling

A Thesis Submitted by Nesma Tarik Mohamed Aboulkhair

To Department of Mechanical Engineering

January/2012

In partial fulfillment of the requirements for the degree of Masters of Science in Engineering

Has been approved by

Dr. Amal M. K. Esawi

Thesis Committee Chair / Adviser _____

Affiliation _____

Dr. Mahmoud Farag

Thesis Committee Reader / examiner _____

Affiliation _____

Dr. Niveen Mawsouf

Thesis Committee Reader / examiner _____

Affiliation _____

_____ _____ _____ ____

Department Chair/ Program Director Date Dean Date

Acknowledgements

I would like to start my dissertation by acknowledging all those who have helped me reach the point of actually writing my dissertation. First, I would love to express my deep gratitude to my supervisor, Professor Amal M. K. Esawi who has continuously nourished me with her guidance and experience.

Second, I am deeply thankful for the Youssef Jameel Sciences and Technology Research Center (YJSTRC), at the American University in Cairo for providing all the facilities, and materials as well as the financial support needed for this research to be accomplished. In addition to the personal help that I received from the YJSTRC team and particularly Abdel Hamid Mostafa, Ahmed Abdel-Gawad, Ahmed El-Ghazaly, Ehab Salama, Hany Salib, Mina Mikhael, Mohamed Taher, Mohie El-din Safwat and Radwa Raafat. Also, special thanks to Ms. Hanady Hussein and Mr. Rami Wasfi for their invaluable technical assistance.

Third, I am really grateful for Professor Hanadi Salem for her unconditional caring and encouragement throughout my years at AUC.

Fourth, I am extremely appreciative to my dear friends, Irene Samy and Mohamed Hegazy, who have always been beside me during my downfalls when I was just about to give up and helped me rise up again and follow the path to where I am today. Also, thanks to Ahmed Hossam who has helped me on a very short notice while writing my dissertation to catch up with my tight schedule.

Fifth, thanks to all the laboratory engineers and technicians (Eng. Khaled Eraqi, Hussein, Mohamed, Saeed, Magdy, and Sobhy) who have contributed hugely to getting this research done smoothly.

Sixth, thanks to the department of chemistry at AUC and specially Mr. Emad Farag for conducting the XRD analysis for the samples.

Seventh, thanks to Durametal Industries, the Egyptian company for wear resistant steels for supplying me with tooling at no cost to carry out this research.

Last and foremost, my beloved family, I can never thank you enough, not in a million years. Thank you my mother for your care, attention, and prayers, thank you for bearing with me and enthusing me during my worst times and never letting me fall. Thank you my father for you have always been my inspiration. Thank you my brother, Ibrahim, for supporting and encouraging me.

Thank you *all* for believing in *me*.

Abstract

Aluminum's many exceptional properties promote it to be as a strong candidate for several applications in the aerospace, automotive, building and packaging industries to name a few. As a result, strengthening Aluminum has been the interest of many researchers over the time. The most commonly followed approaches are alloying and thermal treatments. However, recently, refining the internal structure of materials until reaching the nano-scale range to improve their mechanical properties has been fostered. Specifically speaking, research adopting this approach on various metals has yielded promising results. One of the techniques used to produce nanostructured Aluminum powders, which is the one employed in this research, is mechanical milling.

Aluminum powders were mechanically milled using a high-energy ball mill under argon atmosphere for several milling durations up to 12 hours. The effect of the process control agent used during milling was investigated to determine the suitable amount to be used for best achievable mechanical behavior. Both X-ray diffraction patterns and scanning electron micrographs have revealed the establishment of nanostructured Aluminum by mechanical milling.

Bulk samples were synthesized by powder metallurgy. The success of the process of powder consolidation was determined by examining the degree of densification through density measurements. The effect of mechanical milling on the bulk samples has been studied by evaluating the tensile and compressive behaviors of the developed material. The material after milling for 12 hours exhibited a tensile strength that is four folds that of the starting powders. But this elevated strength was at the cost of sacrificing the ductility of the material. Nevertheless, under compressive loading the material behaved in a ductile manner in addition to the improved strength.

Peaks for secondary phases have been noticed in the X-ray diffraction patterns for the bulk samples after mechanical milling. The types of these phases remain undetermined, although high suspects of oxides and carbides exist, that might have contributed to the material strengthening. Transmission electron micrographs have ascertained achieving a nanocrystalline structure after milling for 12 hours.

The poor ductility of the milled Aluminum acts as a barrier that hinders the utility of the material since almost all the applications require an amount of ductility within certain margins for shaping, manufacturing, and so forth. Hence, post-extrusion annealing was conducted on additional samples in an attempt to improve the ductility. This has been proved quite successful, but still the achieved ductility is nowhere near the range that can help commercialize the newly developed material. It was also remarkable that annealing didn't result in sacrificing the acquired strength; on the contrary, the tensile strength of the material was noticed to have increased.

Another approach to compromise the strength and ductility of mechanically milled Aluminum was to mix soft as-received Aluminum powders with the Aluminum powders mechanically milled for 12 hours to produce bi-modally structured Aluminum composite. Two mixing techniques were tried out that are turbula mixer and the high-energy ball mill.

Using turbula mixer yielded disappointing results by demonstrating a weak bond between the two constituents. Conversely, using the ball mill for mixing allowed a strong bond to form between the constituents leading to enhancing the ductility of mechanically milled Aluminum for 12 hours without depressing the strength beyond the acceptable range.

Table of Contents

List of Figures

List of Tables

Nomenclature

σ_y:	Yield Stress
σ_o:	Intrinsic frictional stress
K_y:	Strengthening coefficient
D:	Grain size
σ_{or}:	Orowan stress
M:	Orowan strengthening formula orientation factor
G:	Shear modulus
b:	Burger's vector
λ:	Wavelength
d:	Diameter of dispersoids
ν:	Poisson's ratio
a:	Lattice parameter
t:	Thickness of crystallite
k:	Crystallite shape constant
2Θ:	Diffraction angle
B:	Full width at half maximum height for an XRD peak
ε:	Strain
τ:	Shear stress
C:	Taylor relationship constant
ρ:	Density of dislocations
f:	Volume fraction

List of Abbreviations

Al:	Aluminum
BM:	Bi-modal
BM AL 0-12:	Bi-modally structured Al mixed using turbula mixer
BM Al 1-13:	Bi-modally structured Al mixed using ball mill
BPR:	Ball-to-Powder ratio
CG:	Coarse-grained
DSC:	Diffraction Scanning Calirometry
ECAP:	Equal Channel Angular Pressing
FCC:	Face-centered Cubic
GB:	Grain Boundary
HPT:	Hot Pressure Torsion
MM:	Mechanical Milling
MM Al X hrs:	Mechanically milled Aluminum for X hours
NC:	Nanocrystalline
PCA:	Process Control Agent
PM:	Powder Metallurgy
PDW:	Polygonized Dislocation Wall
PTB:	Partially Transformed Grain Boundary
SEM:	Scanning Electron Microscope
SPD:	Severe Plastic Deformation
SPS:	Spark Plasma Sintering
TEM:	Transmission Electron Microscope
XRD:	X-Ray Diffraction

Chapter (1)

Introduction

1.1. Aluminum

In 1671, Aluminum was named Alumine for the base of alum that was originally used by the Romans and Greeks. In 1807, the name Aluminium was proposed for the metal, which was later on agreed to be changed to Aluminum. The International Union of Pure and Applied Chemistry IUPAC adopted the name Aluminium in order to conform with the *"ium"* ending of most elements, so Aluminium is the international standard. This spelling was accepted in the United States until 1925 when the American Chemical Society decided to revert back to Aluminum to this day [1].

Of all the non-ferrous metals, Aluminum is the one that is heavily consumed. Annual consumption of aluminum worldwide is 24 million tons. 18 million tons of which is primary Aluminum, i.e. extracted from the ore, and the rest is secondary Aluminum, i.e. derived from scrap metal processing [1].

Aluminum has a very high chemical affinity for oxygen, that's why it can't be found in nature as a metal. Aluminum is ranked the second most plentiful metallic element on earth as it builds 8% of the earth's crust and then comes Iron (5%), Mg (2%), Zn, and Sn (0.004 % each). Although Aluminum's amount on earth is quite huge, it is always found in the form of alumina or any other combined oxide form [1].

Aluminum is a chemical element in the third group of the periodic table of elements. It has an atomic number of 13 and an atomic weight of 26.98 based on

Oxygen. It has no natural isotopes, however artificial isotopes can be produced and they are radioactive ones. Aluminum is a stable element with 14 neutrons and 13 protons. It has a Face-Centered Cubic FCC crystal structure with a co-ordination number of 12 and an atomic packing factor of 0.74. The length of the unit lattice cube was found to contract by decreasing the purity of the metal and this was attributed to the formation of impurity segregations. In Aluminum, the closest distance between two neighboring atoms is ((√2)/2)*Lattice parameter. The atomic radius of Aluminum is normally equal to 2.863 Å [1,2].

Aluminum powders can be found in a wide range of sizes from 0.015 μm to 17,000 μm. It can also be found in different shapes such as spheres, thin flakes, or irregular powders. Aluminum powders are classified according to certain parameters such as apparent density, specific surface (surface area per unit weight), and oxide content [2]. There are different types of powders, such as:

1. Air-atomized powders
2. Spherical atomized powders
3. Water-atomized powders
4. Acicular powders
5. Grained Aluminum
6. Granulated Aluminum
7. Ultrafine powders
8. Fibers
9. Flake powders
10. Flitter
11. Chopped and balled foil
12. Aluminum shot particles

13. Cut foil
14. Machined particles
15. Chopped wire
16. Sintered Aluminum Powder (SAP)
17. Composite powder particles
18. Brittle alloy powders

The degree of purity of Aluminum highly affects the physical properties of the material. Moreover, as the purity of Aluminum increases, its mechanical strength decreases in contrast to the ductility, which increases with increasing the purity of Aluminum. Thus Aluminum powders are classified according to their degree of purity. The classification adopted by the United States standard is shown in Table (1). Aluminum has high reflectivity, electrical, and thermal conductivity [1,2].

Table 1: Aluminum powders classification [1].

Degree of Purity	Classification
99.5 – 99.79%	Commercial Purity
99.8 – 99.949%	High Purity
99.95 – 99.9959	Super Purity
99.996 – 99.999%	Extreme Purity
> 99.9990%	Ultra Purity

Aluminum is a metal with outstanding properties since it has low density (2.7 gm/cm^3), high strength and good corrosion resistance. Commercially pure Aluminum has a value of Young's modulus E in the range of 70 – 72.5 GPa, shear modulus G in

the range of 27 – 28 GPa and a Poisson's ratio ν varying between 0.31 – 0.33. These unique characteristics promote it to be used in conventional and modern applications. Opportunities for Aluminum are expected to increase further as the demand of technologically complex and ecologically sustainable products increases. Aluminum is suitable for numerous applications, such as: [1]

- Automobiles and trucks manufacturing
- Food and beverages packaging
- Building's construction
- Electricity transmission
- Development of infrastructures for transportation
- Manufacturing of defense and aerospace equipment
- Production of machinery and tools
- Durable consumer products

Pure Aluminum is non-heat treatable, consequently it is mostly strengthened by strain hardening if not alloying. One of the techniques to strain harden pure Aluminum is work hardening. Aluminum has high stacking fault energy, hence deformation mainly occurs by dislocation slips. Deformation increases the density of dislocations in the material as well as the stored energy. Cold working is always accompanied by fragmentation and as the amount of severe cold working increases; higher densities of dislocations are produced along with the reduction in fragment size. Heavily deformed Aluminum has a density of dislocations around $10^{15}/m^2$. However, the material can always be reverted back to the original soft and ductile condition through annealing, since annealing eliminates strain hardening and changes the structure achieved through cold working. The cold worked Aluminum is usually

unstable especially in comparison to the strain free Aluminum. Consequently, it tends to revert back to a state of equilibrium or stability through annealing. As the percentage of impurities increases in Aluminum, annealing should be done at a higher temperature and for longer durations. However, this relaxation in the material results in a decrease in the strength of Aluminum since the density of dislocations decreases. The density of dislocations in annealed Aluminum is around $10^{10}/m^2$ [1,2].

Based on the abovementioned facts, Aluminum is a superior candidate in applications where specific strength is a design consideration, owing to its low density and high strength.

1.2. Nanocrystalline materials

Nanocrystalline materials are those composed of grains or crystallites in the nano-meter range (below 100 nm). These materials are characterized by a high density of crystal lattice defects such as grain boundaries, dislocation cells, interfaces, interphases and triple junctions. Consequently, these materials have exceptional chemical, physical, and mechanical properties [3,4]. Nanocrystalline materials have unique properties that are considered extraordinary when compared to the coarse-grained polycrystalline materials, these properties have led to the possibility of designing new materials such as super strong metals, ductile ceramics and wear free materials [5,6].

It has been shown by several studies that the strength of materials is enhanced with grain size reduction and this is supported by the Hall-Petch equation. However, when the grain size is reduced to less than 100 nm, the extrapolation of the Hall-petch equation cannot be used to predict the yield strength of the material. In some cases, the strength does increase with decreasing the grain size following the same trend as

the large-grained materials. In other cases, the strength increases but with a different slope from the one predicted by the Hall-Petch equation whereas sometimes a negative slope is even reported, i.e. the strength decreases with decreasing the grain size. The deviation from the Hall-Petch equation can be attributed to the change in the deformation mechanisms. In coarse-grained materials, deformation is stated to be due to dislocation motion or twinning. Whereas in nano-sized materials, the deformation is believed to be by grain boundary sliding or twinning [4, 7-10].

Recently, synthesizing bulk specimens from nanocrystalline or ultrafine-grained powders has been of great interest due to their outstanding properties that give them superiority over those synthesized from microcrystalline powders [11].

Bulk nanocrystalline aluminum alloys are characterized by their high tensile strength when compared to the conventional microcrystalline equivalents. The enhancement in the strength is mainly referred to grain refinement that is expected from the extrapolation of the Hall-Petch equation [9]. On the other hand, the bulk mechanical properties of pure nanocrystalline aluminum are not fully understood because it is difficult to mechanically mill pure Aluminum powders [4].

1.3. Techniques to synthesize nanocrystalline materials

The rapid progress in technology nowadays had led to an increasing demand on new and advanced materials to replace the conventional materials. Advanced materials are those synthesized controlling their crystal structures and microstructures in order to be tailored to a specific set of properties for demanding applications. The reason behind searching for a replacement to the conventional materials is that the modern applications require materials that are stronger, stiffer, lighter, and have the ability to be used at elevated temperatures. In order to fulfill these needs, several

researchers have been working on modifying the physical, chemical, and mechanical properties of materials to improve their performance. This goal is achievable via two approaches; the first one is the bottom up approach and the second one is the top down approach. In the bottom up approach, the chemical properties of the molecules of the material are studied and tailored to be assembled into the final material. In contrast, the top down approach is when breaking down the material to have an insight of its compositional levels. Fostering the top down approach in the materials research field, significant enhancements have been acquired by subjecting the conventional materials to thermal, mechanical, and thermomechanical processing methods that transform them into nanocrystalline materials [12].

Several investigations have been done in order to study the mechanical behavior of ultrafine-grained (100 - 300 nm) and nanocrystalline materials (<100 nm). These materials showed outstanding mechanical properties and this encouraged researchers to develop different methods to synthesize these materials, and study their mechanical properties using different tests such as micro-hardness and uniaxial tension or compression. Examples for the methods developed to synthesize ultrafine-grained and nanocrystalline materials are inert gas condensation, electro-deposition, crystallization from amorphous materials, rapid solidification processing, spray forming, plasma processing, vapor deposition, severe plastic deformation, and mechanical alloying/milling [7,12].

1.3.1. Mechanical Alloying/Milling

Mechanical alloying (MA) is defined as a solid-state powder processing method that involves repetitive welding, fracturing, and re-welding of powder particles in a high-energy ball mill. This technique allows the production of

homogeneous materials from blended elemental powder mixtures. In the literature, processing powder particles in high-energy ball mills is usually referred to by two different terms; mechanical alloying (MA) and mechanical milling (MM). Mechanical Alloying (MA) is the process of milling mixtures of powders of different metals or alloys/compounds where material transfer is involved to obtain a homogeneous alloy. Milling of uniform (often stoichiometric) composition powders, such as pure metals, intermetallics, or pre-alloyed powders, where homogenization doesn't require material transfer, is termed Mechanical Milling (MM). MM requires half the time required for MA to achieve the same effect. Also, MM of powders reduces oxidation of the constituent powders, as a result of the shortened time of processing. Sometimes MM is referred to as Mechanical Grinding (MG); since grinding is usually thought of as an abrasive machining process involving mainly shear stresses and chip formation. However, the more complex stress states occurring during milling give preference to the term milling. It should also be noted that MA is a generic term, and is sometimes used to include both mechanical alloying and mechanical milling/grinding [13].

Mechanical alloying/milling started in 1966 as an industrial necessity to produce oxide dispersion strengthened Nickel and Iron based super alloys for the aerospace industry. Mechanical alloying is categorized as a dry powder processing technique. It was used for solid-state dispersion in cases when liquid state dispersion was not possible. Since mechanical alloying is a fully solid-state processing technique, phase diagrams are not followed [13].

Mechanical milling is widely used nowadays in research in order to synthesize nanostructured materials in the solid-state [3,4,14]. The growth of the number of publications about mechanical alloying/milling is shown in the bar chart in Figure (1).

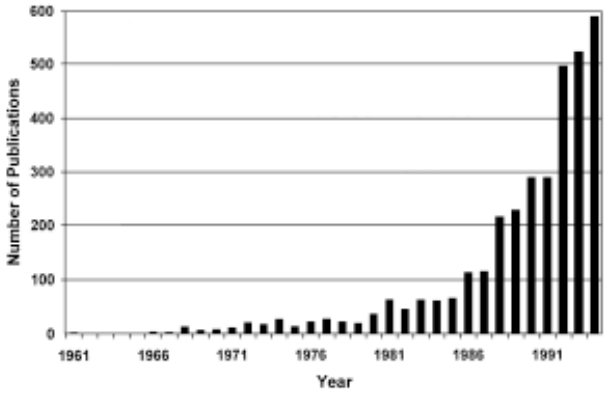

Figure 1: Growth in the number of annual publications about mechanical alloying [12].

Mechanical milling is conducted by loading the powders and balls into the milling jars, according to a specific ball-to-powder weight ratio, along with an amount of process control agent (PCA) and a high-energy ball mill is usually used for the milling process [13]. This process usually takes place in an inert atmosphere [14]. A schematic presentation simulating the motion of the balls and powders in a planetary ball mill during the process of mechanical milling is shown in Figure (2).

During mechanical alloying, the powders are subjected to successive cold welding and then fracturing. To illustrate, the powders are first cold welded together to form laminates. Then these laminates are subjected to further collisions leading to their fracture into finer laminates. After that, the thickness of the lamellae keeps decreasing until this structure disappears [14]. This scenario is clearly demonstrated in Figure (3).

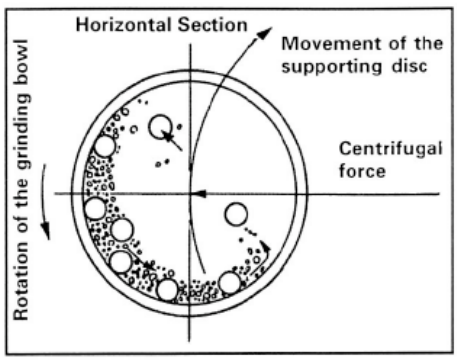

Figure 2: A schematic presentation simulating motion of the balls and powders during milling [13].

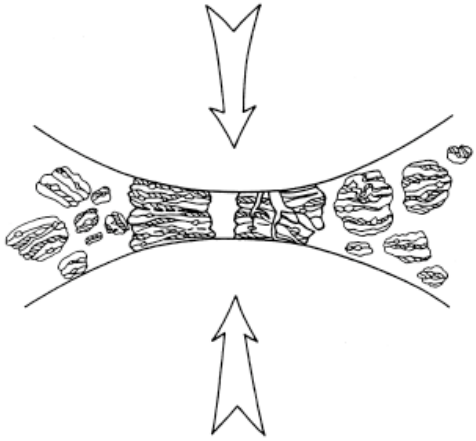

Figure 3: Ball to powder collisions during mechanical alloying [13].

Particles collision with the balls and vial force them to experience high strain rate plastic deformation resulting in high density of dislocations. At the beginning, the density of dislocations keeps increasing until it reaches a certain amount at which the grains get heavily strained and they break up into sub-grains with low angle grain boundaries. These new sub-grains undergo further plastic deformation with the continuation of milling. Hence the orientation of sub-grains becomes random and the size of them reaches the nanometer scale. At this structure, the motion of dislocations becomes difficult, so deformation occurs through grain boundary sliding [3]. Hence, the principle mechanism that controls the operation during mechanical milling is the rate of cold welding and fracturing of the powder particles due to collision and plastic deformation [6].

Grain size reduction that occurs during mechanical milling is also controlled by the rate of recovery during the process. The grain boundary volume increases as a result of mechanical milling leading to an increase in the driving force for recovery and so the recovery rate increases. This results in increasing the final grain size. Consequently, it can be stated that the grain size is dependent on both the energy supplied during milling and the rate of recovery [3].

Generally, in FCC metals the final size of crystallite depends on the competition between the levels of stress induced in the material by mechanical milling and the amount of dynamic recovery. Although it has been previously stated that fracturing and cold welding of the particles is a principle mechanism of operation during milling, it is believed that it is not the major mechanism for grain size refinement. Grain size refinement is also due to localization of plastic deformation as shear bands with high density of dislocations, annihilation of dislocations creating sub-grains and the transformation of these sub-grains into grains by grain rotation and sub-grain boundary sliding [6].

Although the process of mechanical milling has several advantages, there are numerous problems that cannot be ignored, such as: [13]

1. Contamination

The process of mechanical milling mainly operates by collision between the powders to be milled and the vial and balls used in milling. This results in wearing of the vial and balls leading to the presence of minor and unwanted constituents in the milled powders. Several researchers have found that contamination cannot be avoided but it can be reduced to the minimum. The level of contamination was found to increase with the milling time. However, some of the precautions that should be taken into consideration to minimize contamination are as follows:

a. Using high purity metals

b. Using balls and jars made of the same materials being milled

c. Using high-purity atmosphere

d. Self-coating of the balls with the milled material

e. Using the shortest possible milling durations

2. Limited Science content

Although the process has been widely used, the way it works is not yet completely comprehended. One of the main reasons hindering the full understanding of the process is the large number of parameters affecting the produced material such as the type and amount of PCA used, the milling time and temperature, the size, purity, shape and hardness of the powders particles, velocity, angle and frequency of grinding medium, ball to powder weight ratio, milling atmosphere, and size, shape and weight of grinding medium.

1.3.1.1. Variables in the process of milling [12]

Mechanical milling is a complex process that is controlled by numerous parameters. These parameters control the quality of the produced powders and hence the mechanical behavior of the bulk samples synthesized from these powders will be altered as well. These parameters and their effect on the developed material will be discussed in this section.

1.3.1.1.1. The type of mill

There are different types of mills used in mechanical milling; for example, there is the Spex Shaker mills (Figure (4)), Planetary Ball mills (Figure (5)), Attritor mills (Figure (6)), and commercial mills. The selection of which type of mill to use depends on the number of factors that need to be controlled such as the amount of the produced powders, the temperature of the milling process, the acceptable degree of contamination, and the speed of milling.

Figure 4: Spex shaker [15].

Figure 5: Planetary ball mill [16].

Figure 6: Attritor Mill [17].

1.3.1.1.2. Milling container

The material of which the milling container is manufactured hugely affects the developed material. If a hard material is milled in a container made out of a softer material, this will lead to the erosion of the walls of the container and the embedding of this foreign material into the material being milled, causing undesired

contamination. The most common types of milling containers are made of hardened steel, tool steel, hardened chromium steel, tempered steel, stainless steel, WC-Co, WC-lined steel, and bearing steel. Moreover, there are types of milling jars that are used for specific applications only like copper, titanium, sintered corundum, yttria-stabilized zirconia, partially stabilized zirconia + yittria, sapphire, agate, Si_3N_4, and Cu-Be. Moreover, the design of the shape of the container is equally important in order not to use a jar that has dead zones where the powders don't get milled.

1.3.1.1.3. Milling speed

As the milling speed increases, the amount of kinetic energy supplied to the material being milled will definitely increase. Although this increase is quite favorable, the maximum velocity cannot be employed. For instance, considering a high-energy ball mill operating at its maximal speed, the balls will be pinned to the walls of the milling container without exerting any force on the powders to be milled. This is shown schematically in Figure (7). Therefore, it must be noted that based on the equipment used, there is a critical milling speed that shouldn't be exceeded. Moreover, the increase in velocity leads to temperature rise in the jars, which in turn promotes cold welding instead of fracturing. In addition, the high velocity results in excess in the wear rate of the used tool.

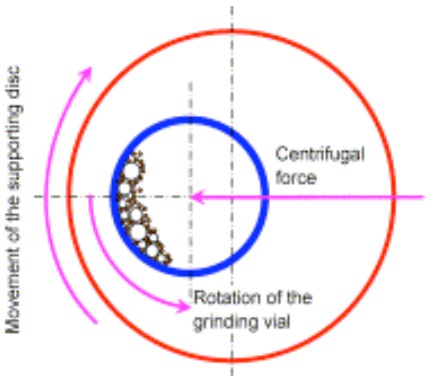

Figure 7: Schematic presentation of the balls pinned to walls at high speeds [18].

1.3.1.1.4. Milling time

The selection of the suitable milling duration depends on numerous parameters such as: type of mill, temperature of milling, ball-to-powder weight ratio, and milling speed. For some materials, exceeding the critical milling time leads to excessive contamination.

1.3.1.1.5. Grinding medium

The most common types of grinding media are hardened steel, tool steel, hardened chromium steel, tempered steel, stainless steel, WC-Co, and bearing steel. The density of the medium should be high enough for the balls to create an effect on the milled powders, i.e. the higher the density, the higher the kinetic energy supplied to the powders.

The size of the grinding medium is also important as it controls the impact of the balls on the powders. Sometimes it is recommended to use a mixture of different sizes of balls in the same milling process.

1.3.1.1.6. Ball-to-powder weight ratio

The ball-to-powder weight ratio BPR is also known as the charge ratio (CR). Several researchers have investigated different ball-to-powder weight ratios from as low as 1:1 up to 1000:1. However, using very high BPR is not recommended. The most commonly used BPR is 10:1, and then comes 4:1 and 30:1.

The BPR is also related to the milling duration and milling speed. All three parameters are interrelated and should work in proportional harmony.

The higher the BPR, the more the possibility of achieving a smaller crystallite size in a shorter time as demonstrated by the graph in Figure (8).

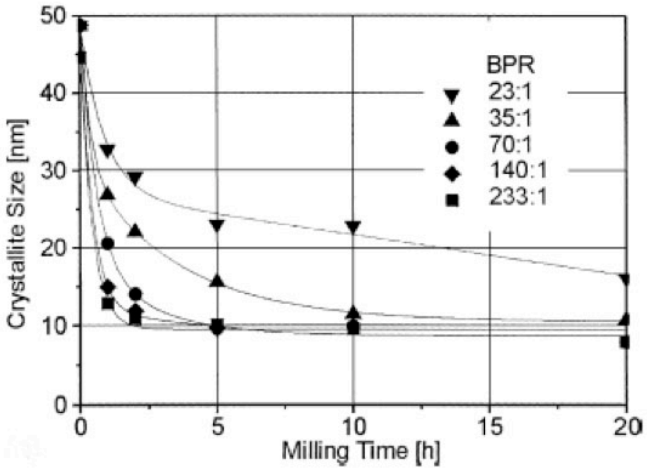

Figure 8: Effect of BPR & MM time on crystallite size of the produced powders [12].

1.3.1.1.7. Milling atmosphere

The process of milling is usually conducted under vacuum or inert atmosphere. The most commonly used gases when milling under inert atmosphere are Argon and Helium. Nitrogen has been proven unsuccessful except when formation of nitrides is required. The driving force behind milling in such specific atmospheres is the need to avoid contamination.

1.3.1.1.8. Nature and amount of process control agent

The process control agent PCA is used in order to promote particles fracturing over cold welding and thus contribute to reducing the particle size. Shown in Figure (9) is a chart plotting the mean particle size of Aluminum versus the amount of PCA used in the milling process demonstrating the decrease in particle size with increasing the amount of PCA [12]. Moreover, it reduces the heat accumulation in the jars during milling and prevents the powders from sticking to the milling media and jar walls. However, PCA can cause the formation of second phases if it reacted with the milled

material during the process of milling or subsequent heat treatments [11]. There are different types of PCA used, the most common of which are Stearic Acid, Hexane, Methanol, and Ethanol. Not only the type of PCA is important but also the amount used is crucial. The amount of PCA affects the final size, shape, and purity of the powders particles. Using a larger amount of PCA leads to decreasing the particle size by 2 - 3 folds. The most commonly used amount of PCA in practice is 1-5% of the powder charge. Research has shown that the relationship between the amount of PCA used and the final size of the particles is an inversely proportional one [12, 13].

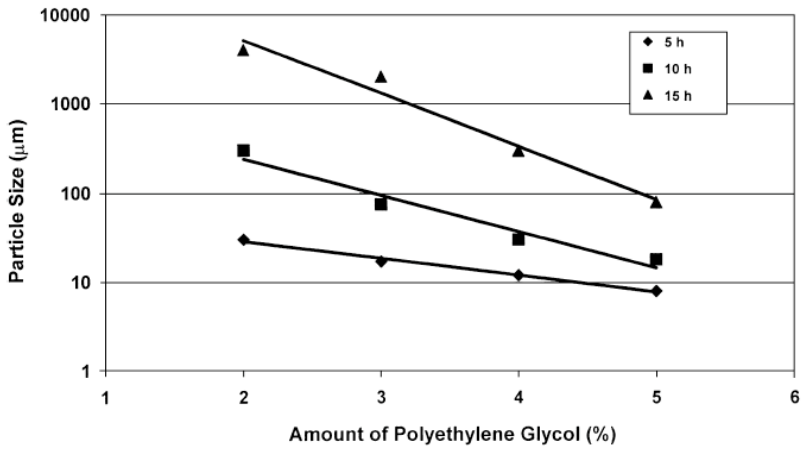

Figure 9: Mean particle size of Al versus the amount of PCA used [12].

1.4. Synthesizing bulk nanostructured samples

Producing bulk samples from nanocrystalline materials can be achieved using two main approaches that are:

1. *Severe plastic deformation of the bulk micro-structured samples*. This approach results in grain refinement due to its large strain without creating porosity in the material in contrast to the second approach, which can produce samples suffering from high porosity. These techniques induce high plastic strain in the materials such

as using high-pressure torsion (HPT) and Equal Channel Angular Pressing (ECAP). However, the minimum grain size achievable using this technique is 200-300 nm, which is not as low as that achievable by the second approach [7,19].

2. *Consolidation of nanocrystalline powders*. The powders produced using mechanical milling for instance can be of grain sizes as small as a few nanometers [7]. Different powder metallurgy (PM) procedures have been adopted to fabricate bulk nanocrystalline samples following this approach such as a combination of cold pressing and hot extrusion, hot pressing, hot isostatic pressing and spark plasma sintering (SPS) [11]. PM techniques involve high temperatures, which might result in grain growth in the samples especially when exposed to heat for long durations. Grain growth results in softening the material, which is not favored when aiming at strengthening the material.

Powder metallurgy helps in producing near net shape products, which is a mean to reduce the cost of production. However, it is not very convenient to be used for small production rates as the cost of tooling will be high and the revenue won't be feasible. But when considering military or automobile industries, powder metallurgy of aluminum is a promising candidate to replace ferrous parts made by powder metallurgy. One of the common techniques for producing aluminum profiles is extrusion and especially direct extrusion. The temperature at which extrusion of aluminum takes place is in the range of 450 to 600°C [1].

1.5. Strength and Ductility dilemma in nanocrystalline materials

The motivation behind developing new materials is the promise of better strength and ductility. Nanocrystalline materials have satisfied this expectation strength wise, however, the ductility of these new materials has been greatly

disappointing. The enhanced strength when compared to their coarse-grained counterparts is already expected beforehand by extrapolation of Hall-Petch equation. However, observations of any enhancement in ductility of nanocrystalline materials were very rare, elongation to failure even rarely exceeded 5% [20]. This lack of the ability to change shape without fracture under tensile stresses is the major drawback that faces virtually all the producers of bulk nanocrystalline metals. In other words, it can be stated that the ductility of these metals is as low as bordering the brittle behavior, although their conventional counterparts are ductile. Ductility is crucial for many applications, as it controls the ability of the material to be shaped and formed, to avoid catastrophic failure in load bearing applications. Therefore, this downside renders these materials unusable [4,5,21-26].

Grain size refinement is one of the approaches that are adopted to strengthen materials as it increases the density of obstacles facing the dislocations by increasing the volume of grain boundaries. However, extremely fine grains are not preferable because they affect the formability and the fracture toughness of the material. Extremely fine grains lead to grain boundaries acting as sinks for dislocations, which in its turn leads to a drop in strain hardening capacity during forming.

The poor ductility of bulk nanocrystalline metals is the main motivation behind researchers' shift to ultrafine-grained metals; those of grain size above 100 nm but below 1 μm, and they have high-angle grain boundaries. Their elongation to failure is usually around 10%, which is better than that of nanocrystalline metals but still not sufficient enough to be used in industrial applications. However, it must be noted that although the elongation to failure in ultrafine-grained metals is better than in nanocrystalline metals, sometimes their strength isn't as impressively strong as in the nanocrystalline metals [21].

In nanocrystalline metals, there are three main reasons behind the fracture strength depression, these are: [23]

- In some extremely small grain-sized metals, the dislocation driven plasticity is reduced concurrent with a hugely increased grain boundaries population with high interface energy that would permit crack propagation in an intergrannular manner
- It is difficult to produce full density bulk specimens with tiny grains; hence they are often small and thin. In this case a minor surface flaw or even roughness becomes a threat for initiation of cracks that are sufficient to cause catastrophic failure, even if there are no flaw or porosity inside the bulk.
- Another reason for the apparent low ductility is the plastic instability, if in the form of catastrophic shear banding in the initial stage of straining. This hypothesis is supported by the shape of the stress-strain curves, where the tensile curve peaks at low plastic strains and then slumps down rapidly, since the plastic deformation is localized in narrow regions (eg. shear bands), that are pulled apart in absence of spatial confinement under tension.

Either these factors acting alone or in concert; the result is a limited ductility of nanocrystalline metals by early fracture due to instability of crack nucleation and growth.

Strength and ductility of materials are mainly dependent on the mode of plastic deformation in the material. In the conventional coarse-grained materials, the plastic deformation is mainly carried by the motion of dislocations within individual grains. However, in nanocrystalline materials this is not the scenario fostered. The

nature of plasticity is that increasing the dislocations leads to their entanglement; consequently their motion is decreased increasing the strength and decreasing the ductility [5].

The failure behavior of nanocrystalline materials is not yet well defined. One theory is that failure primarily starts at the grain boundaries and triple junctions by the creation of voids. These voids, in addition to the readily existing ones, act as nucleation sites for dimples so that the fracture is not along the grain boundaries. Yingguang Liu et al. [25] summarized the scenario of ductile fracture in nanocrystalline metals as follows; under loading, nano-voids are first created at the interfaces. As the plastic flow and diffusion increase, additional nano-voids appear. Then they coalesce and grow into micro-voids and necking takes place.

It is also claimed that the deformation mechanisms in different materials can be categorized into three categories according to their grain sizes. These categories are listed hereunder: [24]

1. Materials with grain sizes larger than 1 μm are deformed by dislocation activity

2. Materials with grain sizes less than 10 nm are deformed by grain boundary shear.

3. For materials with intermediate grain sizes ranging from 10 nm to 1 μm, the deformation mechanism of these materials is not well understood. However, it is believed that it occurs by dislocation activity generated by grain boundary sources.

In order to better understand the lack of ductility in nanocrystalline materials, it is important to compare the tensile and compressive behaviors of nanocrystalline materials, as compression test is not susceptible to minor processing defects, in

addition to avoiding the problem of tensile necking instability. Some information can better be obtained from compression test, especially when dealing with a material that exhibits very limited plastic deformation in tension, such as understanding the strain hardening and strain rate behavior, and determining the on set and propagation instabilities (necking or shear localization) [20].

1.6. Ductility Enhancement in nanocrystalline materials

A basic approach towards retaining some of the lost ductility is by sacrificing some of the gained strength. This idea is very simple and straightforward, for example, it is well established that cold working enhances the strength at the expense of ductility, so to retain some of the ductility, one should consider backing off by decreasing the amount of cold working as a trade off. Also, if the strengthening mechanism was to refine the grain structure of the material, it is recommended to decrease the amount of reduction to be applied in order to maintain some of the ductility in the material [23,26].

Another approach that is of great interest nowadays is producing materials with bi-modal or multimodal grain size distribution in order to provide good yield strength along with good ductility. This structure can be achieved through thermomechanical means or simply mixing powders of different grain sizes and then consolidating the mixture into bulk. One major problem facing this technique is that the distribution of different grain sizes is not easily controlled since the outcome depends on several parameters, which affects the repeatability in these samples. Thus the mechanical response of these materials cannot be predicted beforehand [26].

A method that does not depend mainly on tailoring the microstructure of the materials is to use cryogenic temperatures during deformation. This encourages strain hardening and lowers the rate of dynamic recovery [26].

The extremely important and vital key point that must always be considered, no matter which approach is adopted to enhance ductility, is to aim at producing truly flaw free samples as processing flaws can always lead to premature failure [7,23,25,26].

Research has focused on plastic instabilities, which are demonstrated by the low ductility of nanocrystalline aluminum consolidated using ball-milled powders. However, higher ductility can be reached in compact specimens with fewer voids, as the increase in grain boundary area makes nanocrystalline materials subject to crack propagation across grain boundaries [10, 23]. Another trial to enhance the ductility of MM Al that has been deteriorated as a result of milling process; is to blend Al powders with some cryomilled powders. So the strategy would be to mix the hardened powders with an amount of different powders before consolidation [23,27].

Chapter (2)

Objective

The objective of this research is to develop nanocrystalline/ultrafine-grained Aluminum powders following a top down approach via mechanical milling aiming at strengthening Aluminum. Various parameters affect the quality of the produced powders in terms of morphology, which in turn affects the mechanical behavior of the material. Two of these parameters are to be investigated meticulously that are the mechanical milling duration and the amount of process control agent added to the powders while milling.

The effect of mechanical milling on the mechanical behavior of the produced Aluminum is to be studied by processing bulk samples from the mechanically milled powders and evaluating the tensile and compressive behaviors of the material. The effect of annealing on the synthesized samples will be tested as well.

It is expected beforehand that the strengthening of Aluminum using mechanical milling will be at the expense of ductility, so the second objective of this research is to work out a solution to this dilemma by producing bi-modally structured Aluminum in an attempt to retain some of the lost ductility without significantly wasting the achieved strength.

Chapter (3)

Literature Review

3.1. Synthesis of nanocrystalline materials

Reviewing the literature, one can find numerous trials to produce nanocrystalline materials using the techniques mentioned earlier in the introduction section. The most common techniques adopting a top down approach are Equal Channel Angular Pressing (ECAP), Hot Pressure Torsion (HPT), and Mechanical Milling (MM). Some of these attempts from the literature are illustrated hereunder.

D. Jia *et al*. [20] used equal channel angular pressing (ECAP) at 450°C to process ultrafine-grained Ti, followed by cold rolling to reduce cross-section area by 73%. Compression test results show that the flow stress of ultrafine-grained Ti is more than twice that of the coarse-grained Ti. Moreover, ultrafine-grained Ti shows little strain hardening, with nearly perfectly plastic behavior, whereas coarse-grained Ti shows obvious strain hardening, part of which is attributed to deformation twinning.

D. Jia *et al*. [20] stated that compression test helped in rationalizing the observed tensile behaviors. They've also shown that ultrafine-grained Ti has an enhanced strength over the coarse-grained one, in addition to showing 10-12% elongation under tension and around 20% elongation under compression, but they reported their material to be ductile in both tension and compression. However, the capacity of strain hardening is decreased due to the decrease in the dislocation activity, in addition to the decrease in strain rate sensitivity. Summing up all these factors results in enhancement in the tendency for plastic instabilities.

Another research that used ECAP to synthesize a nanocrystalline material was that of R. Z. Valiev *et al*. [28] as they used equal channel angular pressing (ECAP) and high pressure torsion (HPT) to subject a metal work piece to arbitrarily large shear strain under high pressure without altering the dimensions, in order to induce severe plastic deformation to produce a metal exhibiting both high strength and high ductility. The distinction between ECAP and HPT, when considering their application to the industry, is that ECAP can be scaled up to produce large work pieces in the industry whereas HPT can only be used to produce thin samples of a thickness that doesn't exceed 1 mm.

In their work, R. Z. Valiev *et al*. [28] applied ECAP to Cu samples and HPT to Ti samples. To evaluate the strength and ductility of both ECAP and HPT samples, uniaxial tensile tests were used. Tension test was carried out on Cu samples at room temperature, and the results showed that the conventional coarse-grained Cu samples exhibited low yield strength but on the other hand it exhibited high strain hardening and elongation to failure. However, an increased strength was observed when testing Cu samples that were subjected to ECAP and then cold rolled but this increase in strength was at the expense of significantly decreasing the ductility. In contrast to that behavior, when applying ECAP to Cu, its strength increases in addition to an observant increase in ductility that was shown experimentally to be directly proportional to the number of ECAP passes. Titanium samples processed by HPT were also evaluated by tensile testing at 250°C, the same results were observed in this case as well, that severe plastic deformation using HPT yielded high strength in addition to acceptable elongation to failure.

R. Z. Valiev *et al*. [28] then concluded that small amounts of severe plastic deformation strains result in an increase in strength at the expense of losing ductility,

while very large amounts of severe plastic deformation strains dramatically increase strength along with further increase in ductility. This behavior is opposite to the classical behavior of metals when subjected to large plastic deformation by conventional techniques that introduces greater strain hardening.

TEM observations made by R. Z. Valiev *et al.* [28] showed that the large amount of severe plastic deformation introduces high angle grain boundaries, high density of dislocations, creates ultrafine grains and internal elastic strains. They also stated that increasing the strain results in grain size reduction, but only to a minimum size that depends on the SPD processing condition. However, after grain size saturation, further SPD results in increasing the fraction of the high angle grain boundaries and the microstructure becomes homogeneous.

In another research, an attempt to produce nanocrystalline Zirconium Diboride (ZrB_2) using mechanical milling was conducted by Carlos A. Galan *et al*. [29], when they ball milled Zirconium Diboride using a shaker mill under Argon atmosphere at room temperature. They used BPR 2:1 & 4:1, and the milling durations were varied between 3 and 180 minutes. The as-purchased powders and the milled ones were characterized using x-ray diffractometry and the authors reported that increasing milling duration both broadened the peaks and decreased their intensity in the XRD patterns. However, they noted that the crystal structure was not altered and there was no evidence of contamination. Moreover, investigating the effect of changing the BPR on the crystallite size evolution showed that increasing the charge ratio leads to increasing the rate of crystallite size refinement. It was noticeable also that the crystallite size refinement keeps on increasing until it approaches a limiting value at which saturation is achieved.

Moreover, the TEM images demonstrated a decrease in the particle size with increasing the milling duration. In addition, the particles' morphology has been changed from being angular to being round with milling [29].

Based on comparing the XRD results with the TEM images, Carlos A. Galan *et al*. [29] suggested that the ultrafine particles that were observed at the early stages of milling were single crystals and by milling furthermore they become polycrystals with nanometer-sized crystals in the form of agglomerates. In addition, the milled powders didn't exhibit lattice micro-strains, which suggests crystallite size refinement via brittle fracture not severe plastic deformation in oppose to the case of ductile materials.

Xiangyu Zhao *et al*. [30] mechanically milled Ni powders (30 μm average particle size – 99.9 at% pure) using a planetary ball mill. The mechanical milling medium was stainless steel balls and the process was carried out under Argon atmosphere. The ball-to-powder weight ratio was 20:1, and the milling speed was set to 300 RPM for 5, 10, 20, and 40 hrs.

It was noticed that the particle size increased with increasing the mechanical milling duration up to 10 hrs and then opposed its trend to decrease with increasing the mechanical milling duration. Figure (10) shows the evolution of the particle size during the process of mechanical milling of Ni powders. At the early stages of milling (up to 10 hrs), cold welding is dominant, whereas from this point forward, fracturing becomes dominant; this explains the increase and decrease of particle size with mechanical milling [30].

Moreover, XRD patterns display a decrease in the grain size with increasing the mechanical milling duration, where as, the lattice parameter increases with increasing the mechanical milling duration [30].

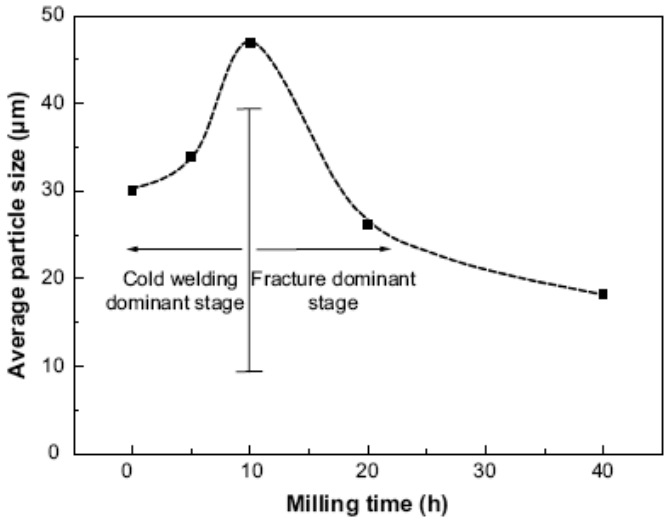

Figure 10: The evolution of particle size during mechanical milling [30].

3.2. Synthesis of nanocrystalline Aluminum by mechanical milling

Since aluminum is a ductile material, its response to the different techniques used to synthesize nanocrystalline materials is expected to be different from other materials. Moreover, the fact that aluminum has a great affinity to forming oxides and carbides impose lots of restrictions on the process adopted to transform the coarse-grained aluminum into ultrafine-grained or even nanocrystalline aluminum following a top down approach.

In addition, researchers cannot give up on synthesizing nanocrystalline aluminum for the evidence of enhanced mechanical behavior that has been shown in several research. For instance, when Khan *et al*. prepared nanocrystalline aluminum powders using active H_2 plasma evaporation and processed the powders by cold compaction and sintering, followed by room temperature rolling into sheets. They have reported an increase in both yield and ultimate tensile strength when comparing to annealed coarse-grained aluminum [4].

3.2.1. Effect of milling duration on mechanically milled Al

H. J. Choi *et al.* [10] produced bulk nanocrystalline Al specimens with different grain sizes down to 48 nm by mechanical milling. Compression and tension tests were carried out in order to evaluate their deformation behavior. The experimental results were then compared with theoretical predictions.

They started with Al powder (≈ 150 μm in diameter and 99.5% in purity) and ball milled the powders in an attritor mill at 550 RPM at room temperature. Samples of ball-milled powders were produced using different milling durations (8, 12, 18, 24, and 48 hrs), in addition to as-received powders used for comparison. The ball-milled powder was containerized in a copper container, then the copper container with the Al powders was heated to 470°C and then rapidly extruded with an extrusion ratio of 15:1 [10].

SEM micrographs of the Al powder ball-milled for 24 hrs showed that the powders were heavily deformed and transformed from the spherical shape initially to be pancake shaped as shown in Figure (11) [10].

Moreover, H. J. Choi *et al.* [10] reported reduction in grain size with increasing the duration of ball milling. The trend of grain size reduction became sluggish on reaching a milling duration of 18 hrs and an apparent steady state was observed for the sample ball-milled for 48 hrs.

For compression and tension tests, the strain rate used was 1×10^{-4} S^{-1} at room temperature. The specimens used in compression test were rectangular with a 2:1 height to width ratio, whereas for tension test, dog-bone type specimens were prepared. Tests were conducted in a direction parallel to that of extrusion and they were stopped at a strain of 0.1 [10].

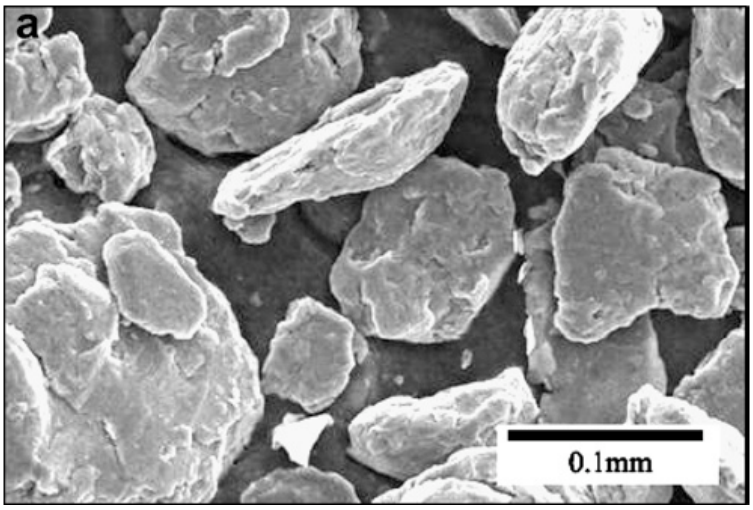

Figure 11: SEM micrograph for Al powders MM for 24 hrs [10].

Results for tension tests showed that the yield strength of the ball-milled specimens increases with increasing the milling duration, or in other words decreasing the grain size. On the other hand, increasing the milling duration leads to a huge decrease in ductility. Moreover, tensile stress-strain curves showed early plastic instability, which led to failure right after yielding. This phenomenon could be attributed to the decrease in the density of lattice dislocation within the grains [10].

They also observed that the fracture surface of nanocrystalline Al specimens after tension test was not very different from that of the microcrystalline Al, although the ductility has significantly decreased in case of nanocrystalline Al. The SEM micrographs in Figure (12) showed that the fracture surface of nanocrystalline Al exhibited elongated dimples that are several times larger than the grain size, which is evidence for ductile failure in nanocrystalline Al [10].

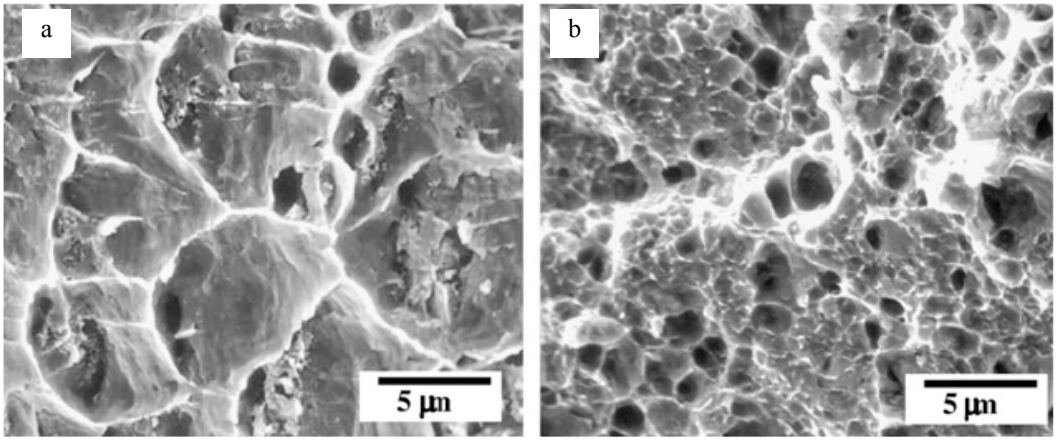

Figure 12: Comparison between the fracture surface of the (a) as-purchased Al and the (b) MM Al using SEM [10].

In addition, they studied the relationship between the yield stress, from both compression and tension tests, and the grain size ($D^{-1/2}$) adopting the Hall-Petch equation to compare the theoretical values with the experimental results.

$$\sigma_y = \sigma_0 + K D^{-1/2}$$

Where K = 0.2 $Kg.mm^{-2/3}$ and σ_0 = 9.8 MPa. Comparing theoretical and experimental results for both the tensile and compressive yield stress, it was noticed that the experimental values approximately followed the Hall-Petch equation until reaching a value for grain size of 70 nm and below, where a positive deviation was observed. This positive deviation is a result of deformation occurring only via activities of dislocations, since activities of twins or grain boundary sliding lead to negative deviation from the Hall-Petch equation [10].

In another attempt to study the effect of mechanical milling on Al powders, Mhadhbi *et al*. [6] started their experiment by annealing Al powders (99.3% pure, 120 – 80 µm) at 500°C for 6 hrs under Argon. The powders were then milled in a vibrator mixer mill for 2, 4, 6, 8, and 10 hrs. Intermittent breaks were allowed every 15 minutes to avoid the formation of intermetallic fractions and heating during milling.

They performed XRD scans for the powders over the range of 20° to 90°. The XRD patterns showed that the line broadening increases with increasing the milling duration. This broadening is related to the change that occurs in microstructure by mechanical milling such as the crystallite size and lattice strain. They found that the lattice parameter increased with increasing milling time and this phenomenon was attributed to grain expansion due to the increase in the density of dislocations with their strain fields. However, the decrease in lattice parameter results from grain compression could be due to the presence of compressive stress fields.

The SEM micrographs showed the unmilled aluminum powders to be ellipsoidal in morphology. However, milling for 4 hrs led to flattening of the particles due to plastic deformation. Whereas further milling up to 10 hrs resulted in welding of very fine powders to the larger particles [6].

In order to study the thermal behavior of the aluminum powders before and after the milling process or in other words to study the effect of milling time on the melting temperature, Mhadhbi *et al*. [6] used Diffraction Scanning Calirometry (DSC). DSC was used over a temperature range 10 - 500°C with a heating rate of 20°C/min. The DSC curves showed that the melting temperature of the powders decreases with increasing milling duration. Furthermore, it was noticed that upon milling for 4 hrs, the endothermic peak was divided into two endothermic peaks. This was attributed to the presence of an oxide layer surrounding the Al particles. One possible scenario is that during milling the oxygen is diffused inside the aluminum particles leading to the formation of an oxide layer surrounding the aluminum grains, so on heating the interior of the grains melt first followed by the melting of the outer layer since the melting temperature of aluminum oxide is higher than that of the aluminum.

Studying the effect of mechanical milling duration on aluminum powders was the subject of another study by Khan *et al*. [4] who mechanically milled pure aluminum powders (325 mesh – 99.5% pure) using a planetary ball mill. The ball to powder weight ratio was set to 20:1 and the milling speed was limited to 100 RPM. Stearic acid was used as a process control agent and 15 minutes breaks were allowed after each 15 minutes of milling to avoid heat rise in the jars. The process was carried out in an inert atmosphere, which is Argon. Several milling durations were tested up to 40 hrs. The milled powders were then cold compacted under a pressure of 2060 MPa for 2 minutes. The compact was then sintered at 600-635°C under a pressure of 900 MPa for 1 hr, followed by no load sintering for 11 hrs. The specimens were then annealed for 1 hr at 600°C.

The authors reported that the grain size decreased with increasing the milling duration up to 10 hrs and then reached a saturation range. Both hardness and compressive strength increased with increasing the milling duration. They reported values of ultimate tensile strength of 110, 200, 250, 450, 550, and 650 MPa for the milling durations 0, 5, 10, 20, 30, and 40 hrs, respectively. However, the ductility was depressed tremendously [4].

In order to investigate the concurrence of the Hall-Petch equation with the mechanical behavior of the mechanically milled Al, E. Bonetti *et al*. [8] milled Aluminum powders (44 μm – 99.9% pure) using an attrition mill with hardened steel balls in a tungsten carbide vial. The ball-to-powder-ratio used was 4:1, and the milling durations were 2, 4, 8, 16, and 32 hrs. The produced powders were then cold consolidated into rectangular bars with high density. Tensile behavior testing showed an increase in the yield strength of nanocrystalline aluminum with increasing the milling duration, however, the values for yield stress were well below those predicted

by the Hall-Petch equation. These results demonstrate the inadequacy of the Hall-Petch equation in the range of nano-scale grain sizes. A broad range of grain size distribution has also been reported, especially for short milling durations.

3.2.2. Effect of milling medium on mechanically milled Al

Caroline B. Reid *et al*. [31] investigated the effect of changing the milling medium on the degree of contamination in the mechanically milled powders. The milling media is mainly the milling vial and the balls. The authors milled alumina using five sets of media that are tabulated in Table (2)

Table 2: Parameters used when investigating different milling media [31].

Test	Vial	Balls	BPR	Time (hrs)
1	Hardened steel	Hardened Fe	10:1	32
2	WC	WC	10:1	32
3	ZrO_2	TZP	10:1	32
4	Al_2O_3	Al_2O_3	10:1	4
5	Al_2O_3	TZP & Al_2O_3	10:1	4

For the combination used in the first run, a considerable amount of 16% Fe contamination was found in the alumina powders. Whereas using WC vial and balls resulted in 35% WC contamination in the alumina powders. However, the most successful experiment was the third one; for in this case a percentage of ZrO_2 contamination of only 3-4% was established. In contrast to all three runs conducted at first, the fourth and fifth tests were totally unsuccessful; since in the fourth test the weight of the balls after milling has decreased by 27%, whereas the powders weight

increased by 438%. An amount of 91% of this increase in powders weight is attributed to mass increase due to breakdown of the balls only after four hours of milling. The remaining 9% are believed to be a result of the degradation of the walls. Test number five has also been considered a failure as the mixture of different balls led to the breaking down of both types, consequently the weight of the balls decreased by 49% [31].

3.2.3. Effect of milling atmosphere on mechanically milled Al

In order to study the influence of the milling atmosphere on the produced powders, T. Cintas *et al*. [32] milled Al powders with a mean particle size of 44 micrometers as starting material. They have conducted the milling process in a vertical attritor for 10 hours using an atmosphere of confined ammonia gas, in addition to another set under vacuum in order to study the effect of the milling atmosphere on the produced material. During the process of milling, they used an amount of process control agent (3 wt%), which is double the amount that they used normally in their laboratories in order to produce powders that are very hard and fine, i.e., with high surface area. The milled powders were then cold compacted under a pressure of 850 MPa using single uniaxial pressing and then vacuum sintered for 1 hr at 650°C followed by furnace cooling.

After milling the powder morphology was found to be equiaxed with a decreased mean particle size. Milling in ammonia atmosphere resulted in a mean particle size of 12.6 μm, whereas milling in vacuum produced powders with a mean particle size of 16.7 μm. It is noticeable that the decrease in mean particle size is significantly higher when milling in ammonia and this is attributed to the presence of

NH_3. Moreover, the grain size was found to be 550 nm and 200 nm for samples milled in vacuum and ammonia gas, respectively [32].

The chemical composition analysis of all samples showed an increase in the percentage of C, N, O, and H due to the reaction of the aluminum powders with the process control agent used. However, the X-ray diffraction patterns didn't show peaks other than those of aluminum, this is probably because of the amounts of these extra elements being below the detectable limit or otherwise they exist in the form of solid solution. Anyhow, the X-ray diffraction of the sintered samples showed the peaks of the compounds that resulted from the reaction of the aluminum with the process control agent and ammonia gas for the samples milled in ammonia atmosphere [32].

The grain refinement is more evident in aluminum powders milled in ammonia because the Nitrogen compounds restricted the grain growth more than the restriction imposed by the carbides and oxides in case of milling in vacuum [32].

Milling in ammonia gas yielded higher relative density, hardness and ultimate tensile strength but lower ductility when compared to as-received aluminum and aluminum that was milled under vacuum. The strengthening that occurred to the milled aluminum was attributed to plastic deformation strengthening, presence of dispersoids or solute atoms and grain refinement [32].

3.2.4. Effect of PCA on mechanically milled Al

It has been already mentioned before that when mechanical milling ductile materials, it is crucial to use an adequate amount of process control agent to avoid excessive cold welding of the particles and promote fracture by collision. For example, a research conducted by Lu and Lai reported that increasing the amount of PCA (stearic acid in their case) from 1wt% to 3wt% while milling aluminum for 5

hrs, reduced the particle size from 500 μm to 10 μm [13]. Although the process control agent is required to act as a surfactant to the particles ensuring clean metal-to-metal contact, there is a drawback to that. The severe thermo-mechanical conditions during milling can lead to the decomposition of the process control agent and its reaction with the milled material to form carbides and oxides since the process control agent is usually an organic material. In some cases, this can be utilized to strengthen materials by dispersion, but on the other hand it can be considered as contamination for other materials where high purity is needed [33].

S. Kleiner *et al*. [33] mixed Al (99.7% pure – 63 μm) with TiO_2 (21 μm) using a planetary ball mill to produce Al - 20wt% TiO_2. The milling speed was set to 250 RPM and intermittent breaks were allowed every 15 minutes. The ball-to-powder weight ratio was 15:1, where hardened steel balls of 20 mm diameter were used. During the process of milling, amounts of 2.5 and 5wt% of stearic acid were added as a PCA. The milling process was conducted under inert atmosphere using Argon gas. The milling times were varied between 1 and 12 hrs when adding 2.5wt% stearic acid and varied between 6 and 48 hrs for the samples with 5wt% stearic acid.

DSC traces of the samples milled with 2.5 and 5wt% PCA are shown in Figures (13 and 14), respectively. These traces show a major endothermic peak at around 665°C, representing melting of Al, for all samples followed by an exothermic reaction. However, a second endothermic peak can be seen in Figure (13) at 875°C, which increases with milling. For the samples with 5wt% PCA, an exothermic peak occurs at 850-900°C, that is converted into an endothermic peak with further milling as shown in Figure (14). Moreover, the XRD patterns showed evidence of formation of oxides and carbides and the TEM images supported the same results [33].

To summarize their work, S. Kleiner *et al*. [33] concluded that the increase of the amount of PCA results in better cooling down during milling, which in return decreases the rate of decomposition of the PCA for short milling times. However, for prolonged milling durations, complete decomposition of the PCA takes place leading to contamination of the powders.

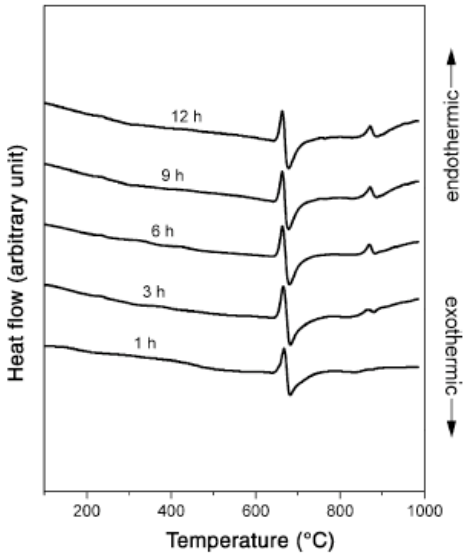

Figure 13: DSC traces for samples milled with 2.5 wt% PCA up to 12 hrs [33].

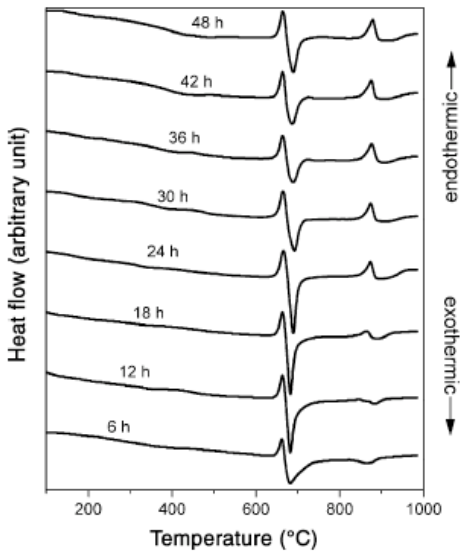

Figure 14: DSC traces for sampled milled with 5 wt% PCA up to 48 hrs [33].

Another research supporting the hypothesis of the decomposition of the PCA during milling was conducted by Kubota *et al*. [11] when they milled aluminum powders (99.9% pure – 100 μm average diameter) using stainless steel balls (7 mm diameter). The milling process was conducted in Argon atmosphere using ball-to-powder weight ratio 7:1, adding stearic acid as a PCA, for 4-8 hrs. They then used Scherrer's equation to determine the crystallite size of the mechanically milled powders using XRD and found it to reach a value of 38 nm. They have reported that they have achieved a fine grain structure after milling for 8 hrs and they have attributed this to the grain boundary pinning as a result of the oxides formed by the reaction between the aluminum powders and the PCA. The decomposition of the PCA, thus, had a favorable effect.

A constant amount of PCA for all milling durations was used by most researchers although some (for example Khan *et al.* [7]) varied the amount according to the milling duration, which according to the experiments mentioned before should follow a directly proportional relationship. Khan *et al*. [7] used Aluminum powders 99.5%, 325 mesh, Alfa Aesar as starting powders. The powders were first degassed and dried under vacuum for 7 hours at 520 °K. Powder handling was always under inert atmosphere in a stainless steel glove box with Argon gas. The powders were then mechanically milled using a planetary ball mill. During the process of milling, it was noticed that the powders flattened, cold welded, fractured and re-welded resulting in a reduced grain size, that's why the process of mechanical milling is considered a severe plastic deformation process. The mechanical milling parameters used were a ball-to-powder weight ratio of 16:1, a small amount of Stearic acid was used as a process control agent to reduce excessive welding, the mechanical milling speed was limited to 120 RPM at room temperature. Intermittent breaks of 15 minutes were

allowed every 15 minutes of milling to avoid heat accumulation in the jars. *The milling durations were 5, 10, and 20 hrs with corresponding amounts of PCA of 0.5, 1, and 1.2 wt%, respectively.*

3.3. Producing bulk samples from nanocrystalline powders by PM

J. J. Fuentes *et al.* [27] attrition milled atomized Al powders (99.7% pure – 44 μm) for 10 hrs. They used ethylene-bis-stearamide EBS powder as a PCA during the process of milling. The milled powders were cold compacted and then sintered. During sintering, 0.6 wt% of Silicon powder (22.4 μm) was used as sintering aid by mixing in a turbula mixer with the milled Al powders before compaction. Cylindrical and dog-bone tension test specimens were produced directly from consolidation without machining.

The optical microscope images of the synthesized samples after compaction and then following sintering have shown that compaction has not resulted in the particles losing their individuality as the metal boundaries are seen clearly. However, sintering the samples led to the loss of entity of each particle. These results demonstrate that cold welding of the particles doesn't occur during compaction and this is generally related to the high micro-hardness of the milled Al powders. The values of ultimate tensile strength of the bulk samples have been 225 and 195 MPa for the samples compacted under a pressure of 1120 and 850 MPa, accordingly. In addition, the values for percent elongation were found to be 2.4% and 1.6%. Investigation of the fracture surfaces using optical microscopy and scanning electron microscopy showed that the type of fracture was brittle. Images from the optical microscope, normal to the fracture profile demonstrated fracture by decohesion of particles. This detachment of particles suggests weak bonding [27].

3.4. Effect of Mechanical Milling on Ductility of nanocrystalline materials

The results of all the trials mentioned before to synthesize nanocrystalline materials have shown that they all suffered from a lack of ductility no matter which technique was used. Many nanocrystalline metals reach their fracture stress in, or slightly beyond the elastic region, upon deformation. Processing flaws and artifacts can all promote brittle behavior, such as residual porosity, insufficient inter-particle bonding, impurities, and large internal stresses. In order to justify this hypothesis, E. Ma [23] tested micro-samples of Cu as well as larger samples for tensile behavior. The micro-samples showed larger yield strength and better ductility, presumably due to lower chances of having large flaws. However, the tensile yield strength for such micro-samples was way lower than that measured under compression for nanocrystalline Cu processed the same way to a similar density. This leaves room for the possibility of existence of residual processing flaws that had a role in decreasing the elongation percent. Consequently, another processing technique was used that resulted in the absence of internal porosity. It was found that the yield strength value has been elevated to one that is close to the best seen in compression tests. However, the ductility was not enhanced, with fracture occurring very soon after yielding. This trial showed that there are other factors affecting the ductility and fracture strength of nanocrystalline metals other than porosity such as propensity for cracking instability and brittle failure, and necking instability.

3.5. Techniques to enhance ductility of nanocrystalline materials

It is well established that decreasing the grain size, decreases the strain hardening capacity of the material. However, annealing of the cold worked material leads to lowering the yield strength of the material, but slightly enhancing the strain

hardening capacity. This enhancement is attributed to the recovery of the cold worked grains, but it is very limited because of the small grain size that decreases the capacity for dislocations accumulation and twin boundaries [20].

D. Jia *et al*. [20] studied the effect of annealing on the Ti samples strengthened by EACP, their strengthening procedure was described earlier in section (3.1). Some of the specimens were annealed in argon for 30 minutes at 300°C. They also annealed coarse-grained Ti at 705°C for 2 hrs, followed by air-cooling. As shown in Figure (15), annealing has somewhat enhanced the ductility and the capacity of strain hardening in the material, but still the ductility of the strengthened material is no where close to that of the coarse-grained Ti. However, it should be noted that the loss of strength upon annealing was not at all dramatic.

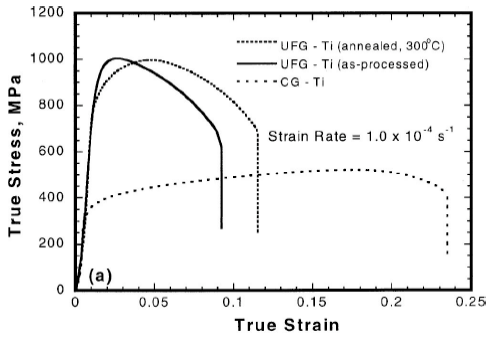

Figure 15: True Stress-strain Curve under tension [20].

Wang *et al.* [34] reported that sintering the FCC samples such as Al and Cu that are strengthened through severe plastic deformation during synthesizing bulk samples has led to the creation of in situ formed composite-like microstructure, such as bimodal grain size distribution. A bimodal grain size distribution is when significant numbers of grains in the material have sizes that are larger or smaller than the rest of the grains. In this case, the material is composed of variable grain sizes. This resulted in an enhanced ductility while maintaining the high strength. Adopting

this approach B. Srinivasarao *et al.* [35] mechanically milled Iron (99+% pure) in a planetary ball mill for 100 hrs allowing intermittent breaks of 2 hrs every 20 hrs, at a speed of 250 RPM. The ball to powder weight ratio used was 10:1 and a controlled atmosphere glove box was used for handling the powders. Spark plasma sintering (SPS) was used to produce bulk samples from the synthesized powders. In order to produce a bimodal grain structure, once the sintering process was completed; the pressure was maintained constant at several temperatures. They reported that increasing the temperature has led to enhancing ductility of the material without drastically losing the strength.

The sinterability of the mechanically milled powders is different from that of the conventional unmilled powders [36]. This is owing to the fact that the mechanically milled powders have irregular shapes and are harder for being heavily cold worked. Based on that, T. Makhlouf *et al*. [36] investigated the effect of annealing on bulk samples of Al alloys synthesized by high-energy ball milling. They reported a decrease in the volume fraction of pores existent in the consolidated samples by increasing the annealing temperature up to 500°C based on microstructural observations. Moreover, XRD patterns of these samples demonstrated an increase in the crystallite size with increasing the annealing temperature.

A trial to retain some of the ductility lost during cold working by annealing was conducted also by Wang *et al* [22]. In doing so, they rolled Cu at liquid nitrogen temperature to reach a high amount of cold work. The cold worked Cu at liquid nitrogen was found to be heavily deformed, with high densities of dislocations in nano-scale networks. The low temperature used was a key factor in limiting the dynamic recovery; this allows the density of accumulated dislocations to be at a higher steady state than that achieved at room temperature. After that, they annealed

the cold worked Cu samples. They noticed that as they increased the annealing temperature, the ductility increased significantly. This phenomenon was further supported by the TEM investigation, which showed recrystallized grains with well-defined high-angle grain boundaries, and the majority of grains were in the nano-scale to ultrafine size. However, they noticed that secondary recrystallization occurred at elevated annealing temperatures. This was demonstrated by the abnormal grain growth that started to produce a volume fraction of coarser grains. The authors attributed the enhancement in ductility without significantly deteriorating the strength to the nanocrystalline/ultrafine grains, as these grains decrease the size of nucleating flaws while increasing the resistance to crack propagation, this leads to a higher fracture stress. They related the significant enhancement in ductility of the samples to the production of bimodal structure during secondary recrystallization. In other words, during processing at liquid nitrogen temperature, large densities of defects and cold working energy were stored in the material, this encouraged nucleation during recrystallization at low temperature. Consequently, the majority of the grains remained in nanocrystalline/ultrafine scale, and only 25% of the grains were coarsened during secondary recrystallization. These coarsened grains were responsible for pronouncing strain hardening to withstand the useful uniform deformation to large strains. Thermomechanical approach adopted by Wang *et al*. [22] thus was able to achieve high strength and ductility in a nanostructured metal. The key factor was to cold work the metal at liquid nitrogen temperature, and then anneal the cold worked samples to produce a bimodal structure that consists of nanocrystalline/ultrafine grains.

A different approach to work out a compromise for the dilemma of strength and ductility in nanocrystalline materials is to develop bimodal structures composed

of micrometer-sized grains embedded within nanometer sized grains. The enhanced ductility is stated to be a result of the larger grains that help stabilize the tensile deformation in the bimodal structured materials in coherency with the nanocrystalline grains that provide strength. This scenario suggests the introduction of new deformation mechanisms including twinning mode [5].

In addition to the attempts to produce bi-modal structured materials in order to enhance the ductility, tri-modally structured materials have been recently of interest to lots of researchers to satisfy the same goal. For example, Ye *et al*. [9] reported some trials to enhance the ductility of nanocrystalline (NC) aluminum by introducing coarse-grained (CG) aluminum to nanocrystalline aluminum reinforced with B_4C particles. This way, they would expect a high strength from the ceramic reinforcement and nanocrystalline aluminum, in addition to appreciable ductility from the coarse-grained aluminum. They used cryomilling to produce 20 wt% B_4C – 80 wt% nanocrystalline 5083 aluminum. They then used a V-blender to mix equal amounts of cryomilled powder and coarse-grained 5083 aluminum. The blended powder was degassed, then consolidated using cold isostatic pressing, followed by hot extrusion at 798°K. The material was then tested for mechanical properties using compression test. Some of the tested samples were as extruded, while the others were annealed at 723°K for 2 hrs and furnace cooled. The optical microscope investigations showed that the coarse-grained Al particles, nanocrystalline aluminum particles and the B_4C particles were uniformly distributed.

Compression test was applied in both longitudinal and transverse directions (with respect to the extrusion direction) and the material showed evidence of anisotropy. The results showed high yield strength in both annealed and un-annealed specimens. The high yield strength of the tri-modal composite was attributed to

different micro-structural features, such as B_4C particles strengthening, reduced grain size of nanocrystalline aluminum, Orwan strengthening from the oxides, nitrides and carbides, and grain size of the coarse-grained aluminum [9].

The effect of each strengthening factor can be demonstrated mathematically as follows: [9]

- *Strengthening by grain size reduction (Using Hall Petch equation):*

$$\sigma_y = \sigma_0 + K\, D^{-1/2} \qquad \{1\}$$

The constants for Al 5083 were σ_0 = 124 MPa, and K = 0.22 MPa √m. The authors selected a grain size for NC Al (D = 165 nm) and for CG Al (D = 800 nm). By direct substitution, for **NC Al** the predicted yield strength was found to be **665 MPa** and for **CG Al** the predicted yield strength was found to be **370 MPa**.

- *Orwan strengthening:*

$$\sigma_{Or} = M \frac{0.4Gb}{\pi(1-\nu)^{1/2}} \frac{\ln(\bar{d}/b)}{\bar{\lambda}} \qquad \{2\}$$

Where *M* is the orientation factor, which is (3.06) for FCC Al, *G* is the shear modulus (25.9 GPa), *b* is burger's vector (0.286 nm), υ is Poisson's ratio (0.33), đ = (√2/3) d (where *d* is the diameter of dispersoids (10 nm)), λ = đ ((√π/4f)-1) where *f* is volume fraction of dispersoids (0.005). By direct substitution, **σ_{or} = 126 MPa.**

Then considering strengthening by both grain size reduction and Orwan strengthening, for **NC Al** (**σ_{NC} = 665+126 = 791 MPa**)

- *Particulate strengthening (using rule of mixtures)*:

$$\sigma = \sigma_m (1-f) + \sigma_f f \quad \{3\}$$

1. Applying rule of mixtures to the bi-modal composite NC Al with B_4C:

Since NC Al is the matrix σ_m = 791 MPa, and B_4C is the reinforcement with a volume fraction *f* of 0.2 and σ_f = 2900 MPa, then for the NC Al – B_4C bi-modal composite, σ = 1213 MPa.

2. Applying rule of mixtures to the tri-modal composite NC Al – B_4C with CG Al:

Since (NC Al-B_4C) is the reinforcement σ_f = 1213 MPa with a volume fraction of 0.5, and CG Al is the matrix σ_m = 370 MPa, then for NC Al – B_4C – CG Al tri-modal composite, σ = 792 MPa.

The theoretical value of strength for the tri-modal composite was found to be far less than the experimental value (1065 MPa), which means that the rule of mixture is invalid in the case of tri-modal composites. This phenomenon was also reported by other researches investigating bi-modal composite-like microstructures [9].

Annealing of the tri-modal composite at 723°K followed by furnace cooling, enhanced the strain to failure from 0.8% to 2.5%. Although annealing leads to grain growth and hence decreases the strength, this didn't occur when annealing a tri-modal composite because of the thermal stability of cryomilled materials [9].

Since both nanocrystalline Al and coarse-grained Al have the same chemical composition, a strong interface is easily developed during consolidation; consequently the load is successfully transferred from the coarse-grained Al to the nanocrystalline Al. That is the justification for why micro-yielding didn't occur, as only a small

fraction of the load is carried by the coarse-grained Al. Moreover, even the load transferred from the CG Al to the NC Al is further transferred to the B_4C particles, because of the clean metallurgical interface developed during cryomilling. This scheme of load transfer behaves like a relay race, and it results in a material with extremely high yield strength [9].

Y. Li *et al.* [37] carried out further investigations on the research conducted by Ye *et al.* [9] by studying the dislocation structure in the produced tri-modal composite using TEM. The TEM images are shown in Figure (16) where Figure (16(a)) shows an area of the CG Al region containing dislocations with various geometries. For example, dislocation networks can be observed clearly in Figure (16(b)) as pointed by the arrow. Tangling of multiple dislocations inside a grain is highlighted by an arrow in Figure (16(c)). In addition, subgrain boundaries are formed due to polygonization of dislocations and an example of that is shown in Figure (16(d)). The dislocation wall in Figure (16(e)) is a result of the re-arrangement of dislocations forming a subgrain boundary. Figure (16(f)) shows several straight and semi-circle dislocations that can be found all over the material.

A clear demonstration the different types of grain boundaries that can exist in a material and how they appear in a TEM image is in Figure (17). Chang *et al.* [38] reported the TEM image in Figure (17) in their research after subjecting commercially pure Al to ECAP. This figure shows the polygonized dislocation wall PDW, the partially transformed grain boundary PTB, and the grain boundaries GB. The author reported the dissociation of the lattice dislocation during deformation is what causes the transformation from PDW to PTB to GB. They attributed the strengthening of their material to the occurrence of this transformation.

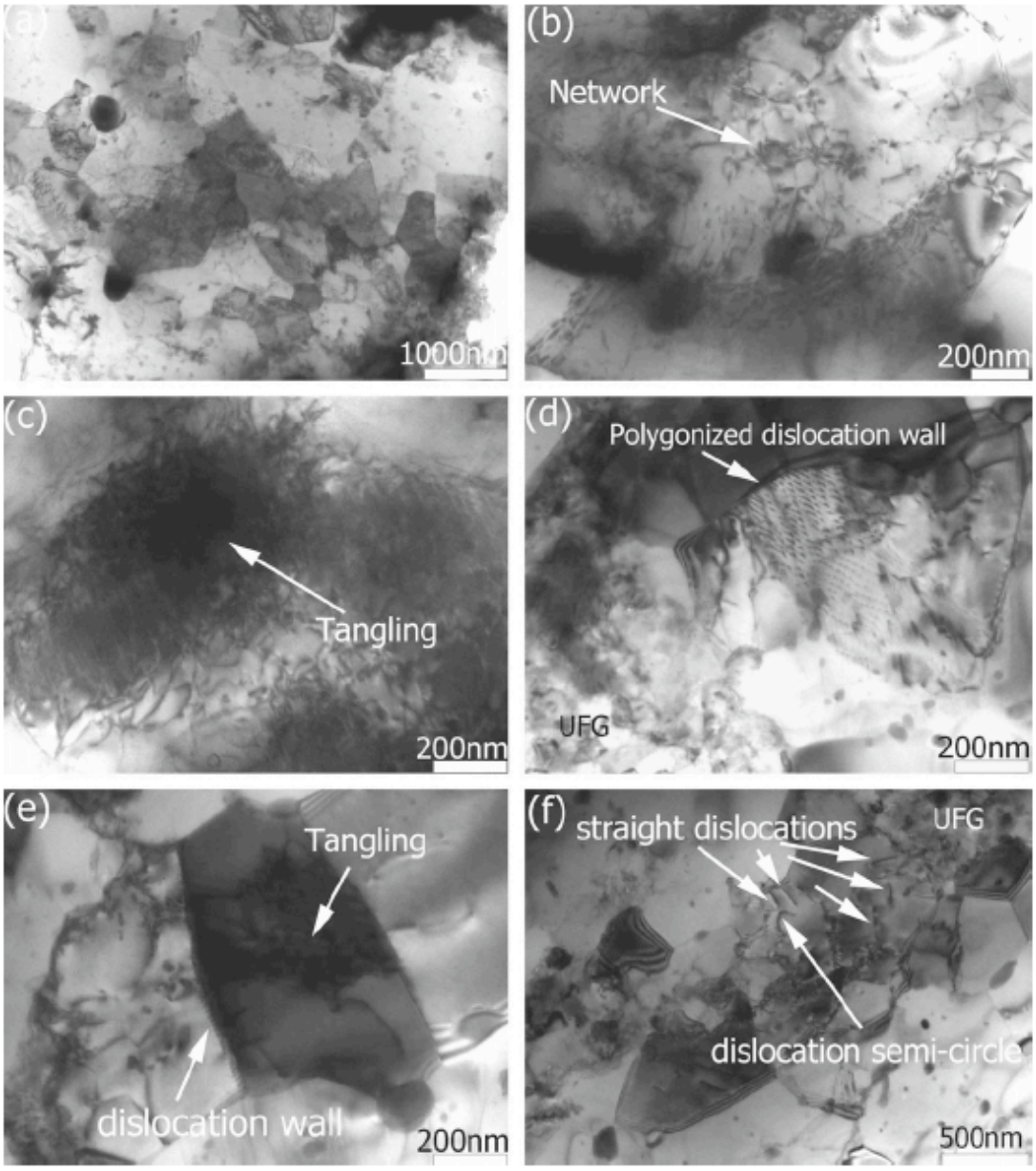

Figure 16: TEM images for the tri-modal aluminum-based composite by Y. Li *et al.* [37].

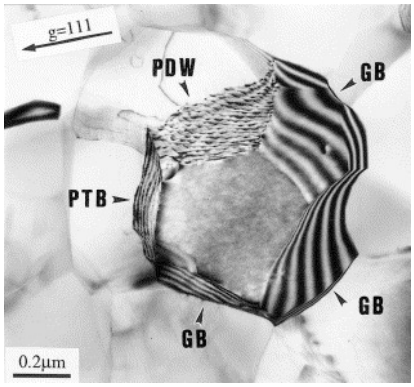

Figure 17: Different types of grain boundaries in a commercially pure Al subjected to ECAP [38].

In a nutshell, the work done on pure Aluminum for strengthening using mechanical milling is very limited. Moreover, the results reported are not yet satisfactory. For instance, the highest tensile strength achieved was around 500 MPa after milling for 48 hrs at 550 RPM using a BPR of 15:1. Although this value of strength is high, the energy consumed to reach it is very extensive and the milling duration needs to be reduced for the process to be commercially feasible. In addition, the problem that faced almost all the researchers was the limited ductility of the nanostructured Aluminum processed by mechanical milling. The reported ductility of the nanostructured materials was rarely higher than 5%. However, shifting to ultrafine-grained materials to be an alternative for the nanostructured ones yielded an enhancement in the ductility to a maximum of 10%, but on the other hand the strength was not as high as that of the nanostructured materials. Further research efforts in this regard are desired.

Chapter (4)

Materials and Experimental procedures

4.1. Synthesis of Mechanically Milled Aluminum (MM Al) specimens

4.1.1. Materials

Pure aluminum powder (99.7% pure - 75 μm) was used in this study; a scanning electron micrograph of the as-received aluminum powders is shown in Figure (18). The aluminum powders were mechanically milled in 250 μL stainless steel jars with 10 mm diameter stainless steel balls (see Figure 19). The process of mechanical milling was carried out using a Retsch PM 400 planetary high-energy ball mill (see Figure 20). The Ball-to-Powder (BPR) weight ratio used was set to 10:1, as it is the most commonly used. Each jar was filled with 30 gm of Aluminum powder in addition to 300 gm of stainless steel balls.

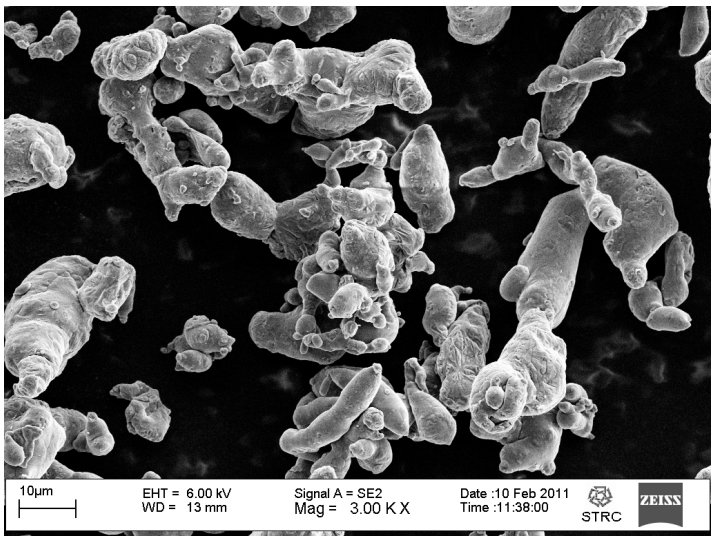

Figure 18: SEM image for as-received Al powders.

Figure 19: Steel Jar and Stainless steel balls used in MM.

Figure 20: Retsch PM400 planetary high-energy ball mill.

4.1.2. The process control agent

Methanol (CH_4OH) was used as a process control agent in order to reduce heat accumulation inside the jars and minimize cold welding of the aluminum particles as a result of high-energy collisions during the process of mechanical milling. The amount of PCA used was found to be a crucial parameter as it controls the size and morphology of the powders produced by mechanical milling and hence it affects the

mechanical behavior of the material. Several trials were carried out using different amounts of PCA in pursuit of reaching the best possible mechanical behavior. As noted before in section (1.3.1.1.8), the amount of PCA follows a directly proportional relationship with the milling duration. It was decided to run the trials on powders milled for 6 hrs. Three amounts of PCA (300, 600 and 1200 µL) were added to the aluminum powders, which were mechanically milled for 6 hrs at 200 RPM. After studying these trials, the amount of PCA decided upon was 1200 µL per 6 hrs of mechanical milling, i.e. 100 µL per 30 minutes of milling. In other words, the amount of PCA added for 30 minutes of mechanical milling is equivalent to 0.26 wt%. This amount was enough to allow the PCA to act as a surfactant for the particles alleviating particle refinement without re-welding of the particles. Although a higher amount could have given better results, the trials were stopped at a certain amount for safety reasons because experiments showed that an excess in the amount of methanol can cause the powder to catch fire upon being subjected to air.

4.1.3. Mechanical Milling Atmosphere

All the powder preparations were carried out in a controlled atmosphere glove box (see Figure 21) with an Argon atmosphere. Moreover, the process of emptying the jars - after mechanical milling - was carried out inside the controlled atmosphere glove box in order to minimize the reaction of the mechanically milled aluminum powders with air forming oxides. Handling the powders inside the controlled atmosphere glove box both reduces the chances of contaminations and helps protect the researcher's safety and health.

Figure 21: Controlled Atmosphere Glove Box.

4.1.4. Mechanical Milling Speed and Durations

The mechanical milling speed used was 200 RPM. In order to study the effect of mechanical milling duration on the mechanical behavior of pure aluminum five sets of mechanically milled aluminum powders were produced varying the mechanical milling durations. These durations were 0.5, 1, 3, 6, and 12 hours. During the process of mechanical milling, intermittent breaks of 15 minutes were allowed every 30 minutes of milling to allow the jars to cool down. The rise in the jar temperature would have promoted particles welding to each other instead of colliding and fracturing as desired. Six samples were produced at each of the abovementioned milling durations, in addition to six samples of as-received pure aluminum for the sake of comparison.

4.1.5. Loose powder X-ray Diffraction

The mechanically milled aluminum powders were investigated by X-ray diffraction (XRD) using Cu Kα in a Scintag XDS 2000 powder diffractometer, operated at 40 kV and 30 mA. Phase analysis as well as the effect of mechanical milling duration on the different structure parameters such as interplanar spacing, lattice parameter, and crystallite size were studied.

4.1.6. Powder Consolidation

The mechanically milled aluminum powders were cold compacted under a pressure of 475 MPa for 30 minutes in a specially manufactured die made of heat-treated W302 Steel giving a cylindrical compact with a diameter of 32 mm and a height of 14 mm. The compaction pressure has been selected after several iterations based on the graph shown in Figure (22) [39].

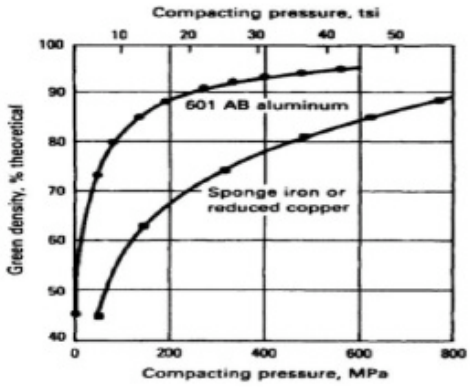

Figure 22: Graph for powder compaction calculation [39].

The green compact along with the die were then placed inside a heating jacket and sintered for 30 minutes at 500°C. The specimen was then directly hot extruded at the same temperature, using an extrusion die ratio of 10:1, to produce 10 mm diameter extrudates. This procedure was successful with all the samples except for the Al powders milled for 12 hrs. The powders milled for 12 hrs wouldn't extrude after sintering for 30 minutes at 500°C. This was probably due to the high amount of strain induced in the particles, which are highly cold-worked. Consequently, the samples were sintered for 3 hrs at 500°C prior to extrusion. The sequence of the powder consolidation process is shown in Figure (23).

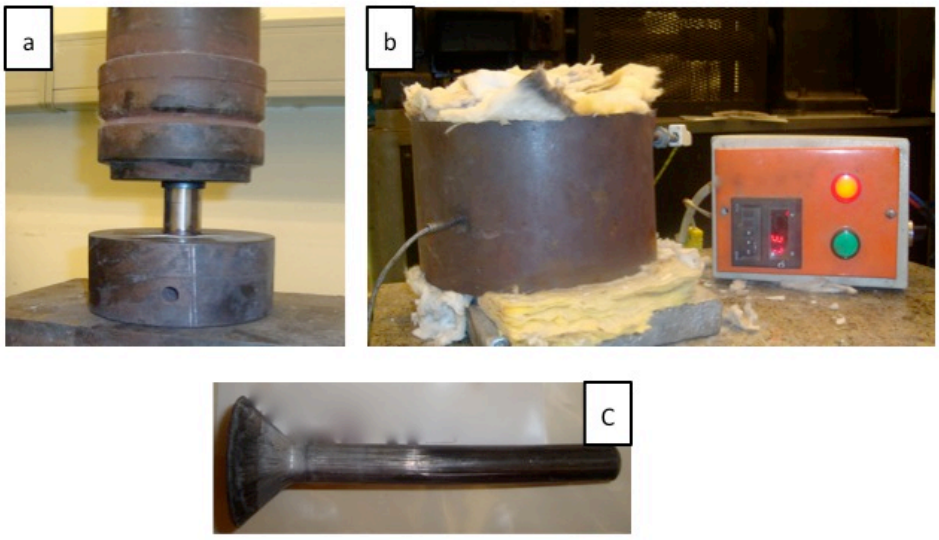

Figure 23: Sequence of the powder consolidation process, (a) Cold compaction, (b) Sintering, and (c) Extrudate.

4.1.7. Tension and compression tests' specimens

The as-extruded samples were machined to produce tension test specimens according to ASTM standard E8. The dimensions of the specimens were [40]:

- Gauge length = 20 mm
- Gauge diameter = 4 mm
- Shoulder length = 10 mm
- Shoulder diameter = 8 mm

Cylindrical compression test specimens were also produced according to the ASTM standard E9 [41], having a length and diameter of 12 and 6 mm, respectively, to yield a length to diameter ratio (L/D) of 2. Both tension and compression test specimens are shown in Figures (24) & (25).

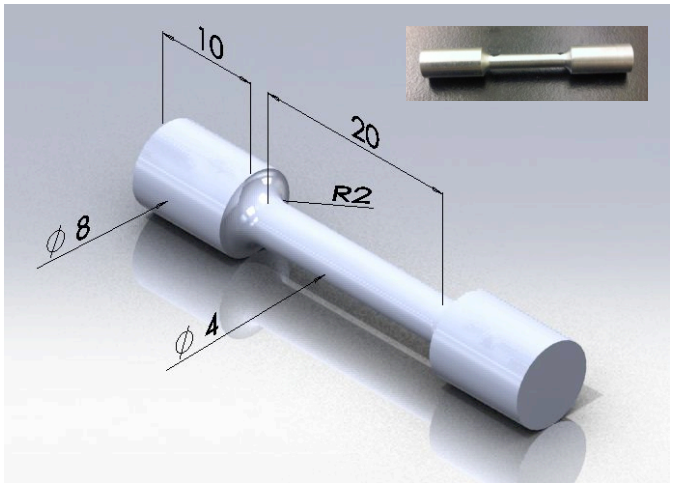

Figure 24: Tension test Specimen.

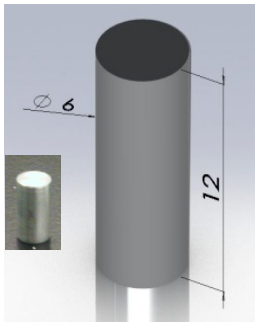

Figure 25: Compression test specimen.

4.1.8. Annealing of machined samples

The effect of annealing on the mechanical behavior of the bulk aluminum specimens that were synthesized from aluminum powders strengthened by mechanical milling was also studied in order to determine whether annealing would help retain some of the ductility that was lost due to the severe plastic deformation to which the aluminum powders were subjected during the process of mechanical milling. Preliminary experiments were carried out to determine the annealing duration that should be used. In these experiments, consolidated powders, which were already

mechanically milled for 6 hrs at 200 RPM, were annealed for different durations (0.5, 1, 2, and 3 hrs) at 500°C in a Thermolyne 6000 furnace. Rockwell (F) hardness test was used to evaluate the hardness of the samples. A Rockwell (F) hardness test, Mitutoyo ATK-600 hardness testing machine with 1/16" diameter ball was used for indentation, with a load of 60 N. The average of ten indentations was determined. Based on this study, three specimens from those produced at each mechanical milling condition were annealed for 3 hrs at 500°C and furnace cooled.

4.1.9. Tension and compression tests

An Instron Screw Drive Universal Testing Machine, with a capacity of 50 KN, was used to test the mechanical behavior - both tensile and compressive - of the produced specimens. Figures (26) and (27) show the specimens mounted on the universal testing machine in tension and compression tests, respectively. The testing parameters for each test were as follows:

- Tension test:
  - Testing speed = 0.5 mm/min
  - Strain rate = 4×10^{-4} /s
  - Testing criteria: Test stopped when load drops by 90%

- Compression test:
  - Testing speed = 0.48 mm/min
  - Strain rate = 6×10^{-4} /s
  - Testing criteria: Test stopped when load drops by 70% or machine maximum travel distance exceeded

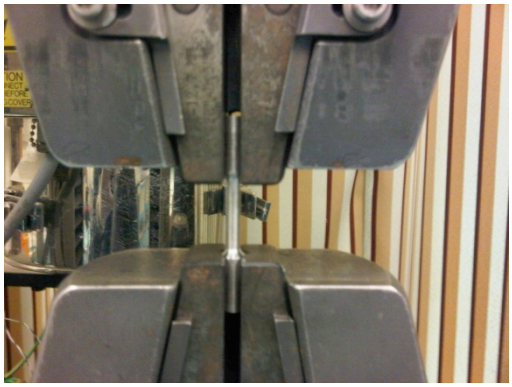

Figure 26: Tension test specimen mounted on the Universal Testing Machine.

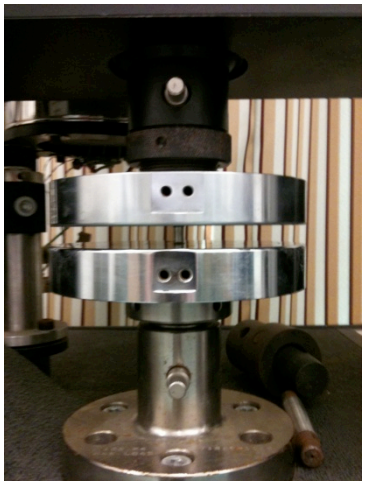

Figure 27: Compression test specimen mounted on the Universal Testing Machine.

Due to the absence of an extensometer in the laboratory that can measure the gauge length extension accurately, gauge marks were carefully placed on the samples and then the failed specimen after tension test was assembled and the final gauge length was recorded by measuring it manually.

4.1.10. Bulk Density Measurement

Cylindrical specimens similar to those of the compression test were produced having length and diameter of 12 and 6 mm, respectively. Bulk density measurement was conducted using a Mettler Toledo densitometer; with Xylene as an auxiliary fluid

whose density is 0.86 g/cm^3. The density determination using this instrument is performed by means of Archimedes' principle, or in other words, the buoyancy method, which states that a body immersed in a fluid apparently loses weight by an amount equal to the weight of the fluid it displaces [42].

4.1.11. Scanning Electron Microscopy

The powders were investigated using a LEO "Supra 55" Field Emission Scanning Electron Microscope (FESEM) to study the effect of mechanical milling on the morphology of aluminum powders. Moreover, the fractography of the mechanically milled aluminum samples, after tension test, was also studied so as to understand the mode of failure and the degree of ductility in these samples.

4.1.12. Transmission Electron Microscopy

Transmission Electron Microscopy TEM analysis was conducted at BegbrokeNano, Oxford Materials Characterization laboratory, UK. The bulk samples were cut into small discs and then prepared on an ULTRATOME microtome at room temperature using DUKKER-ELEMENTSIX diamond knife. A JOEL 2010 analytical TEM was used for the experiments, which has a LaB_6 electron gun and can be operated between 80 and 200 kV. The resolution of this instrument is 0.19 nm, its electron probe size is down to 0.5 nm and the maximum specimen tilt is of ±10° along both axes.

4.1.13. XRD Bulk

A Philips X'PERT multi-purpose X-ray diffractometer with a wavelength of 0.709 nm was used for x-ray diffraction analysis for the bulk samples. Only three bulk

samples were characterized using XRD (as received, MM 6 hrs, and MM 12 hrs samples). All these samples were annealed for three hours at 500°C. The aim of this test was to determine whether secondary phases due to the decomposition of the PCA have formed during the process of sintering or annealing that have contributed to strengthening the material in addition to the strain hardening that resulted from mechanical milling.

4.2. Synthesis of bi-modal Aluminum (BM AL) samples

4.2.1. Powder preparation

To produce bi-modally structured Aluminum samples, equal weights of 12 hrs mechanically milled aluminum powders and as-received aluminum powders were mixed together using solid state mixing techniques. Two techniques were adopted and compared.

The first technique was to mix the powders using a turbula mixer - Figure (28) - at 96 RPM for 30 minutes. In this case no additives were needed. But it was ensured that the process was conducted under an Argon atmosphere.

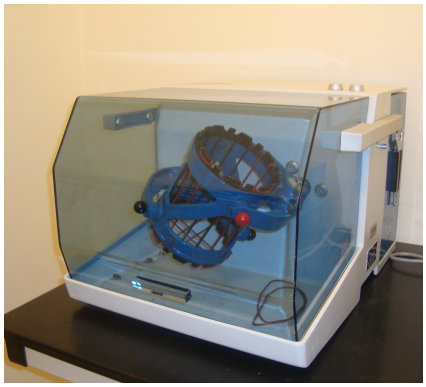

Figure 28: Turbula Mixer.

The second technique was to mix the powders using a high-energy ball mill for 1 hour at 200 RPM using a BPR 5:1. An amount of 200 µL of Methanol was added as a PCA. This technique is considered a hybrid process of mixing and mechanical milling. The whole process was also conducted under an Argon atmosphere.

4.2.2. Bulk samples preparation

The process used to prepare bulk samples of bi-modal Aluminum is similar to that used for the MM Al. The powders were cold compacted under a pressure of 475 MPa for 30 minutes to produce a green compact using a custom made die made of heat-treated W302 steel. The die and the compact were placed in the heating jacket to be sintered for 3 hours at 500°C and then directly hot extruded. After cooling, the extrudates were machined to produce tension and compression tests' specimens; the details of these specimens can be found in section (4.1.7).

4.2.3. Testing and Characterization

The produced samples were tested and characterized using Density measurement, Tension and Compression tests, Scanning Electron Microscopy, and Transmission Electron Microscopy. The specifics of each characterization and testing method can be found in section (4.1).

4.3. Summary of Experimental procedure MM Al

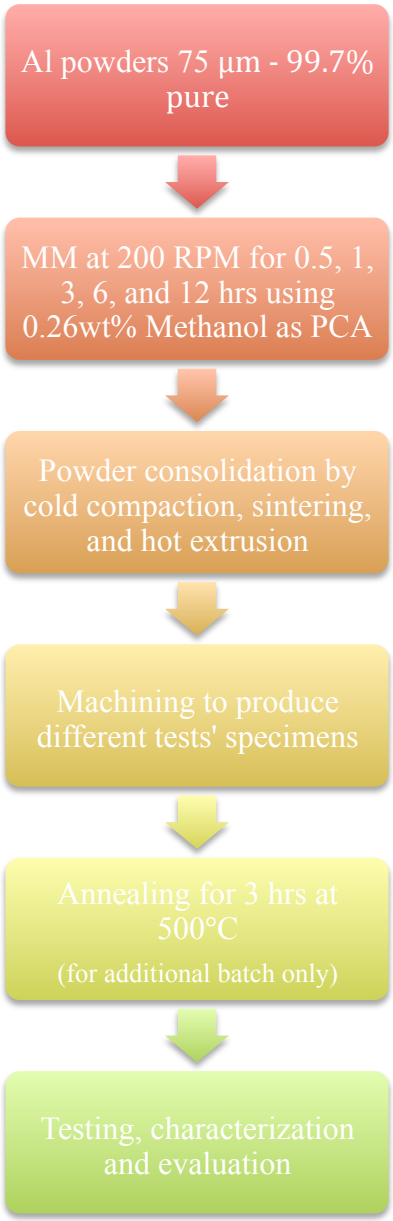

Figure 29: Process chart summarizing the experimental procedure for MM Al.

4.4. Summary of Experimental procedure BM Al

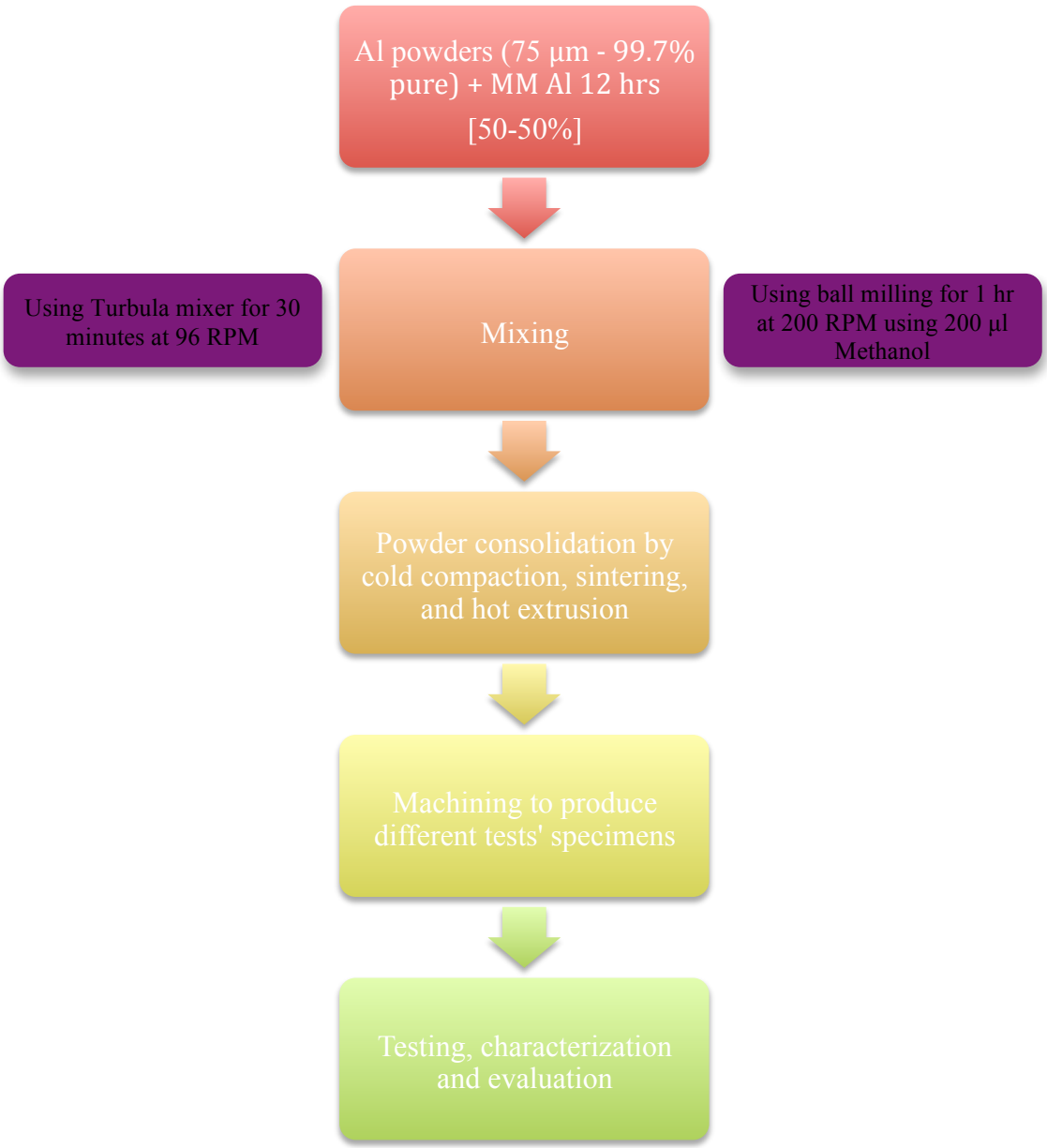

Figure 30: Process Chart summarizing the experimental procedure for BM Al.

Chapter (5)

Results and Discussion

5.1. Mechanically Milled Aluminum (MM Al)

5.1.1. The amount of process control agent

In the attempt to find the optimum amount of process control agent to be used during the process of mechanical milling, which was Methanol in this research, different amounts of methanol were added to the aluminum powder when milled for 6 hrs at 200 RPM. The investigated amounts were 300, 600 and 1200 µL of methanol. The effect of the amount of methanol on the aluminum powder morphology is shown in Figure (31), which shows scanning electron micrographs (SEM) of (a) as-received powders, powders milled with (b) 300 µL, (c) 600 µL, and (d) 1200 µL taken at the same magnification. It is noticeable from Figure (31(b)) that the amount of 300 µL of methanol was not sufficient to allow the particles to collide and fracture into smaller particles. Consequently the particles welded to one another resulting in particle coarsening. The inset in Figure (31(b)) is for the same powder at lower magnification. When an amount of 600 µL of methanol was added to the aluminum powder, although refinement is not clear, it can be noticed that re-welding of the particles was limited (Figure (31(c))). However, when 1200 µL of methanol was added, both requirements occurred; re-welding of the particles was prohibited in addition to refinement of the particles (Figure 31(d))). To conclude, the increase in the amount of methanol during the process of mechanical milling leads to further refinement in the aluminum powder. Measuring the average particle size at each condition also

supported this finding, which conforms to the reported results in the literature [12, 13]. The measured values for the average particle size are listed in Table (3).

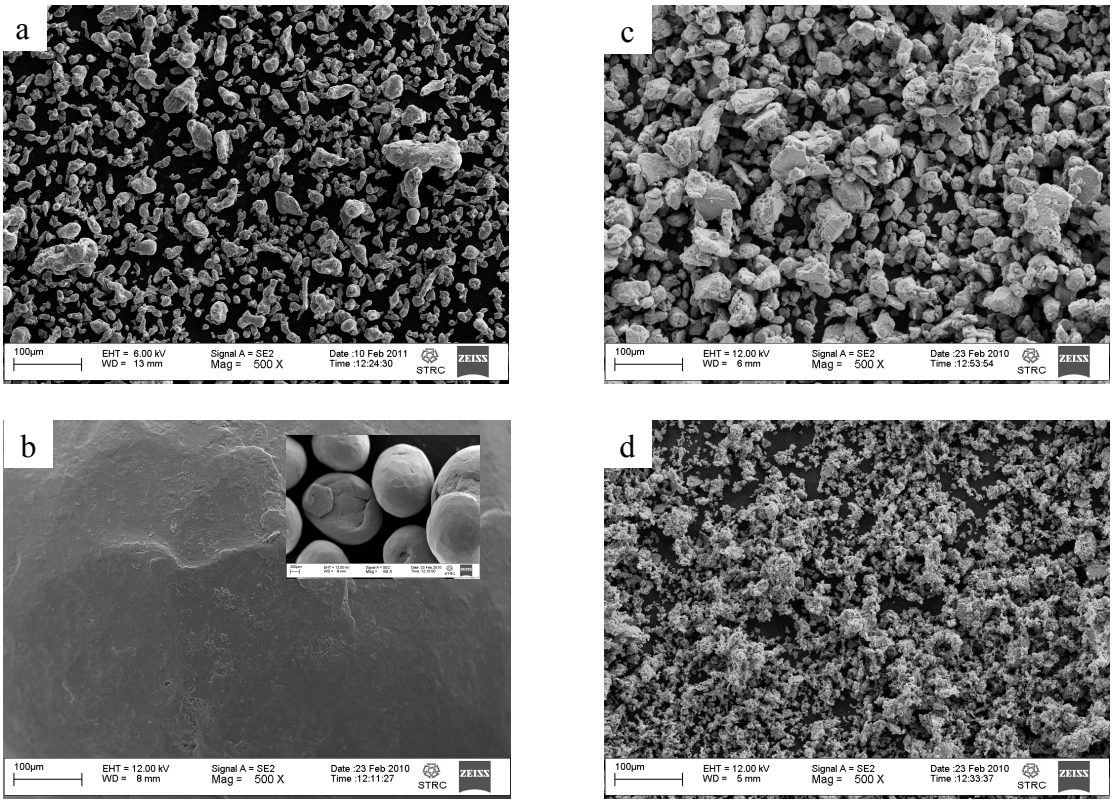

Figure 31: Scanning Electron Micrographs showing the effect of the amount of methanol on the powder morphology of MM Al, (a) as-received Al, (b) MM Al 6 hrs using 300 µL, (c) MM Al 6 hrs using 600 µL, and (d) MM Al 6 hrs using 1200 µL.

Table 3: Average particle size Vs. the amount of methanol added during MM for 6 hrs at 200 RPM.

Amount of PCA (µL)	Average Particle size (µm)
300	1487.18
600	28.58
1200	4.13

Bulk specimens were produced from the powders milled using the three amounts of methanol under investigation and their tensile behavior was studied; the ultimate tensile strength is plotted vs. the corresponding amounts of methanol in Figure (32). This graph demonstrates a direct proportionality between the amount of methanol added during the process of mechanical milling and the ultimate tensile strength of the bulk specimens synthesized from these mechanically milled powders, recording the highest value when using 1200 µL of methanol. Consequently, the amount of methanol was set to be 1200 µL for 6 hrs of mechanical milling, which is equivalent to 3.16 wt%. Trials also showed that the amount of methanol should be varied when changing the milling duration in order to achieve approximately the same degree of fineness in the mechanically milled powders. In order to maintain the proportionality between the amount of methanol and the mechanical milling duration, the amount of methanol was set to be multiples of 100 µL per 30 minutes of milling. The amounts of methanol vs. the milling durations used are shown in Table (4).

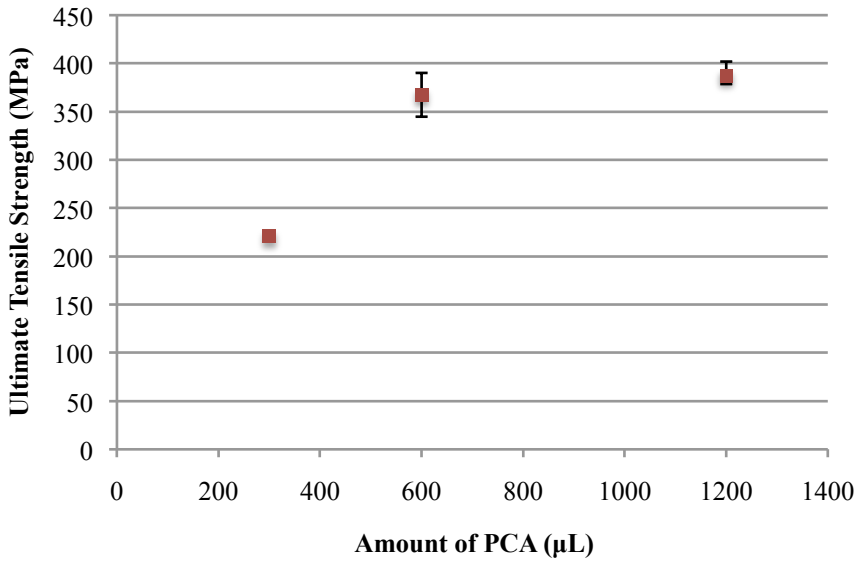

Figure 32: Ultimate tensile strength of bulk specimens synthesized from MM Al for 6 hrs Vs. the amount of methanol used.

Table 4: The amount of methanol used for each of the milling durations.

Milling duration (hrs)	Amount of methanol (µL)	Amount of methanol (wt%)
0.5	100	0.26
1	200	0.53
3	600	1.58
6	1200	3.16
12	2400	6.33

5.1.2. Annealing time

The results of the samples annealed for different durations as well as the calculated average and standard deviation for the Rockwell (F) hardness measurements are shown in Table (5). The effect of annealing time on the hardness of the mechanically milled aluminum for 6 hrs at 200 RPM is clearly demonstrated in Figure (33). As the annealing time increases, the hardness of the specimens increases until reaching 2 hrs of annealing, after which a state of equilibrium is nearly setting in. However, the highest value for hardness was achieved after annealing for 3 hrs, so this was the duration used for specimens' annealing.

Table 5: Rockwell F Hardness Vs. annealing time for Al samples MM for 6 hrs at 200 RPM.

Annealing time (hrs)	0	0.5	1	2	3
Average Hardness (HRF)	84.39	88.13	90.43	93.88	94.31
Standard deviation	3.11	1.83	1.74	5.41	4.37

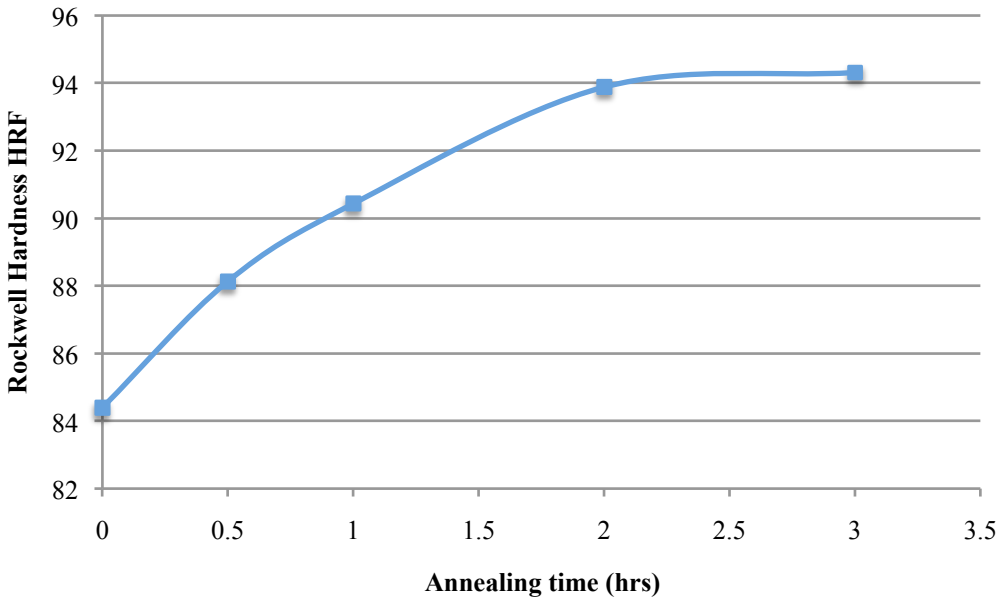

Figure 33: Effect of annealing time on hardness of Al samples MM for 6 hrs at 200 RPM.

5.1.3. Powder X-ray Diffraction

The aluminum powders mechanically milled for different durations were analyzed using x-ray diffraction (XRD) in order to study the effect of mechanical milling on the internal structures (crystallite size, lattice parameter, interplanar spacing) as well as to investigate whether or not any secondary phases (oxides or carbides) have formed following milling in the presence of PCA. The XRD patterns for as-received aluminum powder, and mechanically milled aluminum powders milled for 0.5, 1, 3, 6, and 12 hrs are shown in Figure (34). Broadening and shortening of the peaks, when increasing the mechanical milling duration, are apparent in these XRD patterns, which confirm the expected structure refinement. Figures (35) through (38) show the effect of mechanical milling duration on the XRD pattern of each of the aluminum peaks, i.e. (111), (200), (220), and (311) peaks. Studying the broadening of each peak show that the increase in refinement of the

aluminum powder is directly proportional to the milling duration. However, the rate of refinement was noticed to be lower after 6 hrs of mechanical milling. This suggests that the refinement has approached, but not reached, the critical value after which no further refinement can be achieved.

Similar results were also reported by Xiangyu Zhao *et al.* [30] when they milled Ni powders, and Mhadhbi *et al.* [6] who milled Al powders. Broadening and shortening of the peaks was evident in their work, which was attributed to the refinement in the internal structure of the material.

Concerning phase analysis, no new peaks or even traces were detected. However secondary phases could have formed as a result of reactions with the PCA during milling but below the detectable limits. These findings agree with the results reported by Carlos A. Galan *et al.* [29].

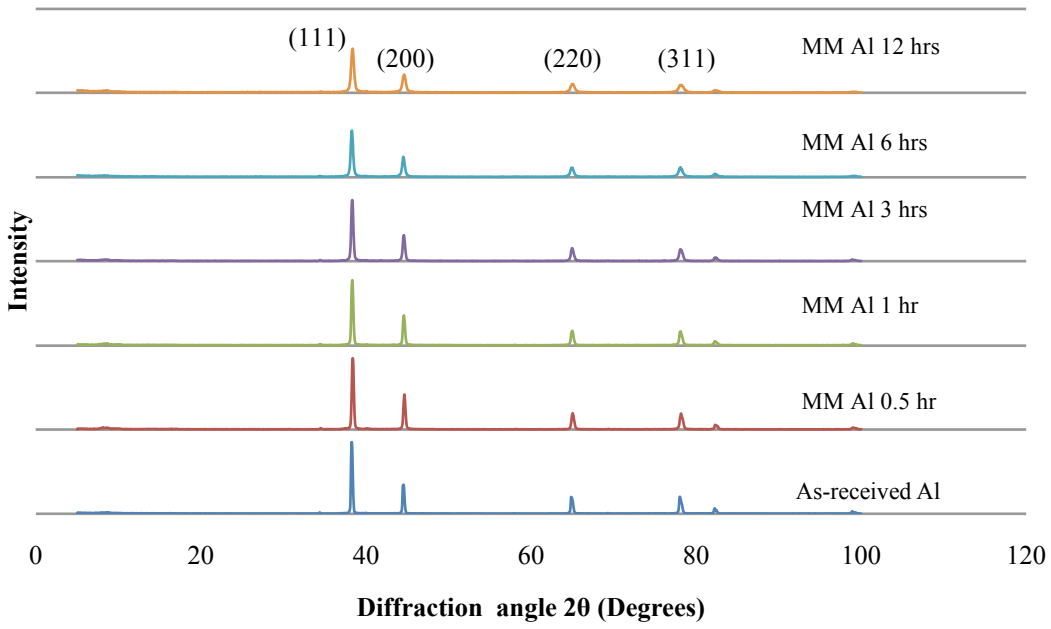

Figure 34: XRD patterns for Al powders mechanically milled for different milling durations at 200 RPM.

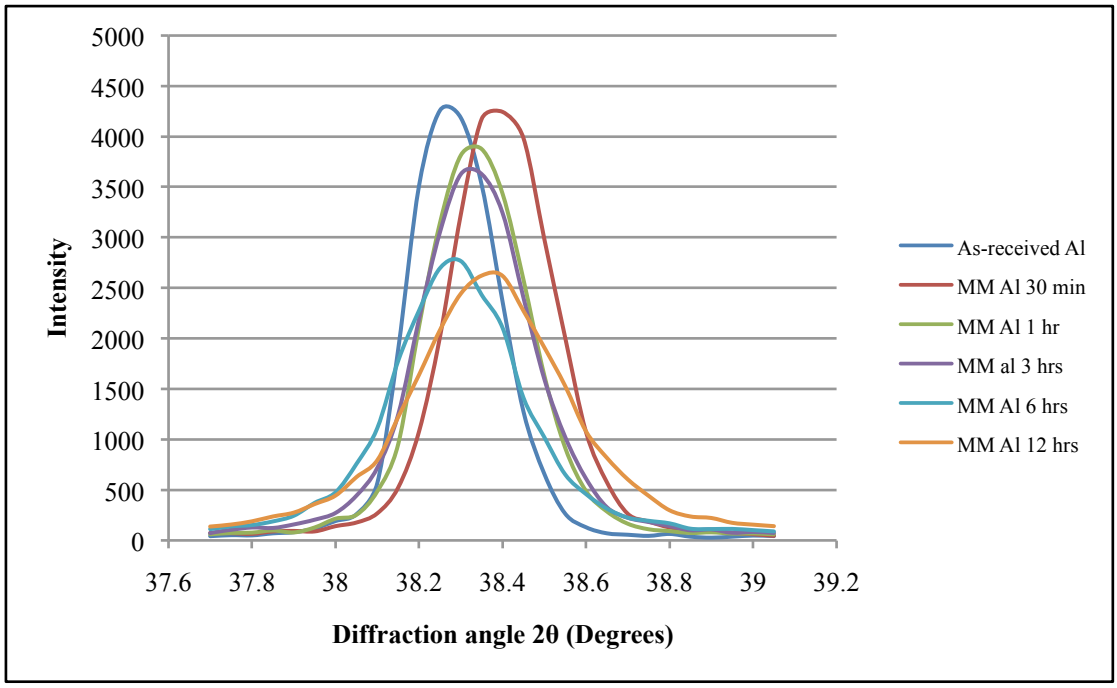

Figure 35: Effect of increasing MM duration on XRD pattern of the (111) peak.

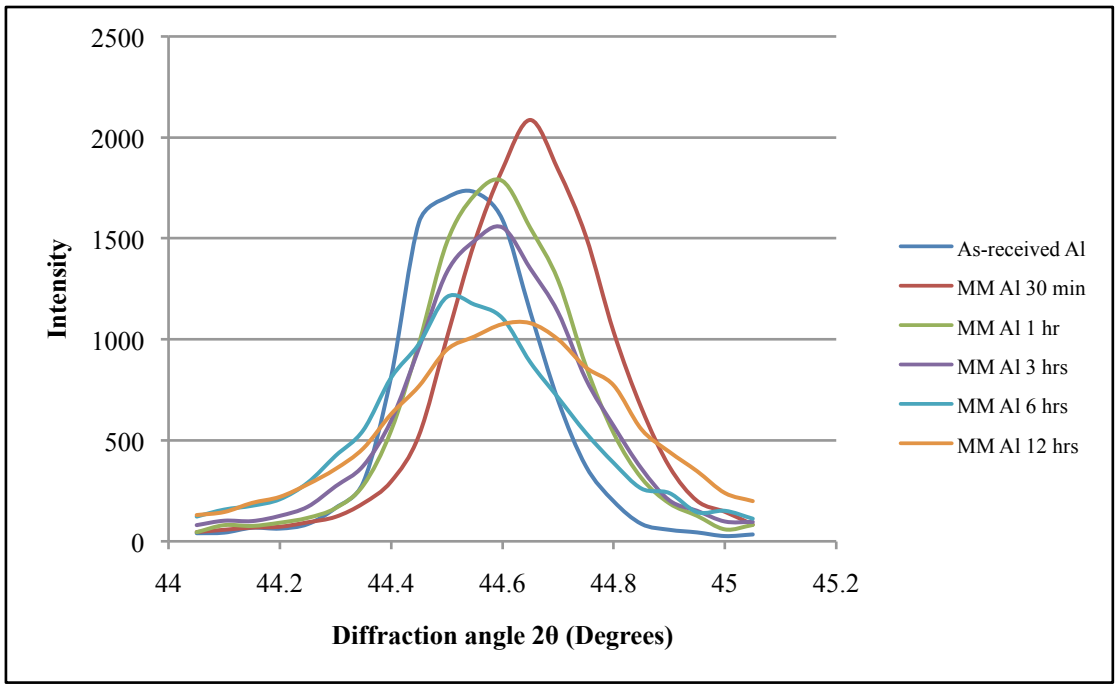

Figure 36: Effect of increasing MM duration on the XRD pattern of the (200) peak.

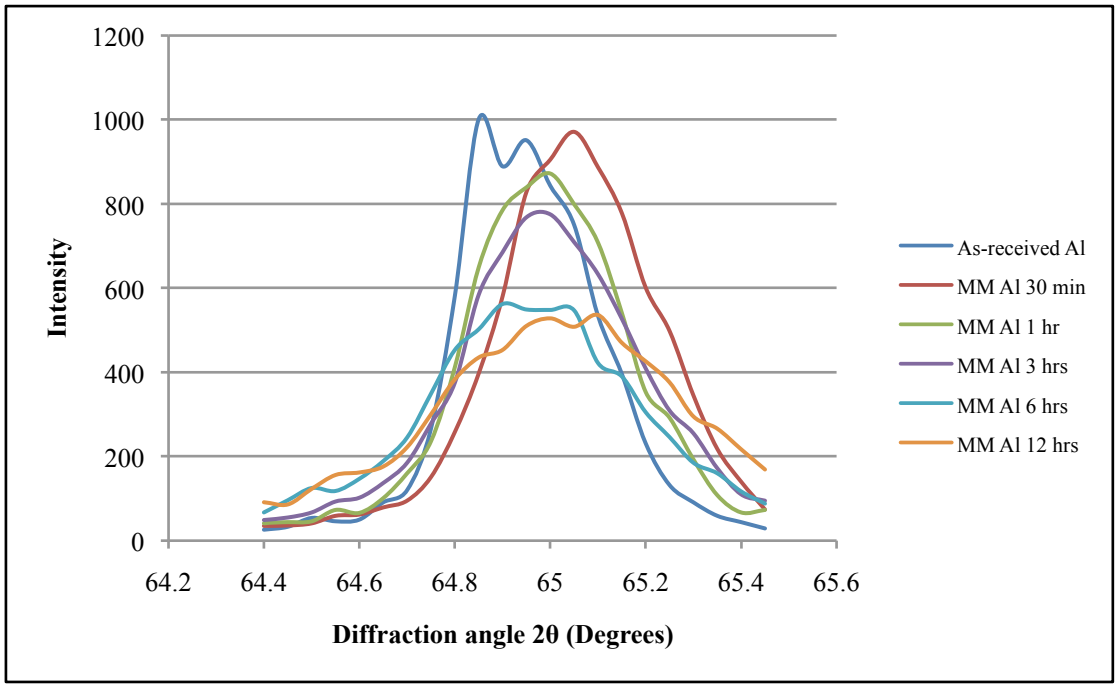

Figure 37: Effect of increasing MM duration on the XRD pattern of the (220) peak.

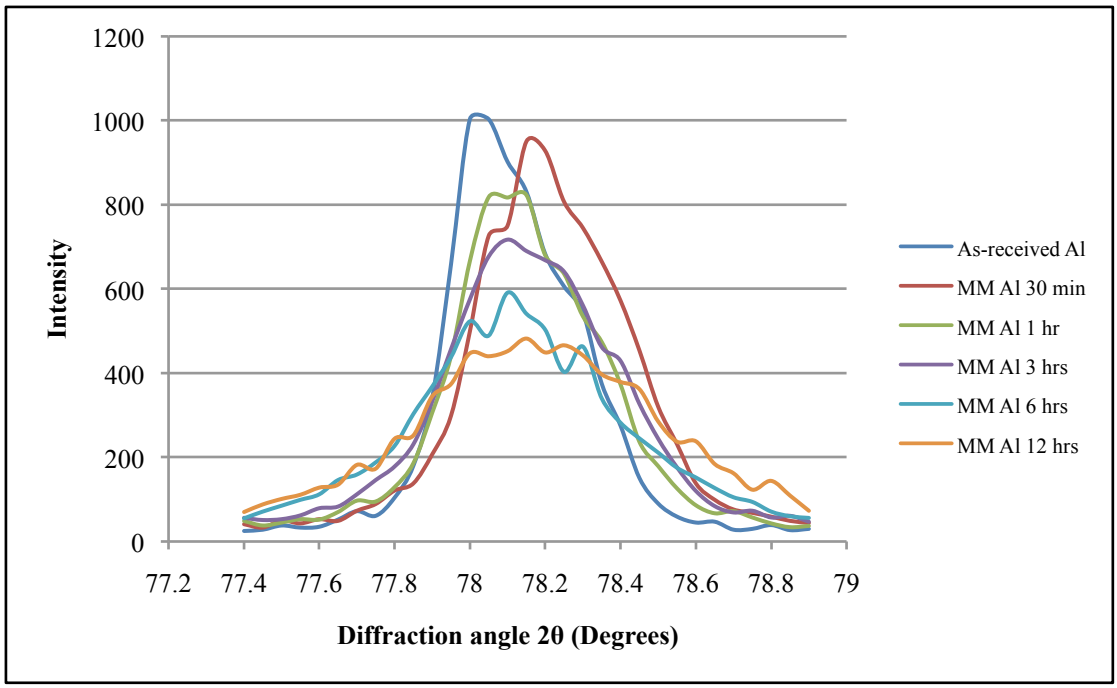

Figure 38: Effect of increasing MM duration on the XRD pattern of the (311) peak.

In order to quantify the refinement that is demonstrated by the XRD patterns, three parameters were calculated for each peak at each of the milling durations; these parameters are the interplanar spacing (d), the spacing between the nearest neighbors/or lattice parameter (a), and the thickness of the crystallite (t). The results of these calculations are listed in Tables (6) through (11).

The interplanar spacing (d) was calculated using Bragg's law [43]:

$$n \lambda = 2 d \sin(\theta) \quad \{4\}$$

Where *n* is the order of reflection (n = 1), λ is the X-ray wavelength (λ = 0.154 nm), and θ is the angle between the incident ray and the scattering planes, which is Bragg's law diffraction angle.

The distance between the nearest neighbors (a) was calculated using the following relation [43]:

$$a = d * \sqrt{(h^2 + j^2 + k^2)} \quad \{5\}$$

Where h, j, and k are the miller indices of the plane.

The thickness of the crystallite (t) was calculated using Scherrer's formula [44]:

$$t = (K*\lambda) / (B*\sin(\theta)) \quad \{6\}$$

Where *t* is the crystallite size, *K* is a constant dependent on the crystallite shape (*K* = 0.9), λ is the X-ray wavelength (λ = 0.154 nm), *B* is the full width of the peak at half the maximum height, and θ is Bragg's law diffraction angle.

Table 6: XRD analysis for as-received Al powders.

Plane	(111)	(200)	(220)	(311)
Interplanar spacing (d) (nm)	0.23502	0.20314	0.1436	0.12232
Spacing between nearest neighbors (a) (nm)	0.40505	0.40628	0.40617	0.40569
Thickness of crystallite (t) (nm)	33.6375	31.2216	29.4148	26.219

Table 7: XRD analysis for Al powders MM for 30 minutes.

Plane	(111)	(200)	(220)	(311)
Interplanar spacing (d) (nm)	0.234137	0.202706	0.143211	0.122157
Spacing between nearest neighbors (a) (nm)	0.405538	0.405413	0.405062	0.405148
Thickness of crystallite (t) (nm)	29.01102	28.63007	24.79785	21.54621

Table 8: XRD analysis for Al powders MM for 1 hr.

Plane	(111)	(200)	(220)	(311)
Interplanar spacing (d) (nm)	0.234431	0.202922	0.143309	0.122157
Spacing between nearest neighbors (a) (nm)	0.406047	0.405844	0.40534	0.405148
Thickness of crystallite (t) (nm)	29.00661	28.62494	25.46098	23.80104

Table 9: XRD analysis for Al powders MM for 3 hrs.

Plane	(111)	(200)	(220)	(311)
Interplanar spacing (d) (nm)	0.234431	0.202922	0.143309	0.122223
Spacing between nearest neighbors (a) (nm)	0.406047	0.405844	0.40534	0.405366
Thickness of crystallite (t) (nm)	27.13522	26.83589	22.97698	19.67466

Table 10: XRD analysis for Al powders MM for 6 hrs.

Plane	(111)	(200)	(220)	(311)
Interplanar spacing (d) (nm)	0.234726	0.203355	0.143506	0.122223
Spacing between nearest neighbors (a) (nm)	0.406557	0.40671	0.405896	0.405366
Thickness of crystallite (t) (nm)	25.4868	23.51894	18.83067	19.30344

Table 11: XRD analysis for Al powders MM for 12 hrs.

Plane	(111)	(200)	(220)	(311)
Interplanar spacing (d) (nm)	0.234431	0.202706	0.143113	0.122157
Spacing between nearest neighbors (a) (nm)	0.406047	0.405413	0.404785	0.405148
Thickness of crystallite (t) (nm)	20.02838	17.89379	15.20292	13.46638

To better demonstrate the effect of mechanical milling duration on the structure of aluminum powder, and in an attempt to comprehend the trend by which the different parameters - interplanar spacing, lattice parameter, and crystallite size - respond to the process of mechanical milling; the values calculated earlier for these parameters are plotted vs. the duration of mechanical milling in Figures (39), (40), and (41).

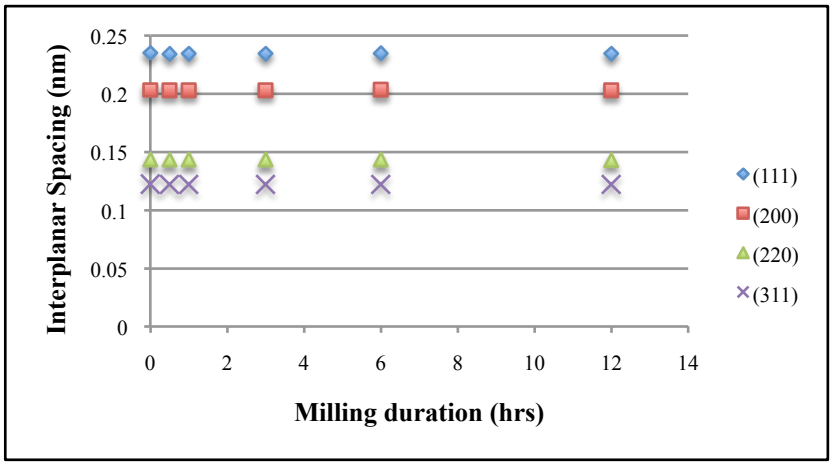

Figure 39: Interplanar spacing *d* Vs. MM duration.

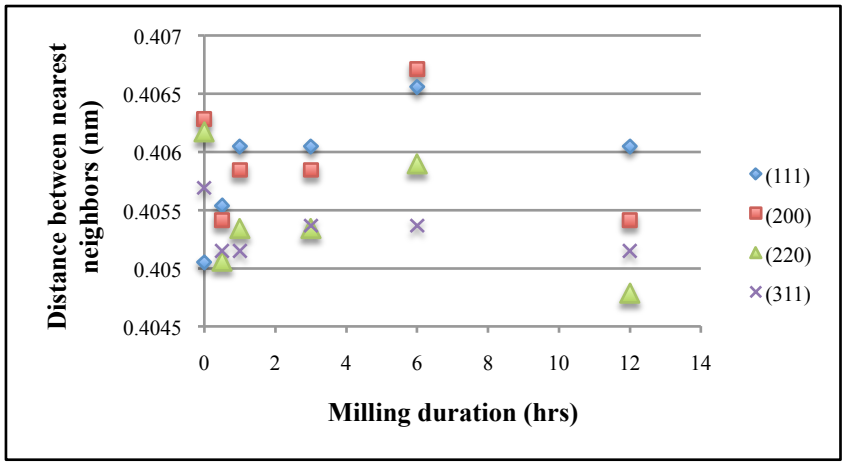

Figure 40: Lattice parameter *a* Vs. MM duration.

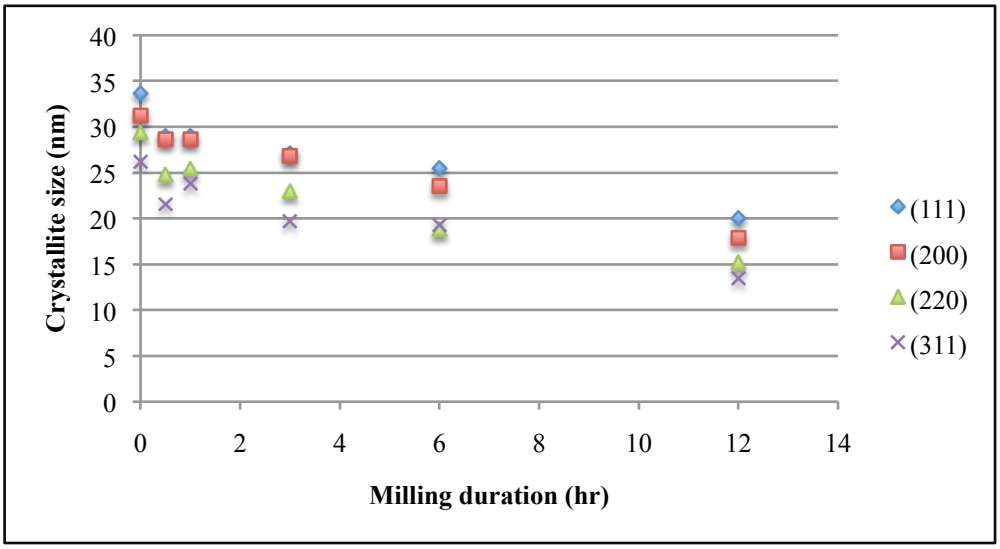

Figure 41: Crystallite size *t* Vs. MM duration.

Figure (41) shows that as the milling duration is increased, the thickness of the crystallite is decreased. The same trend was followed by all the four characteristic planes (111), (200), (220), and (311). This is a proof that structure refinement did occur as a result of mechanical milling.

5.1.4. Tensile behavior

5.1.4.1. The as-extruded specimens

Representative stress-strain curves for the tensile behavior of the as-extruded bulk aluminum samples synthesized from mechanically milled powders are shown in Figure (42). This graph shows that mechanical milling does strengthen the aluminum specimens in tension, and the amount of strengthening gained is directly proportional to the duration of mechanical milling. A strange phenomenon that was noticed from the results was that the samples mechanically milled for 1 hr showed deteriorated mechanical behavior -whether strength or ductility- compared to those mechanically

milled for 30 minutes. This was not a one-off phenomenon as all the samples produced with these conditions showed the same behavior consistently.

The enhancements observed for all the milled samples, however, were at the cost of sacrificing the ductility of the material, reaching the limit of failing in a perfectly brittle manner when milling for 12 hrs as shown in Figure (43), bearing in mind that this sole condition was sintered for 3 hrs pre-extrusion unlike all the other samples that were sintered for 30 minutes only.

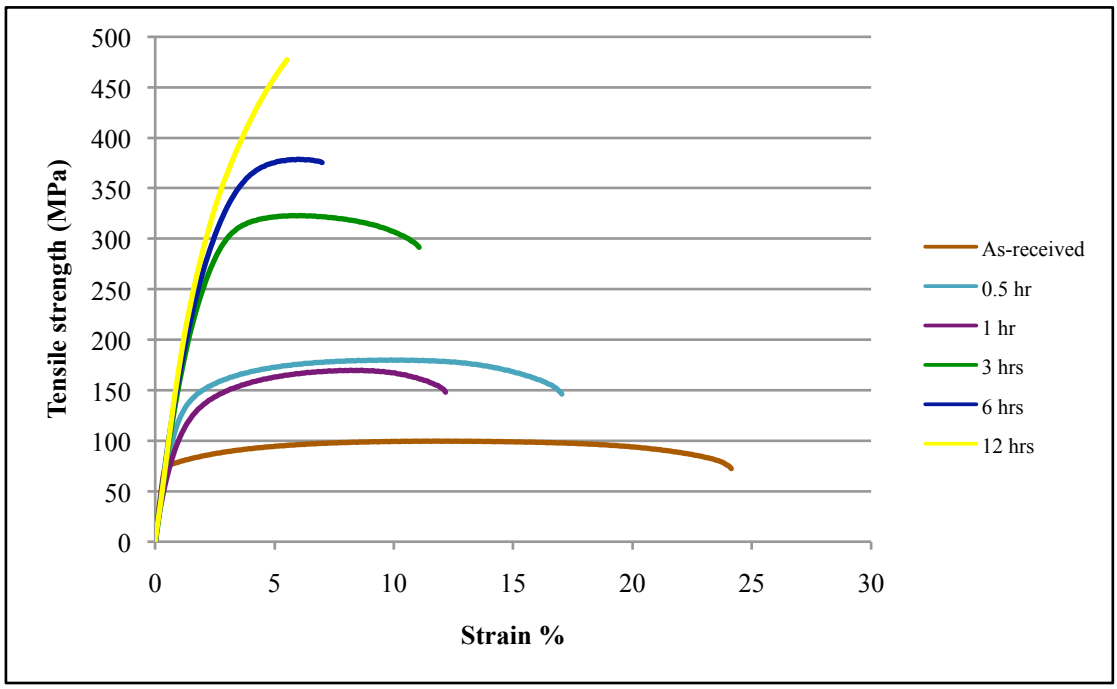

Figure 42: Representative stress-strain curves showing the effect of MM duration on the tensile behavior of as-extruded Al specimens.

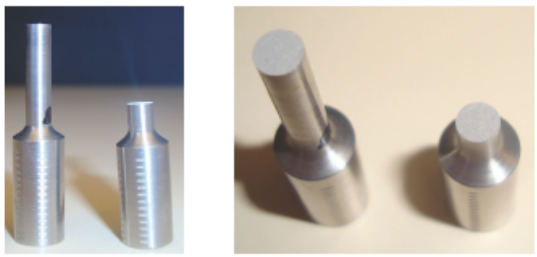

Figure 43: Failed Al specimen MM for 12 hrs under tension.

The highest tensile strength achieved in this work by mechanical milling of pure Al was after 12 hrs at 200 rpm, which is around 460 MPa. Comparing this achievement to the values reported in the literature, for example the work done by Choi *et al.* [10] that is explained in section (3.2.1) as they reached a tensile strength of 500 MPa after 48 hrs of milling at 550 RPM, it could be established that this research has successfully reached a high strength at lower energy consumption (lower rotational speed and shorter milling duration). In another research, Khan *et al.* reported a tensile strength of 450 MPa after milling for 20 hrs at 100 RPM using a BPR of 20:1, although they used a milling speed lower than that used in this research, the time needed to reach approximately the same strength is relatively long.

5.1.4.2. The annealed specimens

Representative stress-strain curves for the tensile behavior of the bulk aluminum specimens that were annealed for 3 hrs at 500°C and then furnace cooled are shown in Figure (44). Comparing the tensile behavior of the as extruded and annealed specimens, it can be deduced that annealing has increased the strain hardening capacity of the mechanically milled aluminum specimens. It is also noticed that annealing has enhanced the ductility of the material and this is clearly demonstrated in the chart in Figure (45).

It was decided not to anneal the Al samples MM for 12 hrs since they were already sintered for 3 hrs prior to extrusion in order not to subject the samples to any additional post extrusion annealing so that the total annealing time for all samples would be equivalent and hence comparable.

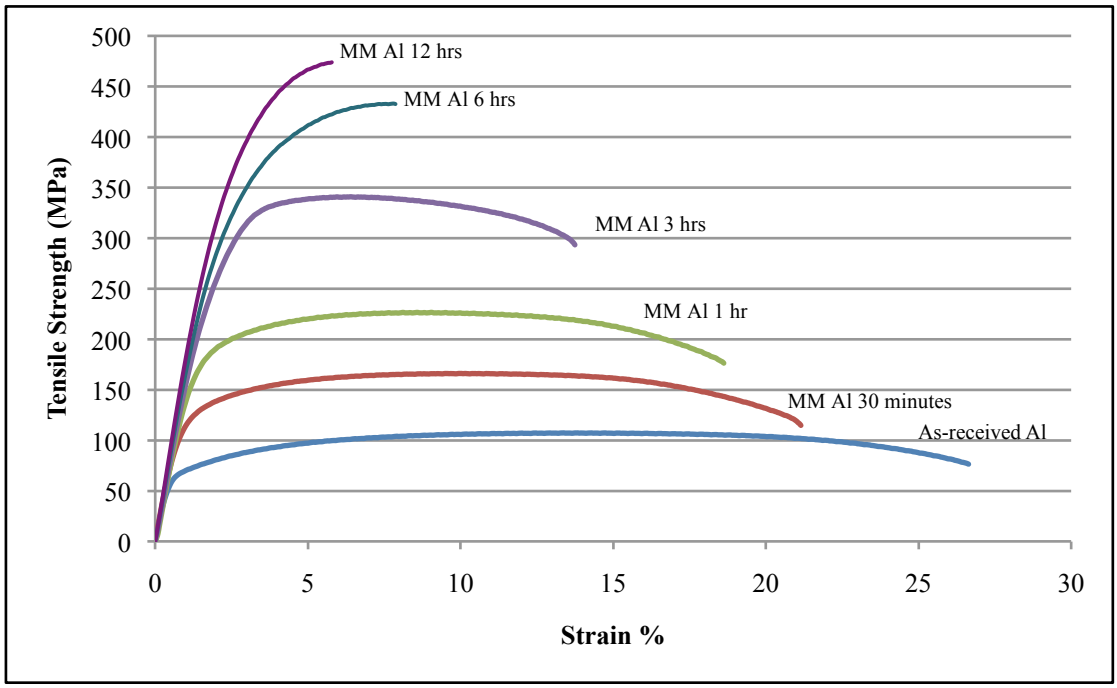

Figure 44: Representative stress-strain curves showing the effect of MM duration on the tensile behavior of the annealed Al specimens.

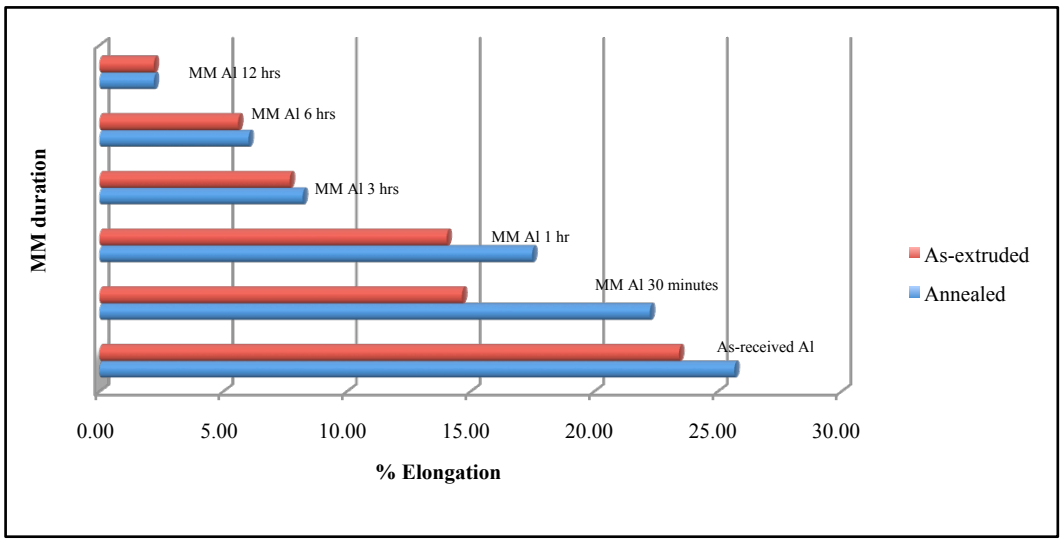

Figure 45: Effect of annealing on the ductility of MM Al.

Although the elongation percent of the material has been increased by annealing, the loss of strength was not significant, if any. In some cases the ultimate

tensile strength of the material was even slightly enhanced such as the samples MM Al for 3 and 6 hrs. The average of the results for the yield strength and ultimate tensile strength and elongation percent are shown in Table (12). The results in Table (12) show that both the yield tensile strength and ultimate tensile strength increase with mechanical milling at the expense of the % elongation.

It cannot be overlooked that annealing has brought stability to the behavior of MM Al samples as demonstrated by the yield strength values before and after annealing. The variation between the samples produced using the same conditions was high leading to a large standard deviation, which diminished after annealing.

Table 12: Comparing the tensile behavior of MM Al samples before and after annealing.

MM duration (hrs)	As-extruded			Annealed		
	Yield Strength (MPa)	Ultimate Tensile Strength (MPa)	%Elongation	Yield Strength (MPa)	Ultimate Tensile Strength (MPa)	%Elongation
0	98.50 ± 21.50	114.34 ± 14.67	20.38 ± 6.68	68.75 ± 6.25	112.48 ± 5.23	25.61 ± 1.72
0.5	112.00 ± 27.00	187.37 ± 3.11	14.08 ± 0.58	129.58 ± 6.66	171.25 ± 9.736	22.09 ± 1.6
1	91.00 ± 39.00	98.01 ± 35.15	14.69 ± 2.21	178.13 ± 5.21	216.86 ± 9.75	18.05 ± 1.86
3	223.00 ± 74.00	333.86 ± 9.92	8.3 ± 2.6	262.00 ± 4.00	333.75 ± 7.26	8.2 ± 3.7
6	242.50 ± 55.50	393.58 ± 7.42	7.02 ± 2.09	280.00 ± 2.00	401.8 ± 31.2	5.99 ± 0.70
12	299.00 ± 25.00	459.46 ± 17.84	2.35 ± 0.45	N/A	N/A	N/A

5.1.5. Compressive behavior

5.1.5.1. The as-extruded specimens

The effect of the mechanical milling duration on the compressive behavior of the as-extruded MM Al samples is demonstrated by the selection of representative stress-strain curves shown in Figure (46). Unlike the tensile behavior, the as extruded samples were ductile under compressive loading. The samples showed ductility to the extent of not fracturing under continuous loading. Most specimens kept on deforming until they transformed to discs instead of the rod samples. An example of a sample before and after the compression test in shown in Figure (47). Only the samples mechanically milled for 12 hrs showed a brittle behavior under compression. An example of these specimens is shown in Figure (48).

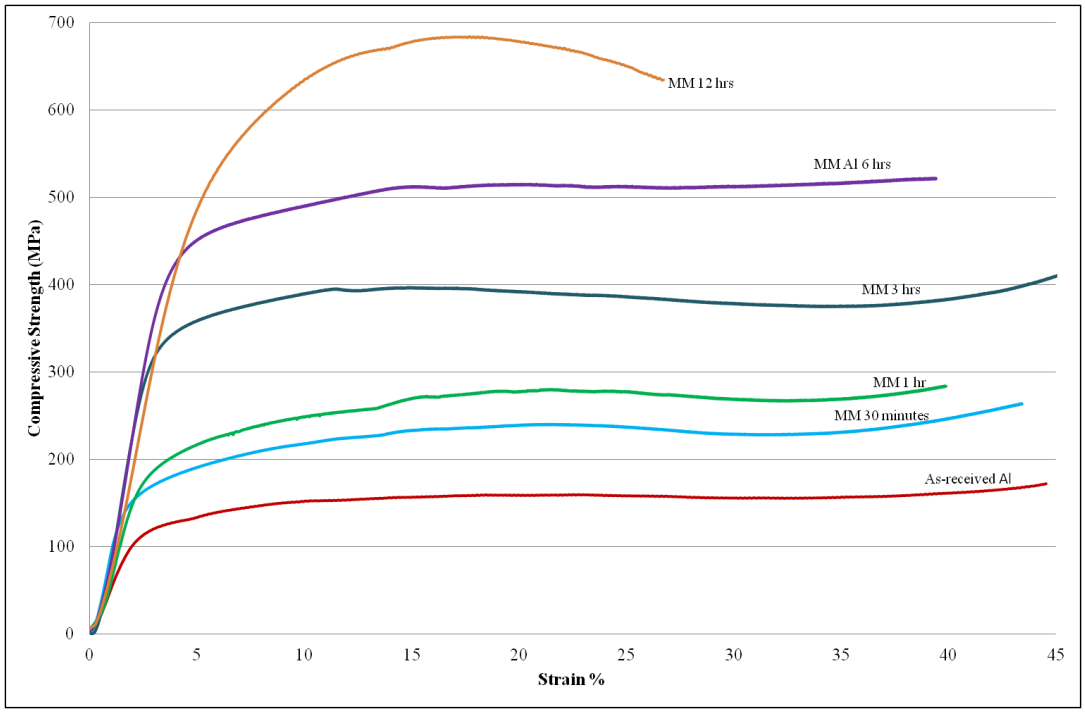

Figure 46: Representative stress-strain curves showing the effect of MM duration on the compressive behavior of the as-extruded MM Al samples.

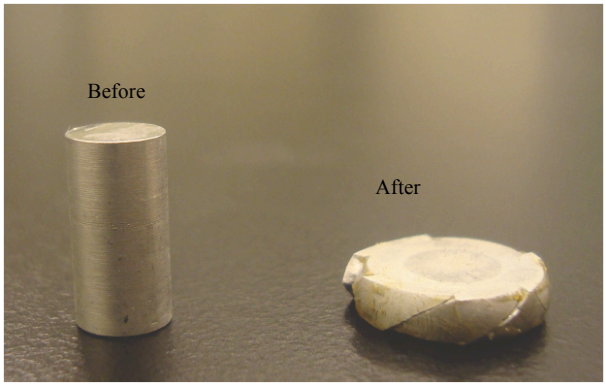

Figure 47: As-extruded MM Al specimen before and after compression test.

Figure 48: Failed MM Al sample for 12 hrs under compression.

5.1.5.2. The annealed specimens

The process of annealing was expected to enhance the ductility of MM al specimens. However, since the samples already behaved in a ductile manner under compression before annealing, there was no difference after annealing regarding ductility. On the other hand, annealing is known to soften materials, but this didn't occur in this case either. The representative stress-strain curves for the annealed samples under compression, presented in Figure (49), show that the opposite of softening has actually occurred as the compressive strength of the annealed samples was found to be slightly higher than that of the as-extruded ones. A comparison

between the compressive behaviors (yield strength and ultimate strength) of MM Al samples before and after annealing is shown in Table (13). The changes in values before and after annealing are noticed to be inconsistent under compressive loading.

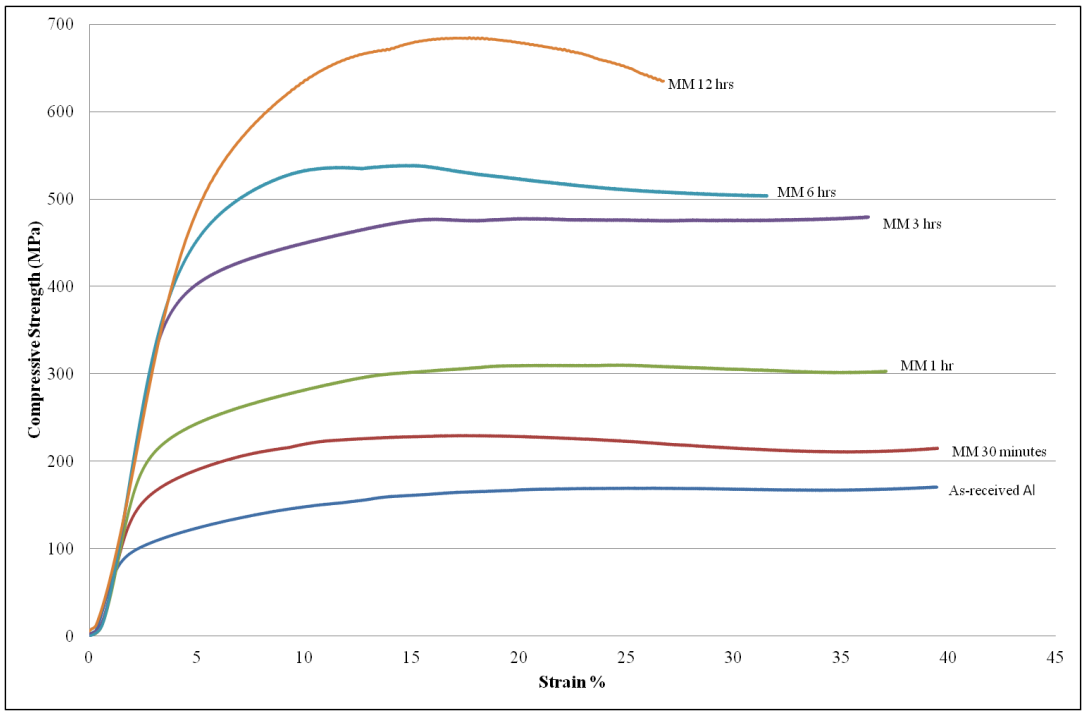

Figure 49: Representative stress-strain curves showing the effect of MM duration on the compressive behavior of the as-extruded MM Al samples.

Table 13: Comparing the compressive behavior of MM Al before and after annealing.

MM duration (hrs)	As-extruded		Annealed	
	Yield Compressive (MPa)	Ultimate Compressive Strength (MPa)	Yield Compressive (MPa)	Ultimate Compressive Strength (MPa)
0	108.50 ± 20.50	180.00 ± 20.00	98.08 ± 5.77	186.55 ± 13.45
0.5	164.30 ± 6.00	246.60 ± 16.40	151.93 ± 1.93	223.07 ± 7.69
1	189.40 ± 0.10	263.15 ± 14.45	207.69 ± 7.69	297.12 ± 12.50
3	359.45 ± 11.65	289.35 ± 10.65	327.89 ± 41.35	450 ± 34.62
6	437.25 ± 28.75	475.00 ± 47.00	415.39 ± 3.84	506.73 ± 31.73
12	497.72 ± 37.71	609.33 ± 75.17	N/A	N/A

5.1.6. Density measurements

5.1.6.1. As-extruded samples

The values of density measured for the as-extruded samples of the mechanically milled Al samples were found to be high and this is clearly demonstrated by the tabulated data in Table (14) in which the relative density (density of the specimen measured using the densitometer divided by the theoretical density of Al, which is 2.7 gm/cm^3) of the samples is listed versus the MM duration. The variations between the values of the samples mechanically milled at different durations are minimal. Anyhow, these results are proof of good compressibility of the samples as well as the success of the process of powder consolidation.

The density of the annealed mechanically milled Al samples showed high density as well. The values of the relative densities of these samples are also presented in Table (14). However, the densities of the annealed samples were found to be significantly higher than that of the as-extruded samples.

Table 14: Relative density for bulk as-extruded MM Al samples.

Milling duration (hrs)	Relative Density (%)	
	As-extruded	Annealed
0	98.80 ± 0.04	98.34 ± 0.12
0.5	98.70 ± 0.28	99.17 ± 0.22
1	98.23 ± 0.36	99.16 ± 0.09
3	98.78 ± 0.23	98.96 ± 0.30
6	98.93 ± 0.22	99.08 ± 0.11
12	97.97 ± 0.52	N/A

5.1.7. Scanning Electron Microscopy

5.1.7.1. Powder Morphology

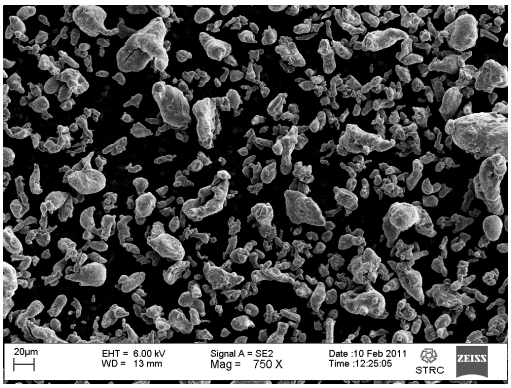

(a)

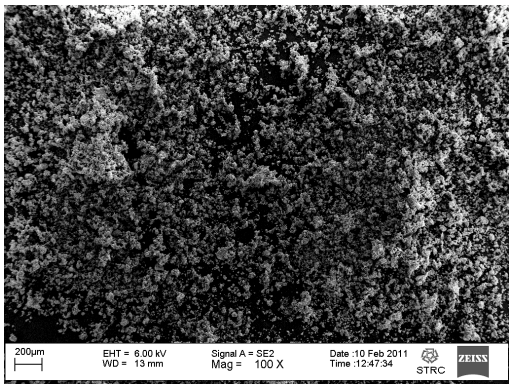

(d)

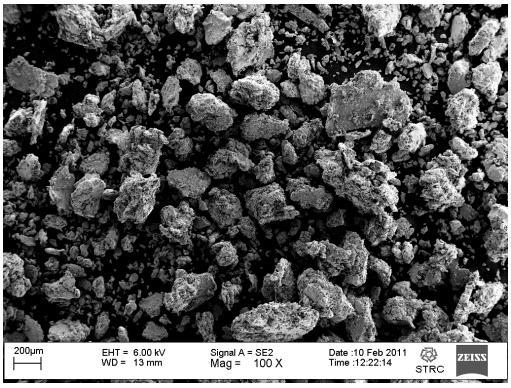

(b)

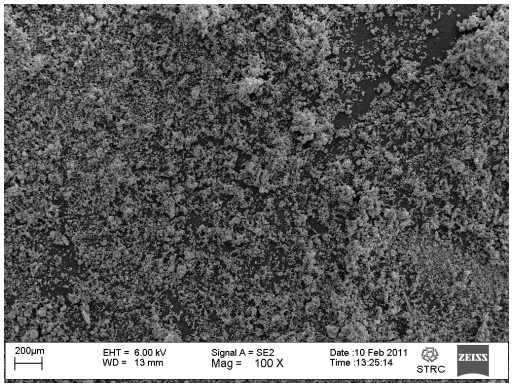

(e)

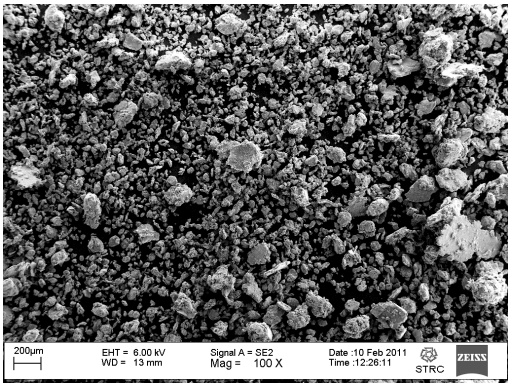

(c)

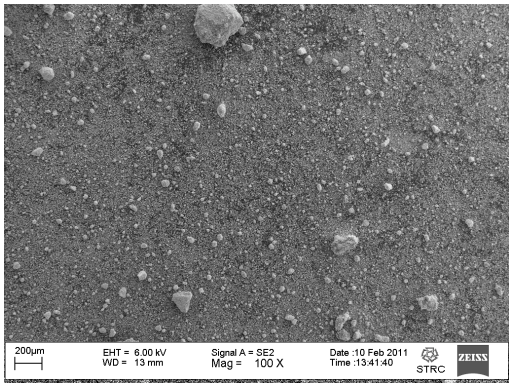

(f)

Figure 50: SEM micrographs showing the effect of MM duration on the Al powder morphology – low magnification (a) as-received Al, (b) MM Al 0.5 hr, (c) MM Al 1 hr, (d) MM Al 3 hrs, (e) MM Al 6 hrs, and (f) MM Al 12 hrs.

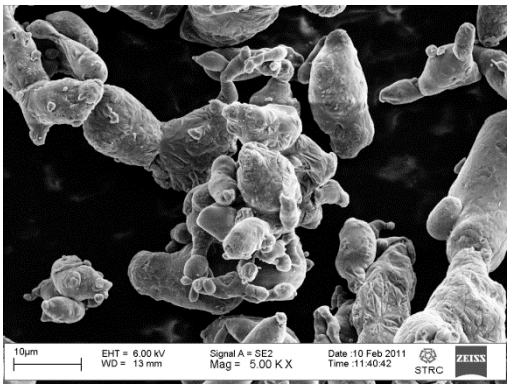

(a)

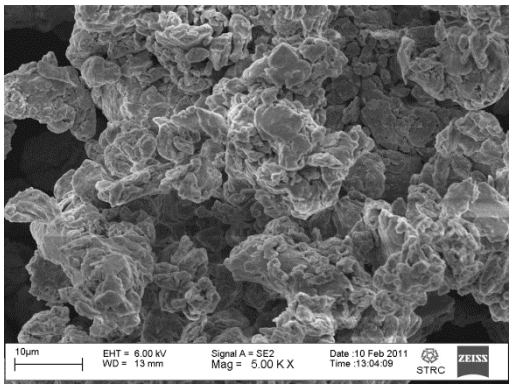

(d)

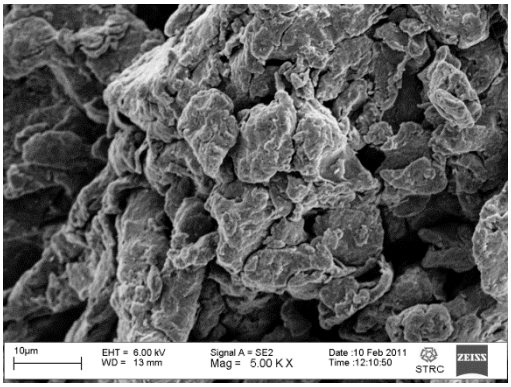

(b)

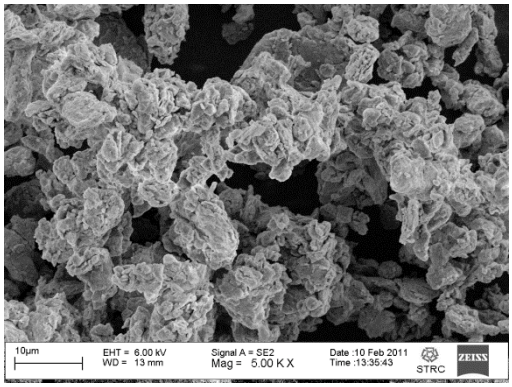

(e)

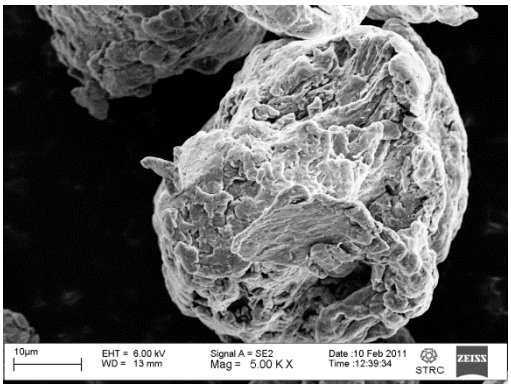

(c)

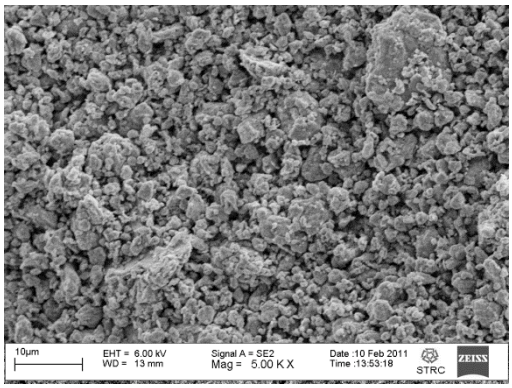

(f)

Figure 51: SEM micrographs showing the effect of MM duration on the Al powder morphology – high magnification (a) as-received Al, (b) MM Al 0.5 hr, (c) MM Al 1 hr, (d) MM Al 3 hrs, (e) MM Al 6 hrs, and (f) MM Al 12 hrs.

The SEM micrographs shown in Figures (50) & (51) illustrate the effect of the mechanical milling duration on the morphology of the Al powder's particles. For instance, considering the low magnification micrographs in Figure (50), it can be deduced that mechanical milling for 30 minutes led to an overall increase in the particles' sizes, which partially decreases with milling up to 1 hr. However, upon milling for 3 hrs, the particles start to be refined significantly. This refinement further increases on reaching 6 hrs of milling. At 12 hrs of mechanical milling, the powder is seen to be extremely fine. This scenario is also supported by the higher magnification images in Figure (51), except that the higher magnification images have cleared out that the large particles that were seen in the lower magnification images after 0.5 and 1 hr of milling, are actually smaller particles that are agglomerating or in other words are cold welded to each other.

Studying the SEM micrographs of the MM Al powders for 12 hrs at low magnification (Figure 50(f)), some random large particles can be observed. Different magnifications of these particles are shown in Figures (52) and (53), that show these particles to be just clusters of very fine powders. These clustered powders are not cold welded powders as air blowing result into their dispersion, so these powders are bonded to each other by Van Der Waal forces due to their large surface areas.

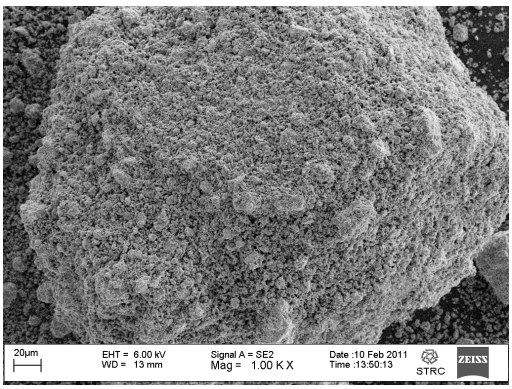

Figure 52: SEM micrograph showing a cluster of particles of MM Al 12 hrs at low magnification.

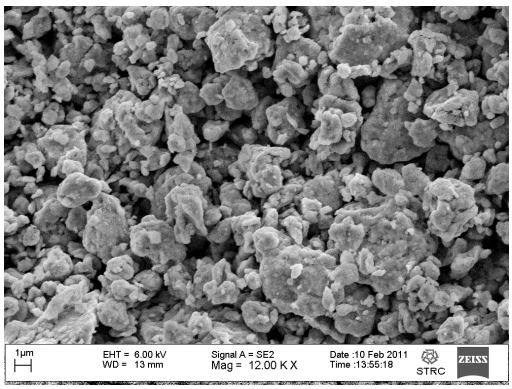

Figure 53: Higher magnification of Figure (52).

In addition to the extreme refinement that the Al particles have encountered after mechanical milling for 12 hrs in addition to the particles of few micrometers size, a significant fraction of particles with sizes in the range of nanometer were also observed. Figures (54) and (55) show SEM images showing some of these nano-scaled particles.

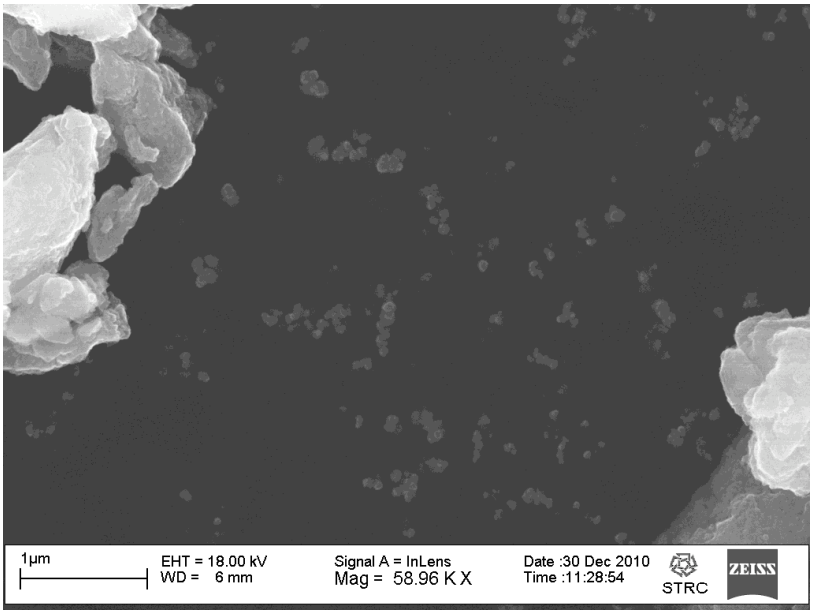

Figure 54: SEM micrograph for MM Al powders showing variation in particle sizes.

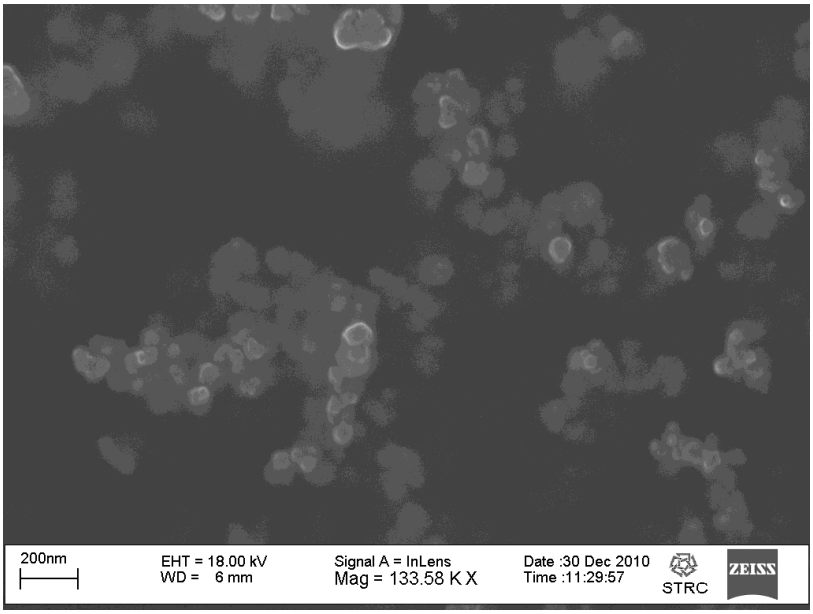

Figure 55: SEM micrograph showing the nano-scale particles in MM Al 12 hrs.

5.1.7.2. Fractography

5.1.7.2.1. The as-extruded specimens

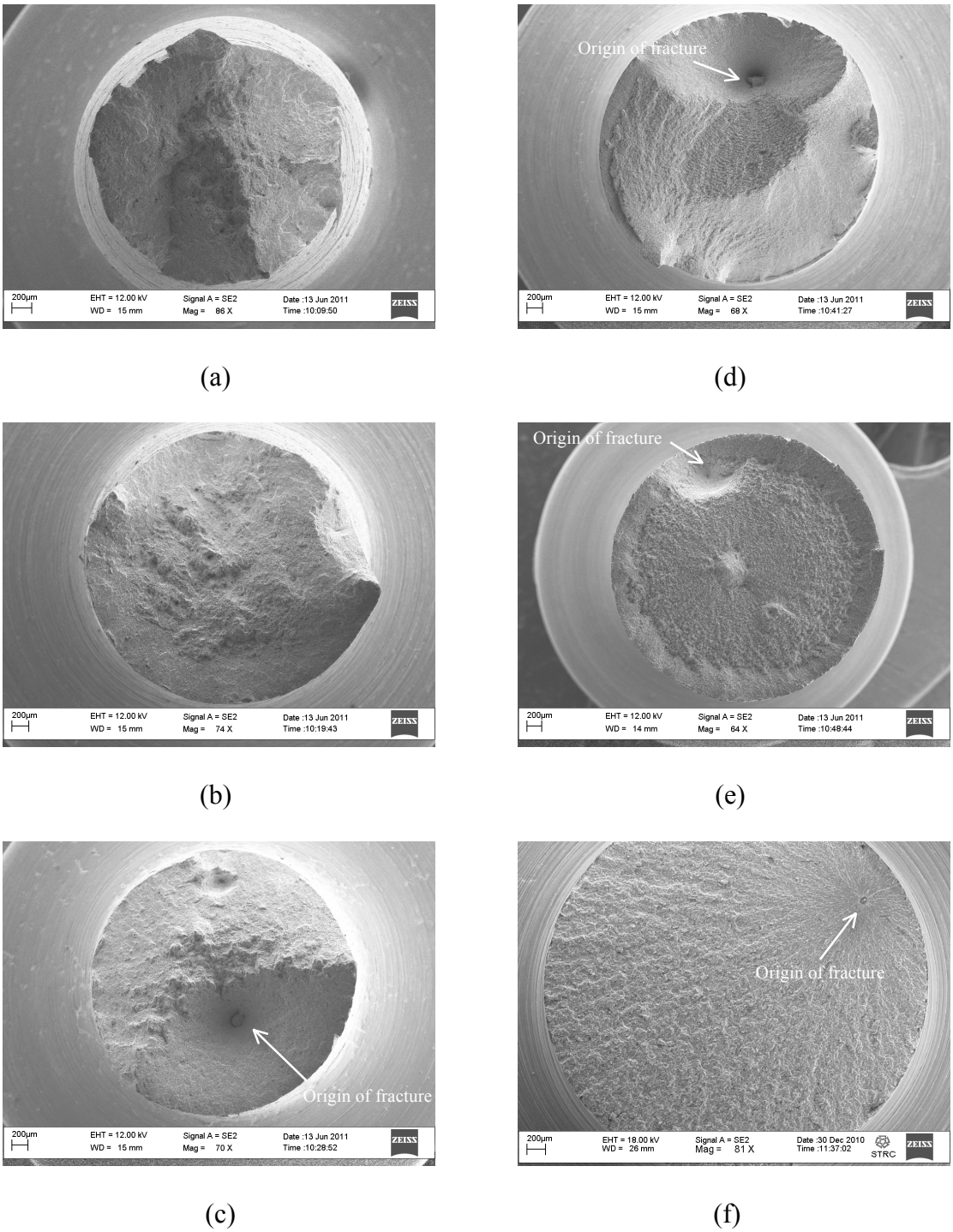

Figure 56: SEM micrographs showing the effect of MM duration on the fracture surface of as-extruded Al samples– low magnification (a) as-received Al, (b) MM Al 0.5 hr, (c) MM Al 1 hr, (d) MM Al 3 hrs, (e) MM Al 6 hrs, and (f) MM Al 12 hrs.

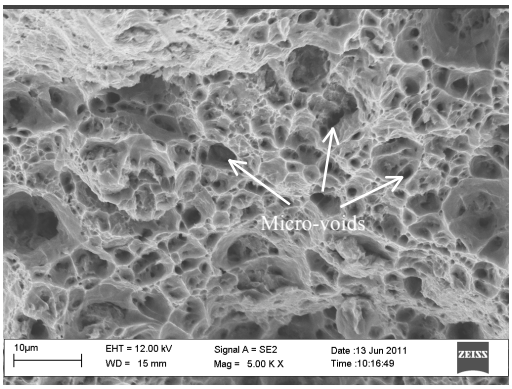

(a)

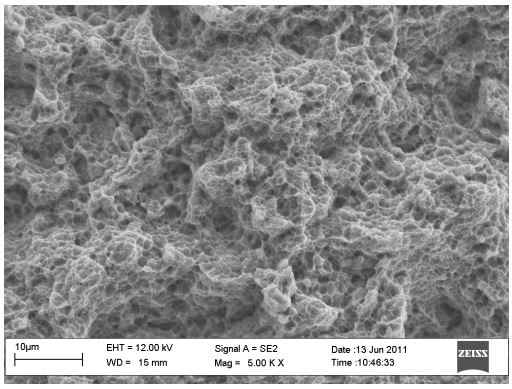

(d)

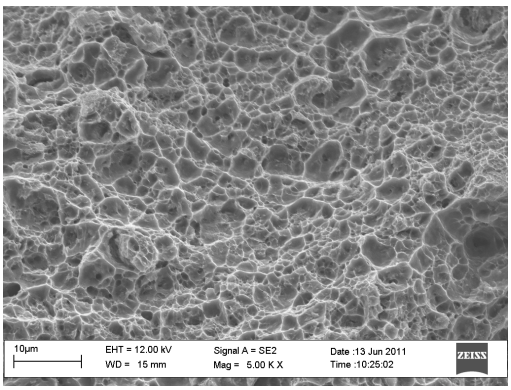

(b)

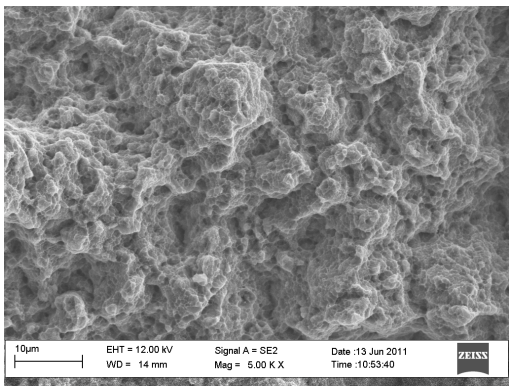

(e)

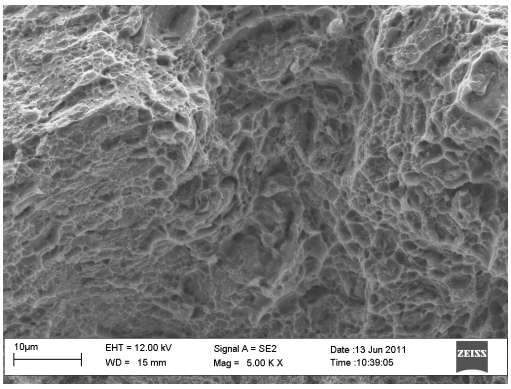

(c)

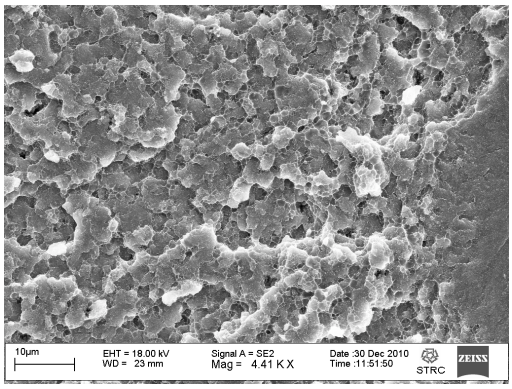

(f)

Figure 57: SEM micrographs showing the effect of MM duration on the fracture surface of as-extruded Al samples– high magnification (a) as-received Al, (b) MM Al 0.5 hr, (c) MM Al 1 hr, (d) MM Al 3 hrs, (e) MM Al 6 hrs, and (f) MM Al 12 hrs.

The fracture surfaces of the different specimens were investigated to better understand the effect of mechanical milling on the mode of failure of the MM Al samples. Figures (56) and (57) show low and high magnification SEM micrographs for the fracture surfaces of the different MM Al samples. The images in Figure (56) demonstrate the increase in the flatness of the fracture surface of the specimen suggesting a refinement in the structure of the material as well as an increase in the brittleness of the material. This is also supported by the images in Figure (57), as dimples and micro-voids can be seen clearly in the fracture surface of the as-received Al sample. These micro-voids coalesce to form an internal crack and the final failure occurs when the shear stress causes the remaining cross section to tear. However, as the milling duration increases, these micro-voids decrease to the minimal, promoting the brittle behavior in the material.

Ductile fracture features can be observed to different degrees in all the specimens except for the sample MM Al 12 hrs, which shows a perfectly brittle behavior as shown in Figure (57(f)). For instance, considering the SEM image for the fracture surface of the Al sample MM for 6 hrs, it totally conforms to the theoretical fracture surface of a ductile failure as shown in Figure (58).

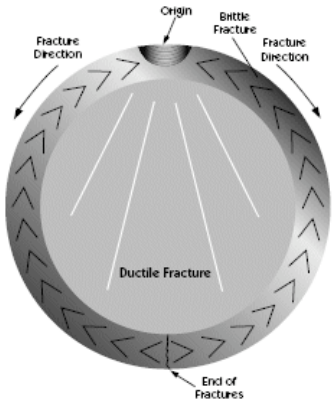

Figure 58: Ductile Failure [45].

Higher magnifications for the origin of crack in the Al samples MM for 12 hrs are shown in Figure (59). A cavity of about 5 µm was observed near the origin of the crack; from which two nano-cracks emerge as pointed by the red arrows. These two cracks seem to be aligned, i.e. they can be connected together using a straight line, hence this cavity occurred as a result of failure and it is not a flaw in the specimen that led to failure.

Moreover, further zooming inside this cavity showed how fine the internal structure of the material is. It is quite noticeable that the specimen is composed of a fraction of particles in the nanometer size range spread between larger particles in the size range of a few micrometers.

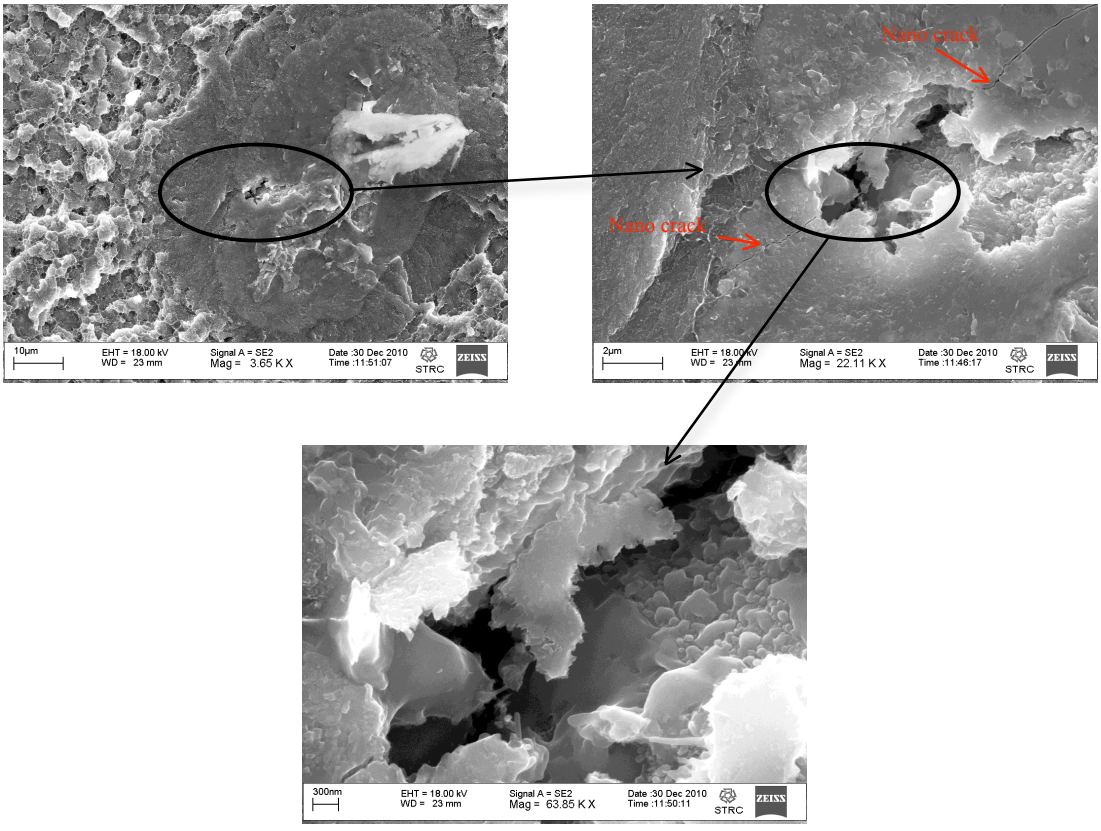

Figure 59: SEM micrographs showing the origin of crack in MM Al 12 hrs.

5.1.7.2.2. The annealed specimens

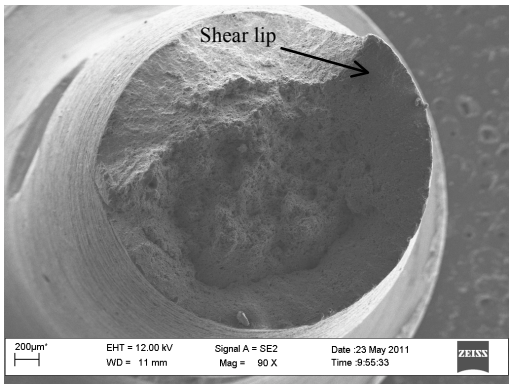

(a)

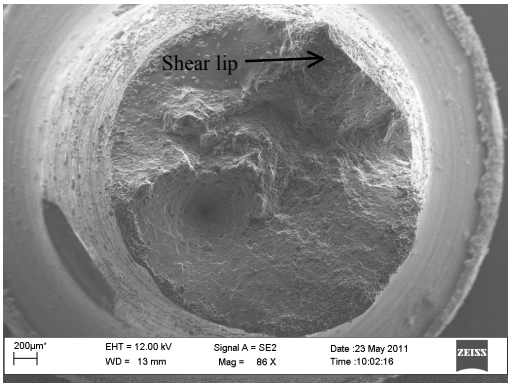

(b)

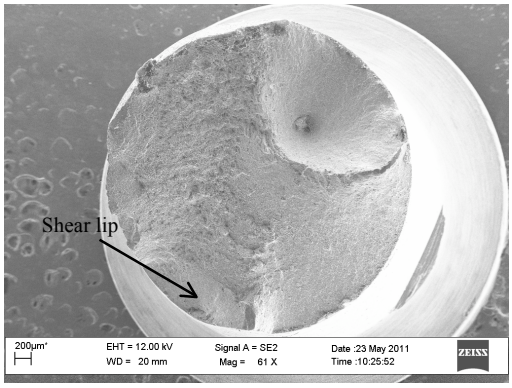

(d)

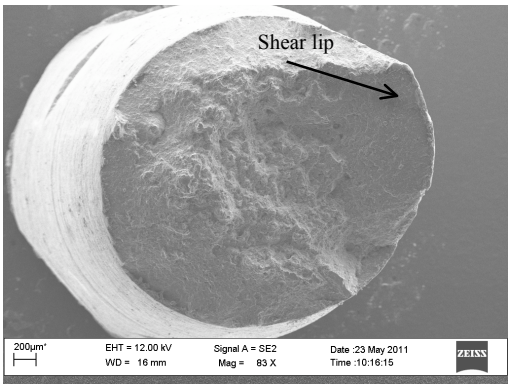

(c)

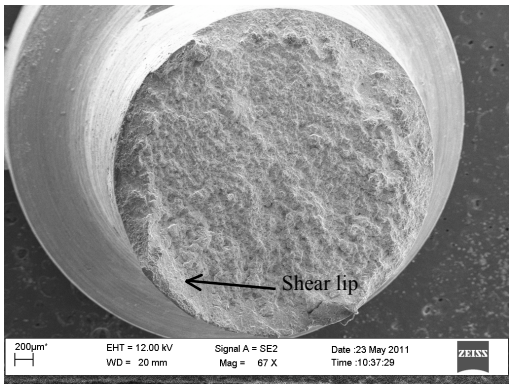

(e)

Figure 60: SEM micrographs showing the effect of MM duration on the fracture surface of annealed Al samples– low magnification (a) as-received Al, (b) MM Al 0.5 hr, (c) MM Al 1 hr, (d) MM Al 3 hrs, and (e) MM Al 6 hrs.

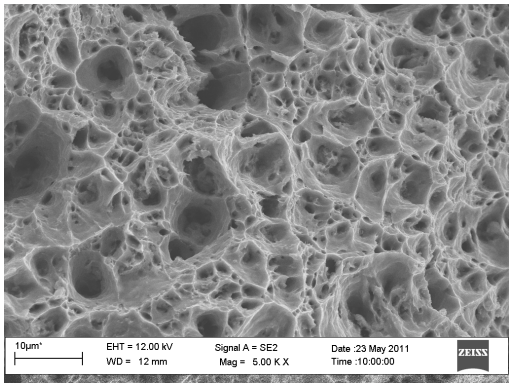

(a)

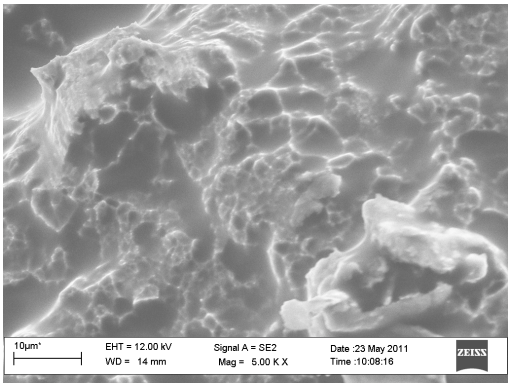

(b)

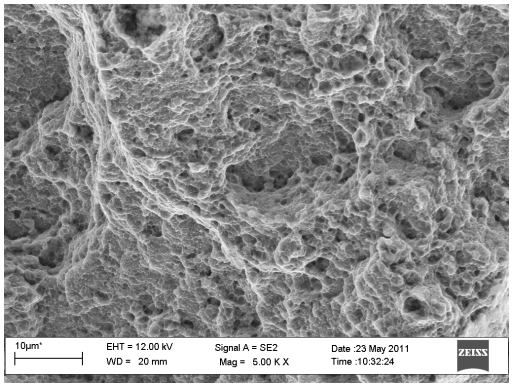

(d)

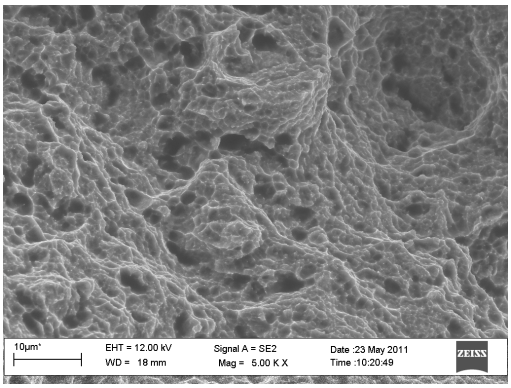

(c)

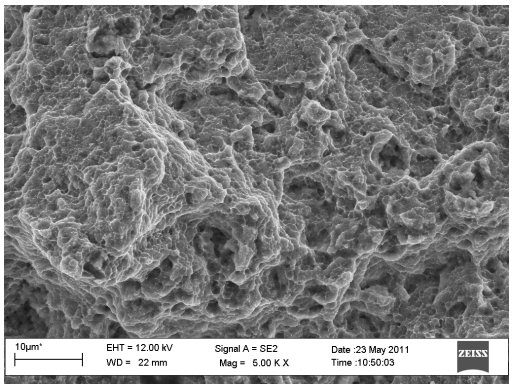

(e)

Figure 61: SEM micrographs showing the effect of MM duration on the fracture surface of annealed Al samples– high magnification (a) as-received Al, (b) MM Al 0.5 hr, (c) MM Al 1 hr, (d) MM Al 3 hrs, and (e) MM Al 6 hrs.

Based on the mechanical behavior of MM Al before and after annealing, the fracture surface after annealing was expected to show more of the ductile features as the ductility of the material increased with annealing. This can be observed in the as-received Al specimen that revealed a cup-and-cone feature that was not existent before annealing as demonstrated in the low magnification SEM images for the fracture surfaces of the annealed samples in Figure (60). Moreover, the shear lip was evident in almost all the annealed specimens as shown by arrows in Figure (60), which supports the ductility enhancement that occurred upon annealing.

Besides, the higher magnification SEM images in Figure (61) show more features of ductile failure when compared to the as-extruded samples. For instance, more dimples and micro-voids can be seen even at higher mechanical milling durations. In addition, coarsening of the particles; that would have deteriorated the strength of the material if occurred, didn't take place.

The increase in the amount of dimples or micro-voids in the material is upon annealing is more significant at early hours of mechanical milling. This is also supported by the mechanical behavior evaluation, as the increase in ductility was more significant at early hours of milling. This could be attributed to the strain hardening to which the specimen is subjected, the more the severe plastic deformation to which the material is subjected, the more its resistance to softening by annealing.

5.1.8. Transmission Electron Microscopy

The transmission electron microscope images of the bulk Aluminum samples mechanically milled for 12 hrs at 200 RPM for both the parallel and perpendicular directions to the extrusion direction are shown in Figures (62) and (63), and Figure (64) respectively.

Figure (62) shows two images for the same area along the direction parallel to the extrusion direction; one is a bright field and the other is a dark field image to illustrate the small grain size that was achieved through mechanical milling.

In both the parallel and perpendicular directions, grain sizes from approximately a few hundred nanometres to a few tens of nanometres could be found in the TEM micrographs. This finding testifies that the process of mechanical milling has led to the refinement of the internal structure of Al after MM 12 hrs and corroborates the XRD results.

Several structural features or defects were observed in the TEM images for the bulk sample MM Al 12 hrs. Examples of these features are single dislocations, dislocation tangle or forests, dislocation walls at the grains' interfaces, polygonized dislocation walls (PDW), as well as partially transformed grain boundaries (PTB) and fully transformed grain boundaries (GB). For the parallel direction, Figure (63(a)) shows dislocation networks circled in red; these networks can be seen spreading all over the material. Dislocation walls at the grains' interfaces can be observed in Figure (63(b)) circled in yellow. Also for the perpendicular direction, dislocation networks and tangles or forests of dislocations can be seen in Figure (64(a)) in addition to transformed grain boundaries, whereas Figure (64(b)) shows polygonized dislocation walls that could be transformed into grain boundaries by deformation according to the reporting of Chang *et al.* [38]. The different features observed in the TEM images conform to the results reported by Y. Li *et al.* [37]

Comparing the TEM images of MM Al 12 hrs in this work to the CG Al TEM images in the work of Y. Li *et al.* [37], it was deduced that the density of dislocations in the MM Al 12 hrs samples is much less than that in the CG Al. This finding also

agrees with what Y. Li *et al.* [37] reported comparing the NC Al to the CG Al in their work. This phenomenon is believed to be for the reason that the extremely small size of the grains doesn't allow it to tolerate a high density of dislocations. They have also suggested that the presence of the small density of dislocations in the NC Al is due to their generation during the process of extrusion as they found that the grain size of the NC Al increased after extrusion, which they attributed to the grain growth that took place during heating the specimens allowing extra space within the grains and hence dislocation were capable of being generated.

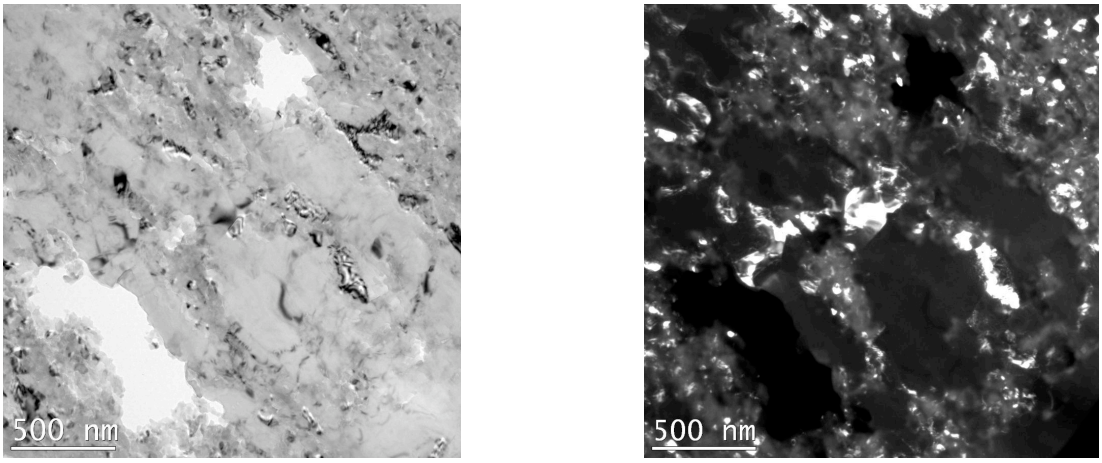

Figure 62: Bright field (left) and dark field (right) TEM images of the same area in a MM Al 12 hrs sample.

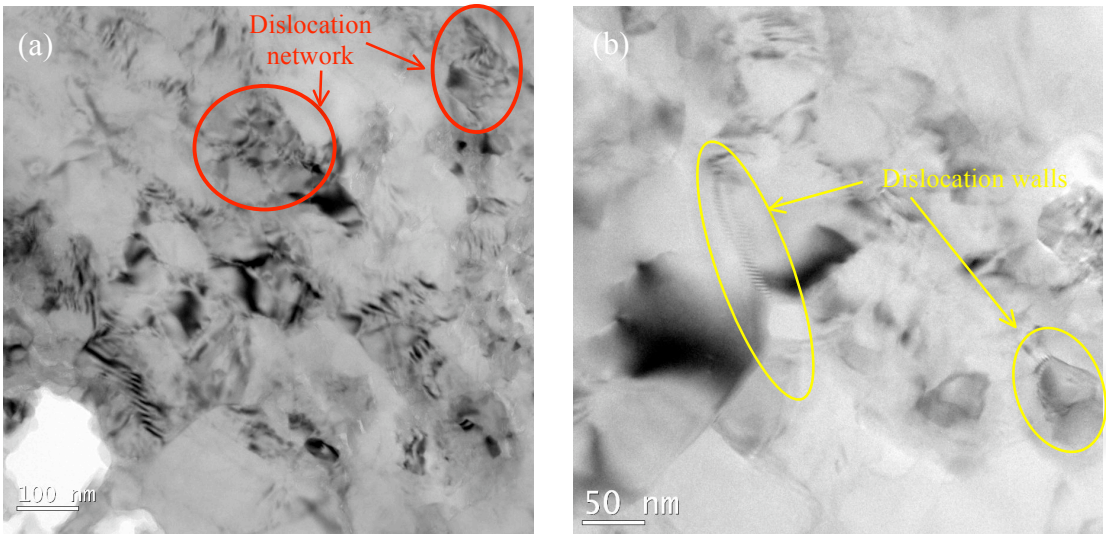

Figure 63: TEM micrographs for MM Al 12 hrs bulk samples along the direction parallel to the extrusion direction.

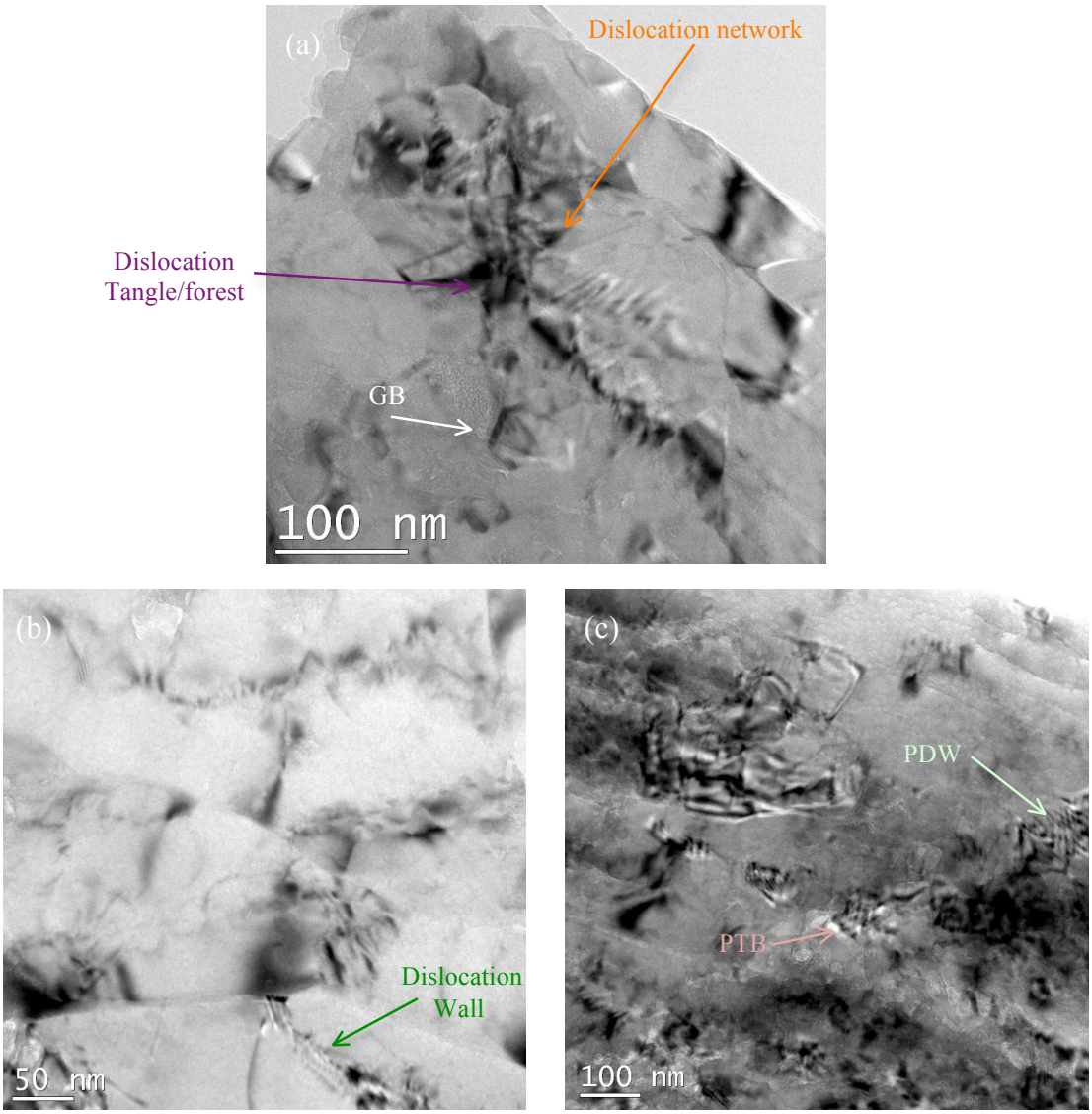

Figure 64: TEM micrographs for MM Al 12 hrs bulk sample along the direction perpendicular to the extrusion direction.

5.1.9. Bulk XRD

The XRD patterns for the bulk samples (as received, MM Al 6 hrs, and MM Al 12 hrs) are shown in Figure (65). These patterns showed broadening and shortening of peaks, which conform to the same outcome of the XRD analysis for the loose powders; that refinement in the internal structure of the material has been achieved via mechanical milling. However, the aim of conducting XRD analysis to the bulk samples was to determine whether secondary phases have been formed

during the stage of sintering or annealing. Studying the XRD patterns for the bulk samples, new peaks appeared after mechanical milling, the most intense of which is that formed right before the (200) peak as pointed by the arrows on the graph. This foreign peak started after 6 hrs of mechanical milling as a very small peak, but after 12 hrs of milling this peak became significantly intense. Phase analysis was conducted to determine the type of the secondary phase formed (suspected to be oxides or carbides), but it is still undetermined, as it needs further investigations.

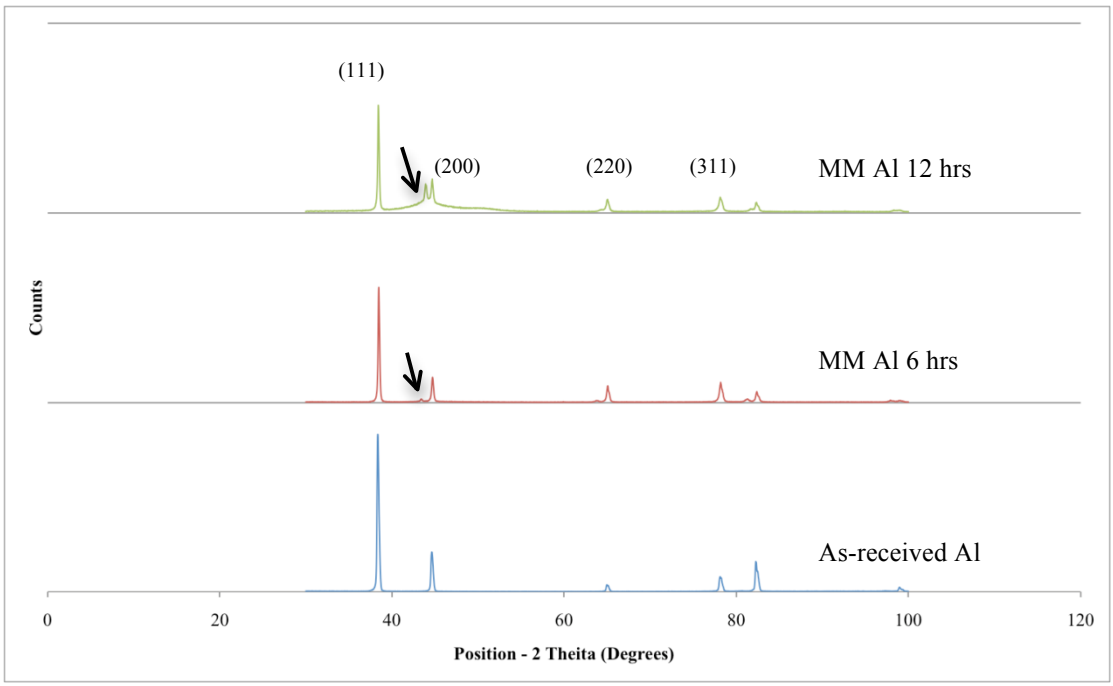

Figure 65: XRD pattern showing the effect of MM on the internal structure of bulk Al samples.

Using Scherrer's formula, the crystallite size for bulk Al milled for 0, 6, and 12 hrs was calculated and the results are tabulated in Table (15) in addition to the corresponding values of crystallite size for the powder samples. Generally speaking, the results show that milling has caused a reduction in the grain size of Al when considering the average of all peaks. However, studying the behavior of the each peak alone, it was noticed that in some directions the crystallite size decreased with milling while in other directions it increased. This suggests that the shape of the grains has

changed from being round shaped to being ellipsoidal in shape upon milling. It is quite noticeable that the crystallite size of MM Al samples is higher in case of bulk samples than the powder samples, this is believed to be due to the heat to which the specimens are subjected during powder metallurgy and annealing.

The findings of the bulk XRD test conform to those of the powder XRD test concerning the crystallite size refinement. However, the secondary phase that appeared in the bulk XRD was not apparent in the one for powders. This could be attributed to the formation of this phase during sintering or annealing, or their increase to the detectable limit upon heating. Moreover, the difference in the parameters used to conduct the test may have differed as a result of using different instruments for both tests.

Table 15: Crystallite size for powder and bulk Al MM for 0, 6, and 12 hrs.

MM duration (hrs)	Crystallite size of Bulk Al (nm)		Crystallite size of Al powder (nm)	
	Average of all peaks	Most intense peak	Average of all peaks	Most intense peak
0	32.40	32.80	30.12	33.63
6	33.20	43.80	21.78	25.49
12	28.40	38.30	16.65	20.03

5.1.10. Microstructure contributions to strength in MM Al

Strengthening of Al by mechanical milling could be attributed to several micro-structural factors such as grain boundary strengthening (grain size reduction), Orowan strengthening (due to the presence of dispersoids), and dislocation strengthening. To evaluate the results obtained for the produced material in the

current research, it was decided to attempt to compare them to theoretical predictions based on the different strengthening mechanisms listed above. This section will present this comparison by using the different formulas to calculate the predicted theoretical strength for MM Al 12 hrs specimens and comparing it to the experimental results reported earlier in this research.

1. ***Grain boundary strengthening using Hall-Petch equation***:

$$\sigma_y = \sigma_0 + K\, D^{-1/2} \qquad \{1\}$$

The constants for Al were σ_0 = 10 MPa, and K = 1.35 MPa √mm [46]. The selected grain size for MM Al 12 hrs is (D = 38.3 nm from bulk XRD results). By direct substitution, for MM Al 12 hrs the predicted yield strength was found to be **228.13 MPa.**

2. ***Orowan Strengthening:***

$$\sigma_{Or} = M \frac{0.4Gb}{\pi(1-\nu)^{1/2}} \frac{\ln(\bar{d}/b)}{\bar{\lambda}}$$

Where *M* is the orientation factor, which is (3.06) for FCC Al, *G* is the shear modulus (25.9 GPa), *b* is burger's vector (0.286 nm), υ is Poisson's ratio (0.33), đ = (√2/3) d (where *d* is the diameter of dispersoids, which is assumed 10 nm), λ = đ ((√π/4f)-1) where *f* is volume fraction of dispersoids, which is assumed 0.0005. By direct substitution, **σ_{or} = 37.55 MPa.**

3. ***Dislocation strengthening using Taylor relationship*** **[37]:**

$$\tau = CGb(\sqrt{(\rho)}) \quad \{7\}$$

Where *C* is a constant assumed to be (0.3), *G* is the shear modulus (25.9 GPa), *b* is burger's vector (0.286 nm), and ρ is the density of dislocations. The value for the density of dislocations was assumed in reference to the work by Y. Li *et al.* to be (4.1×10^7), which is one-tenth the value they used for coarse-grained Al. This assumption was based on the difference in grain size that controls the density of dislocations that can be tolerated within the grain. By direct substitution in equation {7}, τ = 14.23 MPa. Calculating the yield strength of the material using σ = 3.1 τ yields **σ = 44.11 MPa.**

To conclude, considering strengthening by grain size reduction, Orwan strengthening, and dislocation activity for MM Al 12 hrs (**σ = 228.13 + 37.55 + 44.11 = 309.79 MPa)**. Comparing the calculated theoretical value to the experimental value of yield strength for the MM Al 12 hrs samples (299.00 ± 25.00), it is noticed that the experimental results are within the range for the predicted value. It cannot be overlooked that there might be a margin of error in the predicted value due to several factors. First, the value used for the average grain size of MM Al 12 hrs calculated from Scherrer equation without taking into consideration broadening due to instrumental effects, which means it could be underestimated slightly. In addition, the TEM images for the same sample shows grains reaching 100 nm in size in addition to the ones of only few nanometers. Using 100 nm in the Hall-Petch relationship would give a theoretical yield strength of only 145 MPa so a value between 228 and 145 MPa is more probable. Second, for Orwan strengthening, some parameters were assumed due to lack of data and so might have been not reflecting the actual behavior.

Third, measuring the density of dislocations in the material was not possible, and had to be assumed to be a fraction of the value used in the reference by Y. Li et al. [37] for coarse-grained Al 5083, as indicated earlier. Finally, considering that full consolidation couldn't be achieved using powder metallurgy, the presence of micro-voids in the the specimen are expected to depress the yield strength of the material if taken into account.

5.2. Bi-modal Aluminum composite

This section presents the results for the testing and evaluation of the bi-modally structured aluminum samples that were developed using the two techniques explained in section (4.2).

5.2.1. Tensile behavior

The tensile behavior of the bi-modally structured Al samples synthesized by mixing using the turbula mixer was disappointing as the results satisfied neither the expected strength nor the required ductility. A representative stress-strain curve under tensile loading for the bi-modally structured Al in comparison to the parent materials from which the material is composed namely as-received Al and MM Al 12 hrs is shown in Figure (66). As can be seen, the ultimate tensile strength achieved by these conditions was below the average range between the two constituents. Not only was the ductility of the MM Al for 12 hrs not enhanced by the coarser soft particles of the as-received Al but also it was found to be worse. In other words, adding a softer phase using this technique of mixing led to increased brittleness.

On the other hand, using the high-energy ball mill to mix the same constituents yielded better results. As shown in Figure (67), the tensile strength of the material is slightly higher than the expected theoretical strength derived from the rule of mixtures (i.e. weighted average). In addition, adding the as-received soft Al powders was found to enhance the ductility of the MM Al for 12 hrs. Although the produced ductility in the bi-modally structured Al sample is still not satisfactory for this material to be utilized in the industry, but the results are promising that further improvements to the procedure might lead to reaching a compromise between the strength and ductility of the material.

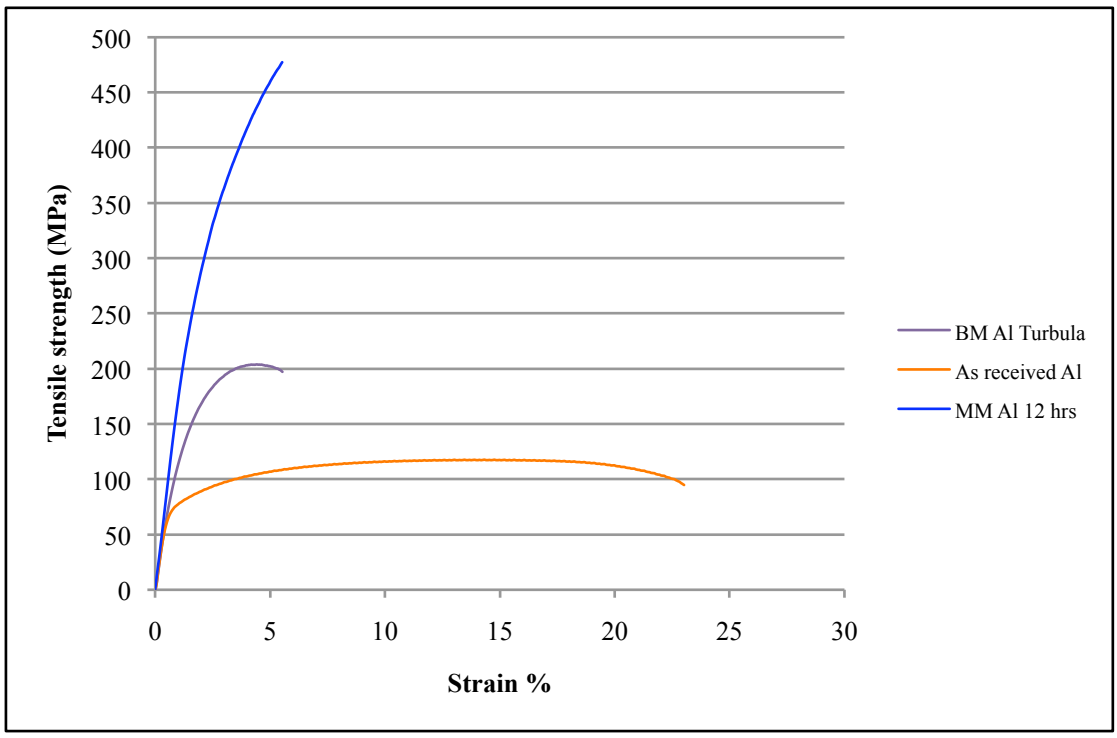

Figure 66: Representative tensile stress-strain curve for bi-modally structured Al synthesized using turbula mixer.

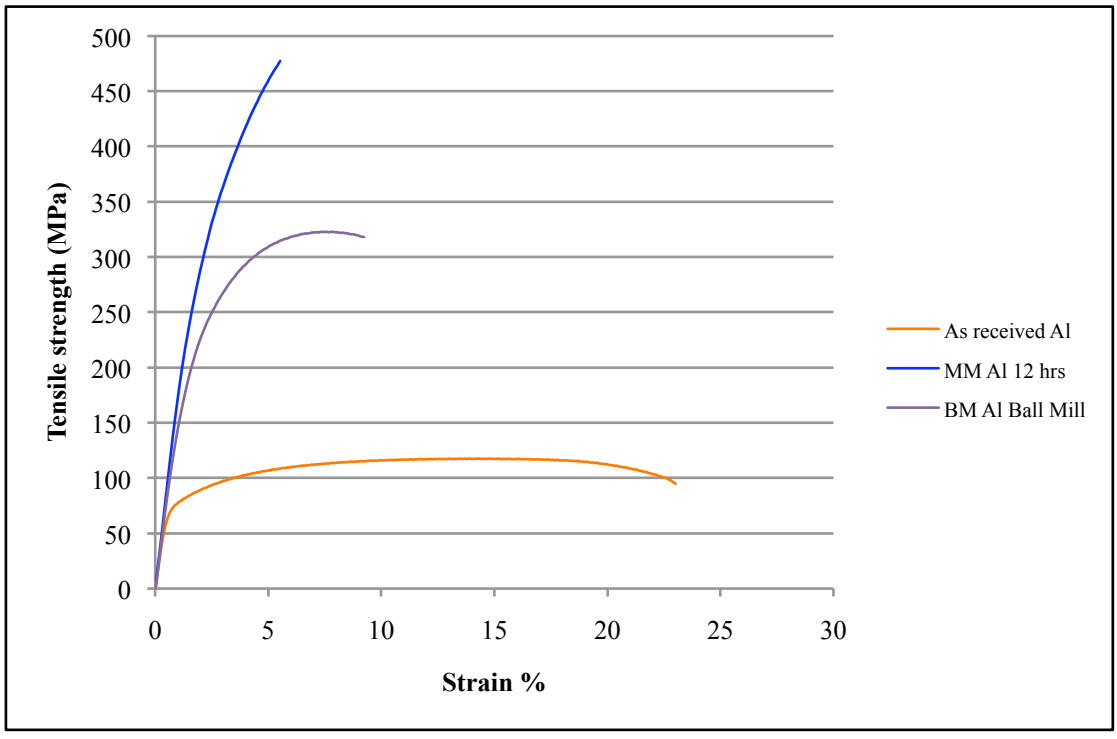

Figure 67: Representative tensile stress-strain curve for bi-modally structured Al synthesized using ball mill.

Table (16) better demonstrates the superiority of the technique of mixing using the high-energy ball mill over the one using turbula mixer. The reason behind that could be the lack of bonding between the particles when mixing using turbula mixer. Whereas in case of using the high-energy ball mill, a better interface is achieved between the two constituents as a result of coating the harder phase (the mechanically milled Al) with the softer phase (as-received Al). This interface is what leads to a chain of load transfer; since a good and sound bond between the two constituents will help the load be transferred from the as-received Al soft particles to the mechanically milled harder ones. Hence, the load will be carried by the hard phase, while the soft phase gives a push of ductility to the material.

Table 16: Comparing mechanical behavior of BM Al samples produced by different techniques.

Mixing technique	Yield Strength (MPa)	Tensile Strength (MPa)	% Elongation
As-received Al	68.75 ± 6.25	112.48 ± 5.22	25.61 ± 1.71
Turbula mixer	126.00 ± 1.00	200.45 ± 3.75	3.95 ± 0.45
Ball mill	232.00 ± 1.50	314.55 ± 9.15	6.94 ± 1.34
MM Al 12 hrs	299.00 ± 25.00	459.46 ± 17.84	2.35 ± 0.45

5.2.2. Compressive behavior

Agreeing with the findings of the tensile behavior testing, the compressive behavior of the bi-modally structured Al yielded almost the same trend. Figure (68) presents representative compressive stress-strain curves for the bi-modally structured Al samples synthesized via mixing by turbula mixer. This graph shows that adding the as-received Al particles to the MM Al 12 hrs led to the deterioration of the mechanical properties under compressive loading. In addition, the ductility of the MM

Al was not enhanced by developing a bi-modal material even under compression. The inset in Figure (68) shows a failed BM Al specimen mixed using the turbula mixer after compression test.

As for the bi-modally structured Al samples that are produced using the high-energy ball mill, the compressive strength curve shown in Figure (69) demonstrate a significantly higher compressive strength than the one observed for the bi-modally turbula mixed sample. However, the compressive strength is reduced compared to the MM Al 12 hrs without changing the ductility of the material under compression. . The inset in Figure (69) shows a failed BM Al specimen mixed by the ball mill after compression test. A comparison between the compressive behaviors of BM Al samples processed by the two different techniques in addition to that of the constituents from which the BM Al samples are composed is shown in Table (17).

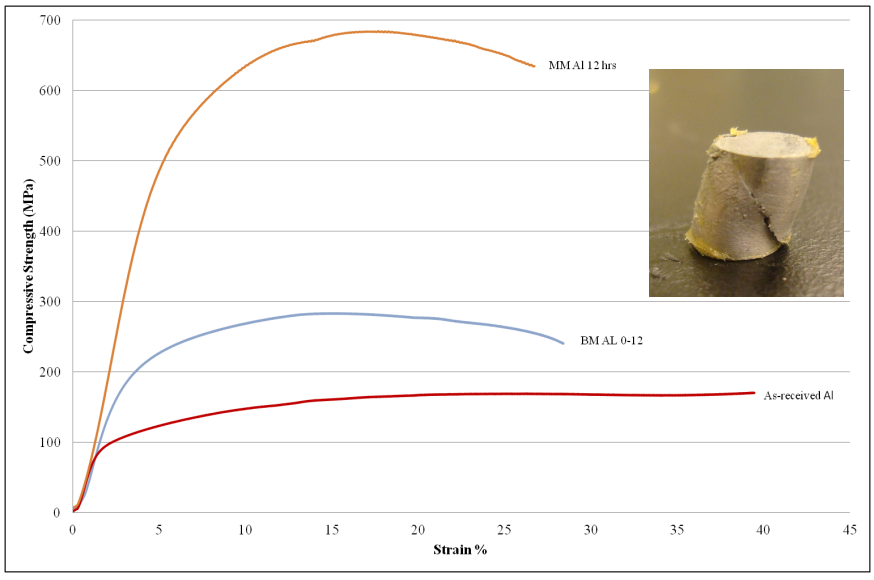

Figure 68: Representative compressive stress-strain curve for bi-modally structured Al synthesized using turbula mixer.

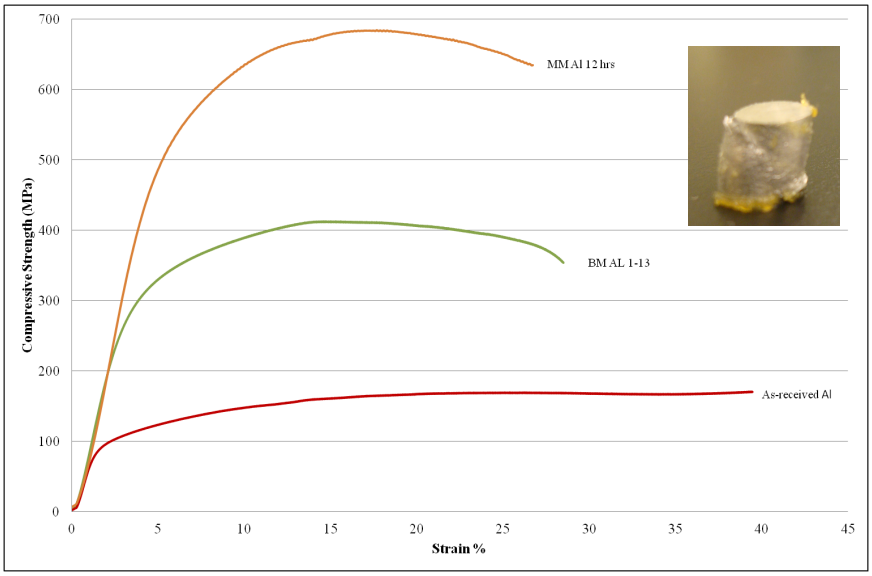

Figure 69: Representative compressive stress-strain curve for bi-modally structured Al synthesized using ball mill.

Table 17: Comparing compressive behavior of BM Al samples produced using different techniques.

Mixing technique	Ultimate Compressive Strength (MPa)	Compressive Yield Strength (MPa)
As-received Al	186.46 ± 13.45	98.08 ± 5.77
Turbula mixer	282.455 ± 8.30	177.60 ± 4.16
Ball mill	393.82 ± 19.09	247.99 ± 10.33
MM Al 12 hrs	459.46 ± 17.84	299.00 ± 25.00

5.2.3. Bulk Density

The average values for the relative density for the bi-modal aluminum samples listed in Table (18) demonstrate good consolidation. Although, the difference between the densities of the samples synthesized by mixing using turbula mixer and those synthesized by mixing using the high-energy ball mill is small, comparatively

speaking, it can be concluded that the samples prepared using the mixing/milling approach exhibit better compressibility.

Table 18: Relative density for BM Al samples.

Mixing technique	Relative Density %
Turbula mixer	98.20 ± 0.07
Ball mill	98.60 ± 0.13

5.2.4. Scanning Electron Microscopy

The SEM micrographs for the fracture surface of the bi-modally structured Al samples synthesized using the different techniques are shown in Figure (70). The images to the left are the ones for the samples synthesized by mixing using the turbula mixer, while those to the right are the ones synthesized by mixing using the high-energy ball mill.

A characteristic feature that is clearly observed in the SEM micrographs of the samples mixed using the turbula mixer is that the overall arrangement of the particles is in the form of a cluster of the MM Al particles surrounded by rivers of the as-received Al particles. This suggests poor dispersion of one phase in the other and hence the two constituents are not mechanically bonded and can be easily distinguished from one another.

On the other hand, the images to the right show that the samples mixed using the ball mill present a better dispersion of the two constituents in one another without clustering. A homogenous distribution of the two constituents is clearly visible. This supports the load transfer scenario suggested in section (5.2.1).

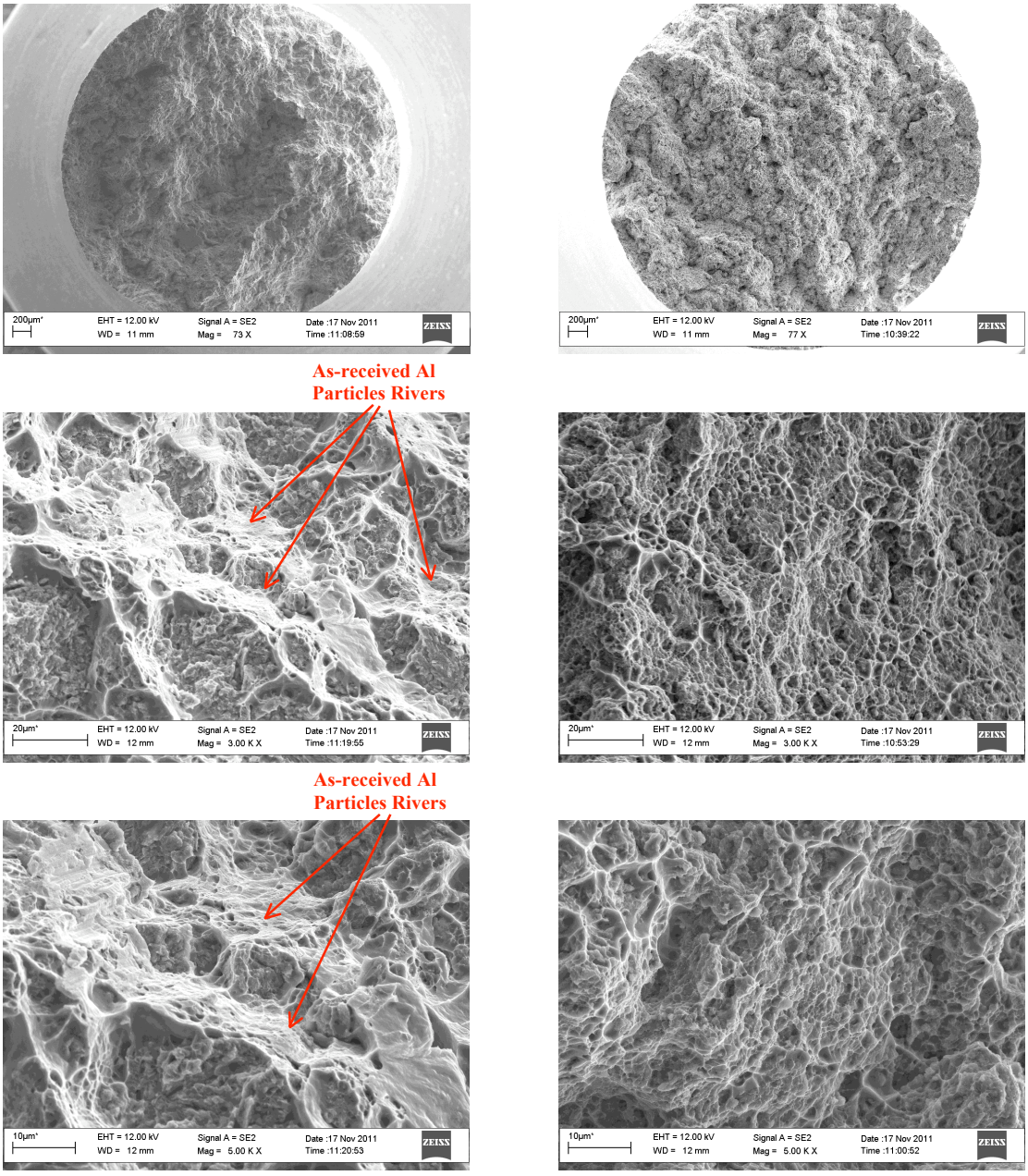

Figure 70: SEM micrographs for fracture surface of BM Al mixed using turbula mixer (left), and ball mill (right).

5.2.5. Transmission Electron Microscopy

The transmission electron microscope images of the bi-modally structured Al agreed with the SEM images that a clean and strong bond was developed when mixing using the high-energy ball mill in addition to the good dispersion of the two constituents with one another. In Figure (71), the red arrows point to the as-received

Al particles (referred to as coarse-grained CG), whereas the blue ones point to the MM Al 12 hrs particles (referred to as mechanically milled MM). It is quite noticeable that the as-received Al particles, being the coarser constituent, contain a higher density of crystal lattice defects (for example, the ones circled in Figure (71)). This supports the hypothesis that the minimal ductility in the nanostructured milled Al is attributed to the lower density of dislocations in the material due to its small grain size that cannot tolerate a high density of crystal lattice defects and suffers from lack of strain hardening capacity [37]. Aside from the interface between the two mixed constituents, which as described earlier appeared defect-free, it was noticed that the interface between the milled Al particles is not smooth. This, however, requires further investigation.

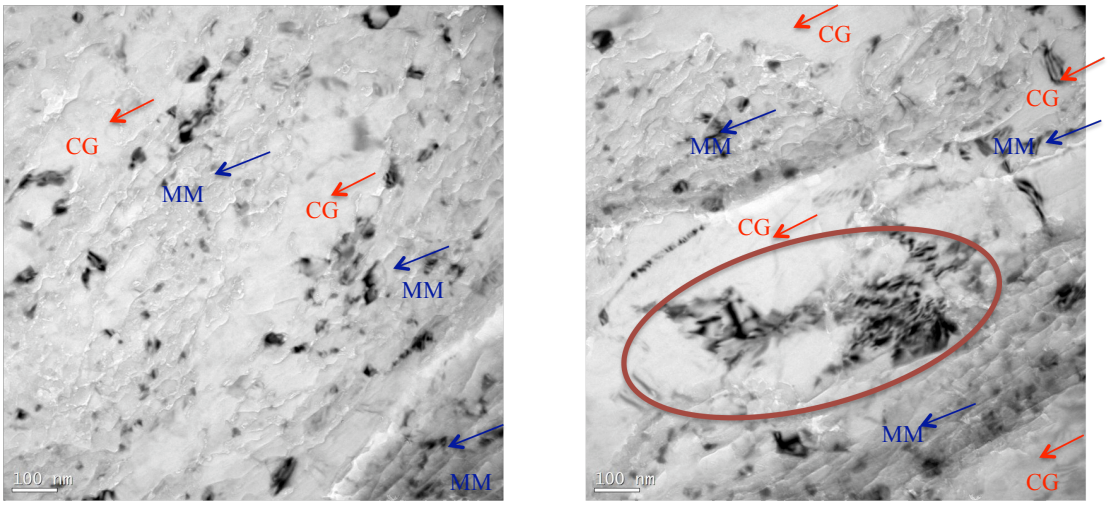

Figure 71: TEM images of BM Al showing the interface between the two constituents and the crystal lattice defects.

5.2.6. Estimated mechanical properties of BM Al

In order to assess the experimentally observed tensile behavior of BM Al, the rule of mixtures was applied to calculate the expected values for yield strength, tensile

strength, and ductility. In this case, there is no matrix or reinforcement by the literal meaning, however, there is a soft constituent, which is the as-received Al and a hard one, which is the MM Al 12 hrs. Equations {8}, {9}, and {10} are used to predict the yield strength, tensile strength, and strain %, respectively using the values in Table (12) in section (5.1.4.2).

$$\sigma_{y\ BM} = \sigma_{y\ Al}\ (68.75).\ f_{Al}\ (0.5) + \sigma_{y\ MM\ Al}\ (299.00).\ f_{MM\ Al}\ (0.5) \quad \{8\}$$

$$\sigma_{BM} = \sigma_{Al}\ (112.48).\ f_{Al}\ (0.5) + \sigma_{MM\ Al}\ (459.46).\ f_{MM\ Al}\ (0.5) \quad \{9\}$$

$$\varepsilon = \varepsilon_{Al}\ (25.61).\ f_{Al}\ (0.5) + \varepsilon_{MM\ Al}\ (2.35).\ f_{MM\ Al}\ (0.5) \quad \{10\}$$

Calculations give the following values:

- Yield strength ($\sigma_{y\ BM\ Al}$) = 183.88 MPa.
- Tensile strength of BM Al ($\sigma_{BM\ Al}$) = 285.97 MPa
- Elongation percent ($\varepsilon_{BM\ Al}$) = 13.98%

Upon comparing the calculated values for the expected yield strength of BM Al (183.33 MPa) to the experimental results in Table (16) in section (5.2.1), it was found that the experimental yield strength of the BM Al mixed using the turbula mixer (126.00 ± 1.00 MPa) is smaller than the predicted value. However, mixing using the high-energy ball mill resulted in a yield strength (232.00 ± 1.50 MPa) that is significantly higher than the predicted value. Moreover, the same phenomenon was also noticed for the tensile strength comparison where the BM Al samples mixed using turbula mixer demonstrated a tensile strength less than the predictions, whereas using the high-energy ball mill showed a tensile strength higher than the predictions.

Studying the difference between the expected and experimental ductility of BM Al samples, it was realized that using either the turbula mixer or the high-energy

ball mill for mixing yielded values that are less than the expectations. The predicted value for the ductility is almost twice the experimental values. This relatively low ductility can be attributed to several factors that need further investigations. For instance, the bond between the two constituents from which the BM Al samples consist might suffer from some defects formed due to the rise in temperature during mixing using the high-energy ball mill despite using methanol as a PCA and allowing intermittent breaks for the jars to cool down during the process of mixing. A clean metallurgical interface is thus a key requirement for a strong interface. The presence of any carbides or oxides dispersoids could have also contributed to the lower ductility.

Chapter (6)

Conclusions

1. Mechanical milling is considered a severe plastic deformation technique that is used to strengthen ductile materials such as Aluminum. In this research, this has been proven by showing the effect of mechanical milling on the mechanical behavior of bulk Al samples synthesized from mechanically milled powders.

2. The outcome of the process of mechanical milling is controlled by several parameters such as those investigated in this research that are the amount of process control agent used during milling and the milling duration.

3. Increasing the amount of process control agent - methanol in this research – promoted particles' refinement and hindered cold welding of the particles. Consequently, the mechanical behavior of the material is enhanced. There are limits against increasing the amount of process control agent, since beyond a certain amount the process becomes hazardous. Based on the studies in this research, an amount of 0.26 wt% of methanol is satisfactory to yield the required mechanical behavior.

4. XRD analysis for loose powders after mechanical milling demonstrated a refinement in the internal structure of the material without the appearance of any foreign peaks, which either eliminates the possibility of the creation of secondary phases during mechanical milling due to the excessive use of the process control agent or suggest that they are below the detection limits.

5. SEM micrographs of the powders before and after mechanical milling showed that the particles' sizes increased at the early stages of milling - up until 1 hr - and then refinement started taking place and was evident in the Al particles milled for 3 hrs and more.

6. Mechanically milled Al powders for 12 hrs were found to consist of fractions of powders with sizes of a few micrometers in addition to fractions of powders with sizes of a few hundreds of nanometers.

7. As the milling duration increases, the tensile behavior of the material increases. The ultimate tensile strength of Al after mechanical milling for 12 hrs at 200 RPM has increased by approximately four folds. Comparing these results with the best comparable results found in the literature, it cannot be overlooked that this research achieved an ultimate tensile strength of (459±17.84 MPa) for MM Al after milling for only 12 hrs at 200 RPM. Whereas as Choi *et al.* [10] reached the value of 500 MPa for the same material after milling for 48 hrs at 550 RPM. However, this strength was gained at the expense of ductility to the extent of behaving in a perfectly brittle manner under tension.

8. The compressive behavior testing showed that mechanical milling has enhanced the material strength under compression, in addition the material was found to be ductile under compression. This finding suggests that the plastic instability under tension could be the result of specimen structural flaws.

9. Annealing was investigated as a process to retain some of the lost ductility. A study was conducted to determine the convenient annealing time, and it was found to be 3 hrs at 500°C. Annealing has been proven to be a suitable process to improve the ductility of mechanically milled Al. Moreover, the ultimate tensile strength and yield tensile strength of the material was not lost; on the contrary it has been slightly increased.

10. Density measurements showed that the bulk samples were well consolidated as the relative density was found to be very high.

11. SEM micrographs for the fracture surfaces before and after annealing revealed ductile failure features until reaching 12 hrs of milling when the specimens failed in a brittle mood.

12. TEM micrographs of bulk Al samples milled for 12 hrs gave evidence for the existence of grain sizes ranging from a few hundreds of nanometers to a few tens of nanometers.

13. XRD analysis for bulk samples conformed to the results from the loose powders regarding the structure refinement. However, foreign peaks were observed after milling for 6 and 12 hrs, suggesting the formation of secondary phases during the stage of sintering or annealing. The type of the secondary phases is yet to be determined as they might be oxides and/or carbides formed due to the decomposition of the process control agent and contributed to strengthening.

14. The production of bi-modally structured Al from as-received Al particles and Al particles milled for 12 hrs using turbula mixer was found to be disappointing as the ductility of the milled Al was depressed even more, besides losing its strength under tension.

15. Using the high-energy ball mill to mix as-received Al powders and milled Al powders for 12 hrs was found to be a promising technique to enhance the material's ductility without tremendously losing the strength under tensile loading below the average theoretical expectation.

16. Compressive behavior of the bi-modally structured Al yielded the same findings as the tensile behavior study.

17. Density measurements for the bi-modally structured Al samples supported full consolidation.

18. SEM micrographs for the fracture surface of the bi-modally structured Al samples mixed using turbula mixer revealed poor bonding between the two constituents and the existence of rivers of as-received Al particles surrounding clusters of MM Al 12 hrs particles.

19. The fracture surface of the bi-modally structured Al samples mixed using ball mill showed evidence of good dispersion of one constituent in the other and the particles were observed to be well bonded.

Chapter (7)

Future work

1. Determine type of secondary phases formed during sintering or annealing to decide whether they contributed to the strengthening of mechanically milled Al.
2. Conduct diffraction scanning calirometry for the milled Al samples to check for the existence of oxides that helped in strengthening the material.
3. Find alternative techniques to produce bulk samples from mechanically milled powders to minimize the defects in the specimens and develop flaw free samples.
4. Conduct fracture toughness test to trace the crack propagation and better understand the plastic instabilities under tensile loading.
5. The observation that hardness of the material increased with increasing the annealing duration is intriguing, so it is recommended to increase the milling duration beyond 3 hrs and determine whether the material's hardness will keep on increasing, and if it does, when will the saturation level be achieved.
6. Investigate why the tensile and compressive strengths of the milled Al samples were increased after annealing in addition to the ductility enhancement although the opposite should be expected given that this behavior is unusual.
7. Try cryomilling when synthesizing bi-modally structured Al using high-energy ball mill in order to assure the creation of clean strong metallurgical interfaces between the particles of the different constituents.
8. The effect of the different parameters in the process of producing BM Al should be studied, i.e. vary the different parameters involved and monitor their effects to achieve the optimum results.

9. The interface between the milled Al particles in the bi-modally structured Al samples requires further investigations as demonstrated by the TEM images.

10. Synthesize tri-modally structured Al from powders mechanically milled for different durations to tailor the mechanical properties in a way that enhanced the ductility besides exhibiting high strength.

References

[1] George E. Totten, D. Scott Mackenzie, “Handbook of Aluminum: Physical Metallurgy and Processes”, New York: Marvel Dekker Inc, 2003.

[2] Brandt, J. L. Aluminum (Properties, physical metallurgy, and phase diagrams). Edited by Kent R. Van Horn. Vol. 1. Ohio: American Society for metals, 1967.

[3] S. Hwang, C. Nishimura, P.G. McCormick. "Mechanical milling of Mg powder." Materials science and Engineering A 318 (2001): 22-33.

[4] Akhtar S. Khan, Yeong S. Suh, Xu Chen, Laszlo Takacs, Haoyue Zhang. "Nanocrystalline Al & Fe: Mechanical behavior at quasi-static and high strain rates, and constitutive modeling." *International Journal of Plasticity* 22 (2006): 195-209.

[5] Valiev, Ruslan. "Nanomaterial Advantage." *Nature* 419 (2002): 887-888.

[6] Mohsen Mhadhbi, Mohamed Khitouni, Myriam Azabou, Abdelwaheb Kolsi. "Characterization of Al & Fe nanosized powders synthesized by high energy mechanical milling." *Materials Characterization* 59 (2008): 944-950.

[7] Akhtar S. Khan, Babak Farrokh, Laszlo Takacs. "Effect of grain refinement on mechanical properties of ball-milled bulk aluminum." *Materials Science and Engineering A* 489 (2008): 77-84.

[8] E. Bonetti, L. Pasquini, E. Sampaolesi. "The influence of grain size on the mechanical properties of nanocrystalline Aluminum." *Nanostructured Materials* 9 (1997): 611-614.

[9] Jichun Ye, Bing Q. Han, Zonghoon Lee, Byungmin Ahn, Steve R. Nutt, Julie M. Schoenung. "A tri-modal aluminum based composite with super-high strength." *Scripta Materialia* 53 (2005): 481-486.

[10] H. J. Choi, S. W. Lee, J. S. Park, and D. H. Bae. "Tensile behavior of bulk nanocrystalline Al synthesized by hot extrusion of ball milled powders." *Scripta Materialia* 59 (2008): 1123-1126.

[11] Wynne, Masahiro Kubota and B. P. "Electron Backscattering diffraction analysis of mechanically milled and spark plasma sintered pure Aluminum." *Scripta Materialia* 57 (2007): 719-722.

[12] Suryanarayana, C. *Mechanical Alloying and Milling.* New York: Marcel Dekker, 2004.

[13] Suryanarayana, C. "Mechanical Alloying and Milling." *Progress in Material Science* 46 (2001): 1-184.

[14] Lai, Li Lu and M. O. "Formation of new materials in the solid state by mechanical alloying." *Materials and Design* 16, no. 1 (1995): 33-39.

[15] http://www.synl.ac.cn/org/non/zu1/english/facilities.asp, November 28th, 2011

[16] http://www.materials-days.eu/advatec/projects/project1.html, November 28th, 2011.

[17] http://www.parts-recycling.com/Metal-Working-Machine-/Stamping-Press-/Out-of-Area-/Union-process-01-hd-lab-attritor-mill.htm, November 28th, 2011

[18] Dongdong Gu, Yifu Shen. "Microstructures and properties of high Cr content coatings on inner surfaces of carbon steel tubular components prepared by a novel mechanical alloying method.", *Applied Surface Science*, 256 (2009): 223-230.

[19] Valiev, T. C. Lowe and R. Z. *Producing nanoscale microstructures through severe plastic deformation.* Journal of the minerals, metals, and materials society, Nanoscale Materials, 2000.

[20] D. Jia, Y. M. Wang, K. T. Ramesh, E. Ma, Y. T. Zhu, R. Z. Valiev. "Deformation behavior and plastic instabilities of ultrafine-grained Ti." *Applied Physics Letters* 79 (2001): 611-613.

[21] Ma, E. "Recent progress in improving ductility of ultra-high strength nanostructured metals." *Metals and Materials International* 10, no. 6 (2004): 527-531.

[22] Yinmin Wang, Minwei Chen, Fenghua Zhou & En Ma. "High tensile ductility in a nanostructured metal." *Letters to Nature* 419 (2002): 887-889.

[23] Ma, E. "Instabilities and ductility of nanocrystalline and ultrafine-grained metals." *Scripta Materialia* 49 (2003): 663-668.

[24] Koch, C. C. "Optimization of strength and ductility in nanocrystalline and ultrafine-grained metals." *Scripta Materialia* 49 (2003): 657-662.

[25] Yingguang Liu, Jiangiu Zhou, Xiang Ling. "Impact of grain size distribution on the multiscale mechanical behavior of nanocrystalline metals." *Materials Science and Engineering A* 527 (2010): 1719-1729.

[26] Ma, E. "Eight routes to improve the tensile ductility of bulk nanostructured metals and alloys." *J*ournal of the minerals, metals, and materials society, Nanoscale Materials, *Nanostructured Materials*, 2006: 59-53.

[27] J. J. Fuentes, J. A. Rodriguez, E. J. Herrera. "Increasing the ductility and strength of submicrometer-grained P/M Al." *Journal of Alloys and Compounds* 484 (2009): 806-811.

[28] R. Z. Valiev, I. V. Alexandrov, Y. T. Zhu, and T. C. Lowe. "Paradox of strength and ductility in metals processed by severe plastic deformation." *Materials Research Soceity* 17, no. 1 (2002): 5-8.

[29] Carlos A. Galan, Angel L. Ortiz, Fernando Guiberteau, and Lean L. Show. "Crystallite size refinement of ZrB2 by high-energy ball milling." *Journal of American Ceramic Soceity* 92, no. 12 (2009): 3114-3117.

[30] Xiangyu Zhao, Yi Ding, Liqun Ma, Xiaodong Shen, and Suyuan Xu. "Structure, morphology, and electrocatalytic characteristics of Ni powders treated by mechanical milling." *International Journal of Hydrogen Energy* 33 (2008): 6351-6356.

[31] Caroline B. Reid, Jennifer S. Forrester, Heather J. Goodshaw, Erich H. Kisi, Gregg J. Suaring. "A study in the mechanical milling of alumina powder." *Ceramics International* 34 (2008): 1551-1556.

[32] J. Cintas, F. G. Cuevas, J. M. Montes, E. J. Herrera. "High strength PM Aluminum by milling in ammonia gas and sintering." *Scripta Materialia* 53 (2005): 1165-1170.

[33] S. Kleiner, F. Bertocco, F. A. Khalid, and O. Beffort. "Decomposition of process control agent during mechanical milling and its influence on displacement reactions in the Al-TiO2 system." *Materials Chemistry and Physics* 89 (2005): 362-366.

[34] Y. M. Wang, E. Ma. "Three strategies to achieve uniform tensile deformation in a nanostructured metal." *Acta Materialia* 52 (2004): 1699-1709.

[35] B. Srinivasarao, K. Oh-ishi, T. Ohkubo, T. Mukai, and K. Hono. "Synthesis of high-strength bimodally grained Iron by Mechanical Alloying and spark plasma sintering." *Scripta Materialia* 58 (2008): 759-762.

[36] T. Makhlouf, M. A. Azabou, M. Ghrib, T. Ghrib, N. Yacoubi, M. Khitouni. "Study of the nanocrystalline bulk Al alloys synthesized by high-energy mechanical milling followed by room temperature high pressing consolidation." *JMSM 2008 conference.* Physics Procedia, 2009. 1411-1419.

[37] Y. Li, Y. H. Zhao, V. Ortatan, W. Liu, Z. H. Zhang, R. G. Vogt, N. D. Browning, E. J. Lavernia, J. M. Scheonung, "Investigation of aluminum-based nanocomposites with ultra-high strength.", *Materials Science and Engineering A* 527 (2009): 305-316.

[38] C. P. Chang, P. L. Sun, P. W. Kao, "Deformation induced grain boundaries in commercially pure Aluminum.", Acta Materialia 48 (2000): 3377-3385.

[39] J. R. Davis and Associates, "Aluminum and Aluminum alloys", ASM International, 1993.

[40] "Standard Test Method for Tension Testing of Metallic Materials", ASTM E8/E8M, American Society for Testing and Materials, 2009.

[41] "Standard Test Method for Compression Testing of Metallic Materials at room temperature", ASTM E9-09, American Society for Testing and Materials, 2009.

[42] http://us.mt.com/us/en/home/applications/Laboratory_weighing/Density_1.html, Last visited on December 29th, 2011 at 11:16 PM.

[43] William D. Callister, "Materials science and engineering: an introduction.", 7th Edition. John Wiley and Sons Inc, 2007

[44] Randall M. German and Seong Jin Park, "Handbook of mathematical relations in particulate materials processing", John Wiley and Sons Inc, 2008.

[45] http://www.nhml.com/resources/2004/1/1/ductile--brittle-fracture, January 6th, 2012.

[46] http://www.dtic.mil/cgi-bin/GetTRDoc?AD=ADA205997, January 15th, 2012.